การกำจัดองค์ประกอบของก๊าซผสมสไตรีนและแอมโมเนียที่ความเข้มข้นต่ำโดยใช้เครื่องปฏิกรณ์ปล่อยโคโรนาที่อุณหภูมิต่างๆ

นายสหัส ไชยโย

วิทยานิพนธ์นี้เป็นส่วนหนึ่งของการศึกษาตามปริญญาวิศวกรรมศาสตรมหาบัณฑิต
สาขาวิชา วิศวกรรมเคมี ภาควิชาวิศวกรรมเคมี
คณะวิศวกรรมศาสตร์ จุฬาลงกรณ์มหาวิทยาลัย
ปีการศึกษา 2544

ISBN 974-03-0232-7

REMOVAL OF DILUTE MIXTURE OF STYRENE AND AMMONIA USING CORONA DISCHARGE REACTOR AT VARIOUS TEMPERATURES

Mr. Sahat Chaiyo

A Thesis Submitted in Partial Fulfillment of the Requirements
for the Degree of Master of Engineering in Chemical Engineering
Department of Chemical Engineering
Faculty of Engineering
Chulalongkorn University
Academic Year 2001

ISBN 974-03-0232-7

Thesis Title Removal of Dilute Mixture of Styrene and Ammonia Using Corona Discharge Reactor at Various Temperatures
By Mr. Sahat Chaiyo
Field of study Chemical Engineering
Thesis Advisor Professor Wiwut Tanthapanichakoon, Ph.D.

Accepted by the Faculty of Engineering, Chulalongkorn University in Partial Fufillment of the Requirements for the Master's Degree.

………………………………………….. Dean of Faculty of Engineering
(Professor Somsak Panyakeow, Dr. Eng.)

Thesis Committee

………………………………………….. Chairman
(Associate Professor Chirakarn Muangnapoh, Dr. Ing.)

………………………………………….. Thesis Advisor
(Professor Wiwut Tanthapanichakoon, Ph.D.)

………………………………………….. Member
(Associate Professor Tawatchai Charinpanitkul, Dr. Eng.)

………………………………………….. Member
(Jirdsak Tscheikuna, Ph.D.)

สหัส ไชยโย : การกำจัดองค์ประกอบของก๊าซผสมสไตรีนและแอมโมเนียที่ความเข้มข้นต่ำโดยใช้เครื่องปฏิกรณ์ปล่อยโคโรนาที่อุณหภูมิต่างๆ (REMOVAL OF DILUTE MIXTURE OF STYRENE AND AMMONIA USING CORONA DISCHARGE REACTOR AT VARIOUS TEMPERATURES) อ.ที่ปรึกษา : ศ.ดร. วิวัฒน์ ตัณฑะพานิชกุล , 185 หน้า. ISBN 974-03-0232-7

จุดประสงค์หลักของงานวิจัยนี้คือ ศึกษาผลของอุณหภูมิที่มีต่อการกำจัดสไตรีนและ/หรือแอมโมเนียโดยอาศัยปฏิกิริยาการเติมอิเล็กตรอน เนื่องจากก๊าซเป้าหมายเหล่านี้เป็นก๊าซองค์ประกอบ 2 ชนิดของก๊าซที่ปล่อยจากเตาเผาศพที่อุณหภูมิสูง ในเบื้องต้นได้ทำการศึกษาถึงลักษณะสมบัติการปล่อยโคโรนาที่เงื่อนไขอุณหภูมิสูง แล้วทำการประยุกต์เครื่องปฏิกรณ์แบบเติมอิเล็กตรอนในการกำจัดก๊าซสไตรีน (C_8H_8) และ/หรือ แอมโมเนีย (NH_3) ออกจากก๊าซไนโตรเจนที่อุณหภูมิห้องถึงอุณหภูมิ 300 องศาเซลเซียส ปัจจัยที่ทำการศึกษาได้แก่ ความเข้มข้นขาเข้าของสไตรีน ร้อยละของออกซิเจนและความเข้มข้นของไอน้ำในกระแสก๊าซ จากผลการทดลองในอดีตและปัจจุบันพบว่า ถ้าความเข้มข้นของก๊าซสไตรีนยิ่งต่ำ ประสิทธิภาพการกำจัดจะยิ่งดีขึ้นโดยไม่ขึ้นกับอุณหภูมิการทดลอง อนึ่งการมีออกซิเจนผสมอยู่ในก๊าซไนโตรเจนจะช่วยเพิ่มประสิทธิภาพการกำจัดก๊าซให้สูงขึ้นทั้งก๊าซสไตรีน และ/หรือแอมโมเนีย ส่วนการมีไอน้ำจะช่วยเพิ่มประสิทธิภาพในการกำจัดก๊าซสไตรีนจากก๊าซไนโตรเจน แต่กรณีที่มีไอน้ำในก๊าซไนโตรเจน-ออกซิเจนจะทำให้ประสิทธิภาพการกำจัดต่ำกว่ากรณีที่ไม่มีไอน้ำ

นอกจากนี้ได้ทำการศึกษาการกำจัดก๊าซผสมสไตรีน และแอมโมเนียแบบพร้อมกัน พบว่าอิทธิพลของก๊าซสไตรีนที่ผสมอยู่ช่วยเพิ่มประสิทธิภาพการกำจัดก๊าซแอมโมเนีย ในขณะที่อิทธิพลของก๊าซแอมโมเนียที่ผสมอยู่ทำให้ประสิทธิภาพการกำจัดก๊าซสไตรีนลดลงเล็กน้อย ดังที่คาดไว้ การมีออกซิเจนผสมอยู่ช่วยเพิ่มประสิทธิภาพในการกำจัดแบบพร้อมกัน เนื่องจากมักเกิดปัญหาการเกิดผลิตภัณฑ์ที่ไม่ต้องการ ปัญหานี้สามารถบรรเทาได้อย่างน่าพอใจโดยการใช้เครื่องปฏิกรณ์สองเครื่องที่ต่อแบบอนุกรม

ภาควิชา ………วิศวกรรมเคมี………. ลายมือชื่อนิสิต……………………………………………..
สาขาวิชา ……….วิศวกรรมเคมี……..... ลายมือชื่ออาจารย์ที่ปรึกษา………………………………..
ปีการศึกษา ………2544……………… ลายมือชื่ออาจารย์ที่ปรึกษาร่วม……………………………

4270587921 : MAJOR CHEMICAL ENGINEERING

KEY WORD GASEOUS POLLUTANT/GAS PURIFICATION/ELECTRON ATTACHMENT/CORONA DISCHARGE

SAHAT CHAIYO: REMOVAL OF DILUTE MIXTURE OF STYRENE AND AMMONIA USING CORONA DISCHARGE REACTOR AT VARIOUS TEMPERATURES
THESIS ADVISOR: PROF. WIWUT TANTHAPANICHAKOON, Ph.D., 185 pp. ISBN 974-03-0232-7

The main objective of this research is to investigate the effect of temperature on styrene and/or ammonia removal using electron attachment reaction because the target gases are two of the malodorous gaseous components that emitted at high temperature from a crematory furnace. The corona-discharge characteristics at various elevated temperatures are studied first. Then the electron attachment reactor is applied to remove styrene(C_8H_8) and/or ammonia(NH_3) from N_2 at room temperature to 300^0C. The factors investigated are inlet gas concentration of styrene, percentage of coexisting oxygen and the concentration of water vapor in the gas stream. Past and present experimental results that, regardless of the temperature, the lower the inlet concentration, the higher the removal efficiency becomes. It has been found that the presence of O_2 enhances the removal efficiency of both styrene and/or ammonia. The presence of water vapor enhances the styrene removal efficiency from N_2. However, the presence of water vapor in N_2-O_2(5%) has adverse effect on the removal efficiency.

Furthermore, simultaneous removal of styrene and ammonia from N_2 has been investigated. The experimental results show that the presence of styrene enhances the removal efficiency of ammonia. In contrast, the presence of ammonia slightly retards the removal efficiency of styrene. As expected, the presence of O_2 enhances the simultaneous removal efficiency. Since some reaction by-products are often generated, using two independently operated reactors in series can satisfactorily minimize this problem.

Department ……..Chemical Engineering…….. Student's signature ………………………………………
Field of study ……Chemical Engineering…….. Advisor's signature ……………………………………..…..
Academic year …………...2001……………….. Co-advisor's signature …………………………………..

ACKNOWLEDGEMENT

I am very grateful to my advisor, Prof. Wiwut Tanthapanichakoon, Department of Chemical Engineering, Chulalongkorn University, for his indispensable advice, and his encouragement to continue the course of this work. I am also grateful to Assoc. Prof. Tawatchai Charinpanitkul, Assoc. Prof. Chirakarn Muangnapoh and Dr. Jirdsak Tscheikuna for their stimulative comments and participation as the thesis committee.

I would like to acknowledge the TJTTP-JBIC Project and the Thailand Research Fund (TRF). Dr. Noriaki Sano of Himeji Institute of Technology and Prof. Hajime Tamon of Kyoto University visited CU and brought research materials here as part of the joint Thailand-Japan Technology Transfer Project. The research work originally received financial support from TRF given to Prof. Wiwut as Team Research Award and subsequently New Fundamental Knowledge Project. I have also received monthly stipends as Research Assistant from these TRF Projects.

I would like to thank Dr. Sano for his on-the-job training, useful guidance, research assistance, and kindness. It has been a great experience learning a lot of things from him and Prof. Tamon.

I would like to thank Assistant Prof. Sanong Ekgasit, Department of Chemistry, Faculty of Science, for carrying out FT-IR spectroscopic analysis to help identify the solid deposits.

I would like to thank Ms. Nantamas Dhattavorn for her training and useful suggestions. It would have been impossible to finish this thesis without her advice.

Thank you very much to all members of the Particle Technology and Material Processing Laboratory for their warm collaborations and kindness especially Mr. Pisit Ariyadetvanit who gives me a lot of suggestions.

Thank you very much for all friends in Environmental Laboratory for the time we have shared together and their hospitality.

Last but not least, the indispensable encouragement from my family that leads me through this course.

CONTENTS

NOMENCLATURE

C_{in} = inlet concentration [ppm]

$C_{out,0mA}$ = outlet concentration [ppm] when using zero current

$C_{out,Any\ mA}$ = outlet concentration [ppm] when using non - zero current

$[\ ]_{in}$ = inlet concentration [ppm]

$[\ ]_{out}$ = outlet concentration [ppm]

ψ = apparent removal efficiency [-]

ψ' = removal efficiency excluding adsorption effect [-]

ψ'' = removal efficiency per unit residence time [-]

I = discharge current [mA]

P = power consumption [W]

SV = space velocity [hr^{-1}]

V = discharge voltage [V]

R = anode radius [m]

R_o = cathode radius [m]

θ = mean residence time, (min)

V = effective volume of the corona discharge reactor,(ml)

A = cross sectional area, (cm^2)

$\langle \upsilon \rangle$ = superficial velocity, (m/s)

CHAPTER I

INTRODUCTION

Nowadays air pollution in Thailand has become one of the most serious environmental problems. There are many sources of air pollutants such as heavy concentration of vehicles that release a large amount of toxic and obnoxious emissions. One of the air pollution problems in Thailand is emission gas from the crematoria during cremation rites. There are nearly 23,000 temples nationwide, including approximately 300 temples with crematory furnaces in Bangkok Metropolitan Area. Various malodorous gases and particulate are emitted during cremation, causing frequent complaints from vicinal communities. Typically crematory gases are emitted from a stack to the atmosphere without adequate treatment. A few rich temples have installed furnaces with after-burning systems but an overwhelming majority of Bangkok temples have inadequate systems. For this reason it is worthwhile to try to develop an alternative gas treatment method that has high efficiency and low energy consumption.

This research investigates the application of corona-discharge reactors in series to the removal of dilute gaseous pollutants. Electron attachment is a reaction involving low energy electrons and an extremely high selectivity for electronegative gases.

Table 1.1 Types and concentrations of gaseous emission from a crematorium after 100-fold dilution (Nishida K. 1981, 1988)

	Components	Concentration
Air	N_2	78 %
	O_2	20~21 %
Low Concentration	CO_2	0.01-0.02 %
	H_2O	0.22 %
	NO_x	80 ppm (max)
	SO_x	5.8 ppm (max)
	Acetic acid (CH_3COOH)	24 ppm
	Hydrocarbons	230 ppm (as propane)
Very dilute concentration (malodorous)	Acetaldehyde	0.04 ppm
	Styrene	0.01 ppm
	Hydrogen sulfide	0.01 ppm
	Methyl mercaptan	0.001 ppm
	Dimethyl sulfide	0.0005 ppm
	Ammonia	0.37 ppm (max)
	Trimethyl amine	0.023 ppm (max)

Table 1.1 shows an example of the types and concentrations of gases emitted from the stack of a crematory furnace after the exhaust gas has been diluted 100-fold with ambient air. Since the above concentrations of the malodorous gases have

been diluted 100 times with ambient air, their original concentrations are nearly 100 times higher before the dilution.

Table 1.2 compares the generic technologies with corona discharge technology for VOC and odor control. Under certain suitable conditions, corona discharge is a novel efficient method that can simultaneously remove several electronegative gas species. With coexisting oxygen, non-electronegative but oxidizable species can also be decomposed and removed. High energy electrons and thermal plasma are not necessary to remove the gas species.

In this research emphasis will be placed on the effect of the gas temperature because it has not sufficiently been investigated despite the fact that the exhaust temperature of most stack gases is always much higher than room temperature. Generally gaseous pollutants are often emitted at high temperatures (typically, the actual exhaust stack gas temperature may range from 150-300 ^{0}C). Therefore it is necessary to investigate corona-discharge properties at various elevated temperatures.

Table 1.2 VOC and odor control methods

Method	Suitable condition/ requirement	Advantage	Disadvantage
After-burning (thermal combustion)	Uniform furnace temperature (800-900 °C). Residence time about 0.5~2 sec. High gas concentrations. Steady state operation.	Simple and widely available.	Unsuitable for unsteady state operation. Large furnace required.
Catalytic reaction (catalytic combustion)	Known unchanged gas species. High gas concentrations preferable. Adequate residence time. Steady state operation.	Can be operated at relatively lower temperatures compared to thermal combustion. High selectivity of targeted gas species.	One catalyst type not effective simultaneously for several gas species. Combustion requires moderate to high temperatures Disposal of spent catalysts and/or regeneration.
Adsorption	Relatively low temperature and low space velocity. Low gas concentrations. Usually unsteady operation. Known types of gas species.	Steady and unsteady operations.	Regeneration is often necessary to reduce costs. Relatively high pressure drop Continuous operation requires multiple units Disposal of solid adsorbents. Complicated operation.
Gas absorption	Low to very high temperature. Usually steady operation. Low to relatively high gas concentrations. Known types of gas species.	Can simultaneously remove particulate and gas species.	Difficult to find the appropriate liquid absorbent Regeneration is often necessary to reduce costs. Complicated operation. Disposal of liquid absorbent.
Corona discharge, electron attachment	Low space velocity. Dilute to low gas concentrations. Electronegative gas species and/or species oxidizable by ozone. Steady and unsteady operation.	Rapidly reach the steady state. Multiple removal mechanisms.	Relatively big reactor. High investment. High voltage entails risks, including gas explosion when the combustible gas concentration is high. Automatic cleaning of the anodic surface may be necessary. Undesirable by-product gas may be produced.

1.1 Objective of research work

1.1.1 Investigate the effect of elevated temperature on the simultaneous removal efficiency of gaseous pollutants at atmospheric pressure using the deposition-type reactor at various conditions.

1.1.2 Investigate the use of two corona-discharge reactors in series on the individual and overall removal efficiency of the reactors.

1.2 Scope of research work

1.2.1 The experimented gases in this research are styrene and ammonia

1.2.2 The influence of coexisting gas components is:

- Oxygen
- Water vapor
- Combination of both components

1.2.3 The experimental conditions investigated are as follows:

- discharge currents 0- 0.50 mA
- cathode diameter is 0.5 mm with 10 cm effective length
- Space velocity gas at room temperature is 55.8 hr^{-1}
- Temperature range is room temperature to 300 °C

CHAPTER II

FUNDAMENTAL KNOWLEDGE

The self-sustaining discharge of electrons in a non-uniform electric field between a thin wire and a coaxial cylinder is called a corona discharge. This name is descriptive of the glowing light effects found when the applied voltage is several kilovolts. High vacuum is not always required and corona discharge can be generated at or near atmospheric pressure. The gas pressure needs not be low for the discharge to occur, but at low gas pressure the corona is not visible. The luminous part of the discharge is usually restricted to a region close to the wire surface, which may be positive or negative with respect to the cylinder. One distinguishes between positive and negative coronas by the applied positive or negative voltage of the central electrode.

Coronas are by no means only artificially produced. It is the natural phenomenon of the glow or corona surrounding the sun but is only visible during a total solar eclipse. In addition, nature produces them between and within electrically charged clouds. A theory on cloud electrification attributes this process to the corona on and around ice particles in the clouds. According to this theory, corona is not only the effect but also the cause of the appearance of charged clouds and therefore of lightning and thunderstorms.

In a corona discharge reactor, there are three regions in the void space between the anode and cathode.

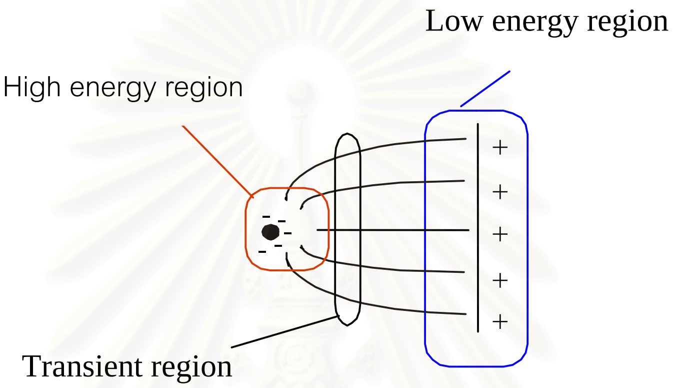

Figure 2.1 Wire to plate electrodes

In the high electron energy region, free electrons are emitted from the cathode surface and rapidly accelerated. Surrounding gas molecules will be ionized after collision with these free electrons and negative ions are produced. In the transient region, the electron energy is just enough to dissociate gas molecules to produce neutral radicals. In the vast region of low-energy electrons, electrons are prone to be captured after collision with gas molecules. Cluster formation and electron attachment reaction generally take place in this region.

2.1 Electron attachment reaction

When low-energy electrons collide with electronegative gas molecules, the law of probability requires that some of the electrons are captured by some gas molecules to form negative ions. This natural phenomenon is called "electron attachment" (Massay, 1976). The probability of electron attachment depends on the electron energy level, the structure of the gas molecule, and its electron affinity (electronegativity). There is a huge difference between the electron attachment probability of the electronegative gas molecules and that of the neutral carrier gas. This high selectivity is reflected in the production of specific negative ions (Caledonia, 1975 and Massay, 1976, 1979). In short, electronegative impurities at very dilute concentration become negative ions by electron attachment, and they can selectively be separated from the neutral gas (for example, N_2) in an electric field.

In the case of an electron with excessively high energy colliding with a gas molecule, the molecule would not only be negatively ionized but may also be either dissociated or positively ionized due to the net loss of one electron from the molecule itself. In contrast, if a free electron whose energy is too low reaches the molecular orbital, the electron can not be captured by the molecule. It is necessary to take into account the moderate (appropriate) range of electron energy level when the electron attachment probability is to be enhanced. A great deal of effort has been devoted to the generation and utilization of discharge electrons with a variety of energy range via a variety of gas-discharge devices. However, the appropriate range of electron energy level contributing more or less exclusively to electron attachment generated by such devices has not been clarified because of the limitation of in-situ measurement devices and/or technique.

At the exact moment when an electron is captured by a gas molecule, the molecule would be placed in an excited state. To become stable, the molecule must release the excess energy in quanta, for example, by collision with another electron, by collision with another gas molecule, by being decomposed, or by irradiation. Various processes for the electron attachment reaction have been reported (Moruzzi and Phelps, 1966) as illustrated by **Eq. (2.1), (2.2), and (2.3).** Here a mixture of an electron-attaching gas, AB, and an appropriate carrier gas, M, is considered in these processes.

Dissociative attachment: $e + AB \rightarrow A^- + B$ (2.1)

Three-body attachment: $e + AB + M \rightarrow AB^- + M$ (2.2)

Radiative attachment: $e + AB \rightarrow AB^- + h\nu$ (2.3)

Since the electron attachment probability of the gas molecule is dependent upon its electron affinity, it is reasonable to expect that a gas molecule that contains one or more atoms with high electron affinity would have a high probability of electron attachment. For example, in a comparison between SF_6 and N_2, the electron affinities of S, F, and N are 200 kJ/mol, 333 kJ/mol, and –26 kJ/mol, respectively. So it is not surprising that the probability of electron attachment for SF_6 molecule is reportedly 10^{11} times that of N_2 molecule (Hickman and Fox, 1956). This extreme difference in the electron attachment probability among various kinds of gas molecules results in high selectivity in the formation of the corresponding negative ions. Therefore, even a specific gas component whose concentration is extremely low can effectively be separated from the main (neutral) gas in an electric field by utilizing the electron attachment reaction. As a consequence, the method based on electron attachment can be expected to be one of the most efficient methods of gas purification.

2.2 Principle of gas purification

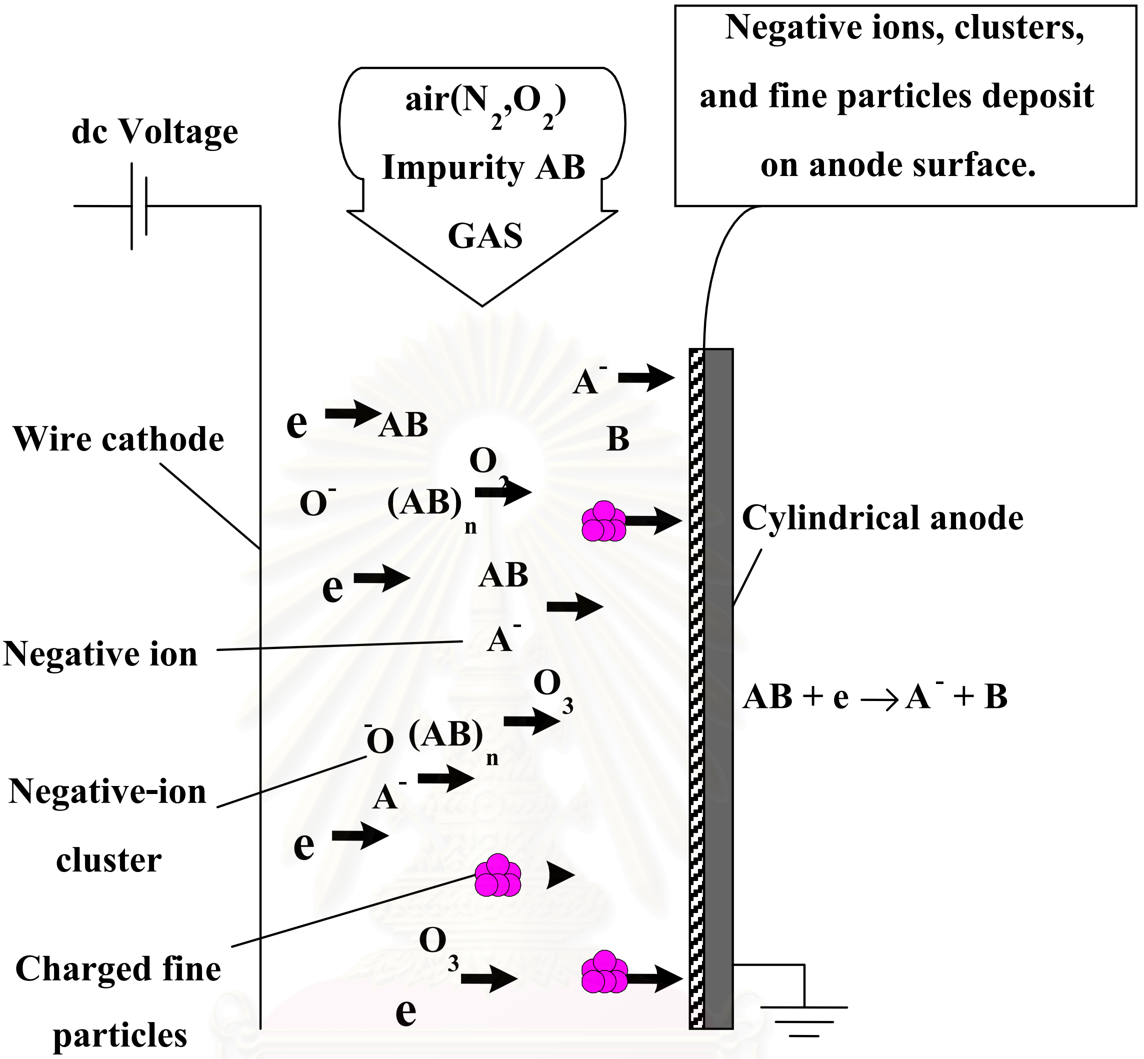

Figure 2.2 Principle of Gas Purification

Figure 2.2 illustrates the principle of gas purification by the removal of an impurity, AB, from an inert gas in a cylindrical corona-discharge reactor (Tamon et al., 1995). The corona discharge is employed here because it is an efficient method to supply a large number of low-energy electrons to the gas stream. The cathode is a wire stretched along the axis of the reactor and the outer cylinder acts as grounded anode. High DC voltage (-5~ -15kV) is applied to the cathode to induce corona discharge in the reactor. Electrons generated at the cathode drift to the anode along the applied electric field. During their drift to the anode, a portion of them collides with the gas molecules. Negative ions, A^-, are thus selectively produced by electron attachment and they likewise drift to the anode as the electrons do.

In an ideal case, the number of electrons generated in the reactor is sufficient for all gaseous impurities to hitch up with the electrons and all negative ions thus generated are able to completely deposit on the anode surface. In other words, the outlet gas is devoid of unwanted impurities and complete removal is achieved. In reality, upon their arrival at the anode, certain kind of negative ions might simply discard their charges without depositing on its surface. In this case these gaseous impurities can not be separated using the simple deposition-type reactor. In any case, it is most desirable to capture most of the negative ions arriving at the anode surface. The idea of how to remove negative ions at the anode will be described later.

Besides the above-mentioned removal mechanism associated with electron attachment reaction in the corona-discharge reactor, it is believed that other removal mechanisms may simultaneously contribute to the removal efficiency. When single negative ions are produced in the reactor, they may possibly interact with other adjacent gas molecules via their electrostatic forces and negative-ion clusters may be formed. Each cluster then contains multiple gas molecules targeted for removal. When the clusters drift to the anode and manage to deposit there, the removal efficiency is greatly enhanced.

Another possible mechanism contributing to the removal efficiency is the so-called radical reaction. When dissociative electron attachment also takes place in the reactor, not only negative ions but also reactive radicals are produced. In particular, the radicals may readily be produced in the immediate vicinity of the cathode surface where high electric field strength exists. It is logical to assume that the removal efficiency would be enhanced by radical reaction, which, however, often results in the generation of reaction by-products.

The reaction of targeted gas molecules with O_3 is frequently mentioned. Ozonation reaction usually takes place when oxygen coexists in the gas stream. High-energy electrons close to the cathode surface collide with O_2 molecules to dissociatively produce O^- radicals. O^- radicals can next react with O_2 molecules to produce O_3, which is reactive with various kinds of gases. Hence, ozonation reaction is expected to contribute to the oxidative destruction of a number of gaseous impurities in the gas stream, thus improving the removal efficiency while yielding by-products.

2.3 Types of reactor

As mentioned in section 2.2, in some cases certain kind of negative ions produced by electron attachment would drift towards but do not easily adhere to the anode surface. Thus they end up as uncaptured negatively charged or uncharged impurities at the outlet of the conventional deposition-type reactor, and cause a decrease in their removal efficiency. It is therefore essential to find out how to effectively remove such negative ions at the anode. This has motivated Tamon et al. to propose three types of reactor, as shown in **Figure 2.3**.

Deposition-type reactor

Some negative ions readily adhere to the anode surface of the reactor after releasing their negative charges there. In this case they may form solid particles or react with the metallic anode. The solid particles form a thin deposition layer on the anode surface. Thus, the so-called deposition-type or (simple) reactor is adequate for the removal of these negative ions. Periodic cleaning of the anode surface or its replacement is often necessary to maintain high removal efficiency.

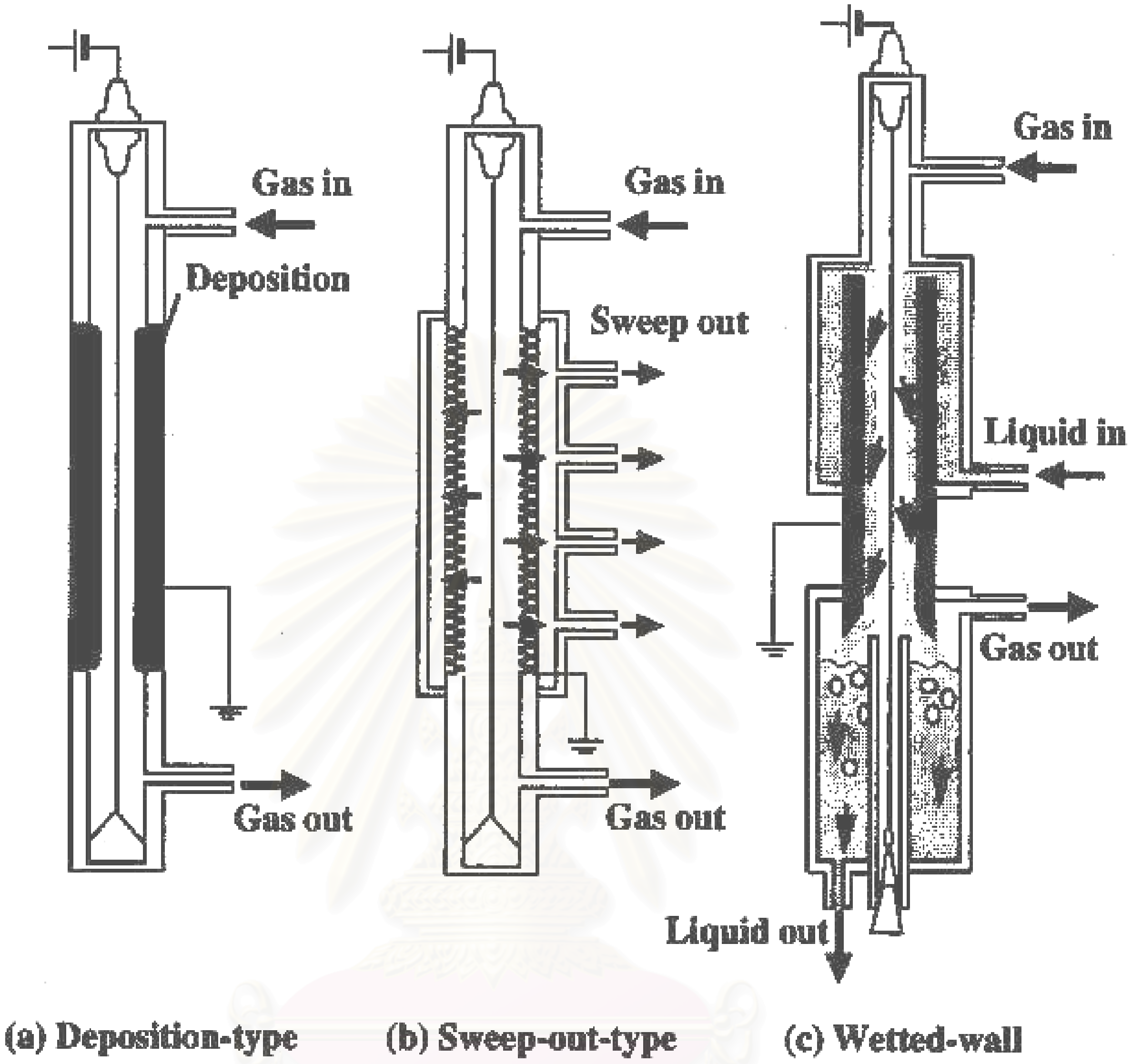

Fig 2.3 Concepts of corona-discharge reactor

Sweep-out-type reactor

In some uncommon cases certain negative ions do not easily deposit on the anode surface but change back to the original uncharged molecules after releasing electrons at the anode surface. In such cases, the deposition-type reactor is not suitable because the original molecules of the gas impurities are not removed but diffuse back to the main gas stream. To solve this problem, the sweep-out-type reactor, which uses a porous pipe wall made of sintered metal as anode is recommended. A small portion of the carrier gas around the anode surface is swept out by suction through this pipe to restrict backward diffusion of the concentrated electronegative impurities so that the removal efficiency would be kept high. The swept-out stream with a much higher concentration of the gas impurities can then be treated using a suitable conventional method.

Wetted-wall reactor

Another option to remove negative ions at the anode surface is the wetted-wall reactor. Negative ions reaching the anode of the reactor can be absorbed into a down-flowing liquid film on the vertical anode surface. This absorption of the ions improves the removal efficiency. The most important advantage is the self-cleaning of the anode, which makes it suitable even for dirty gas streams containing both dust and gaseous pollutants. The major drawback is the need for a liquid (mostly water) treatment and recycle system. Anyway, the corona-discharge reactor to be investigated in this work will be limited to the deposition type because it is easier to construct and operate, and is applicable as a first step of the fundamental study in a laboratory.

Kittisak Laipsuriyakul et al.(1998) and Wiwut Tanthapanichakoon (1998) reported experimental results about the effect of the structure of the corona-discharge reactor on the removal of dilute gases. The smaller the reactor diameter among three equivolume reactors, the higher the removal efficiency as shown in **Figure 2.4**.

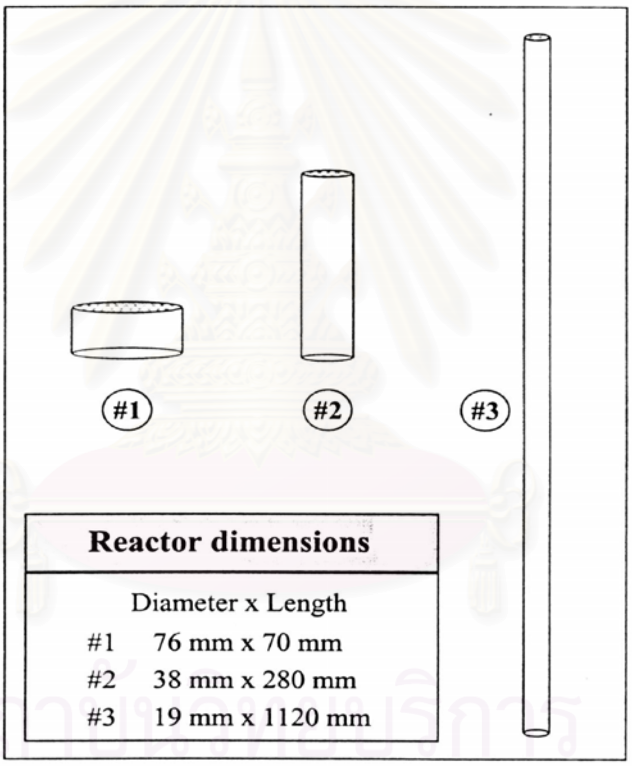

Reactor dimensions

	Diameter x Length
#1	76 mm x 70 mm
#2	38 mm x 280 mm
#3	19 mm x 1120 mm

Fig 2.4 Different shapes of equivolume reactors

As for the number of cathode wires in a single reactor vessel, the single-cathode reactor always exhibited a higher removal efficiency than the 5-cathode one as shown in **Figure 2.5**.

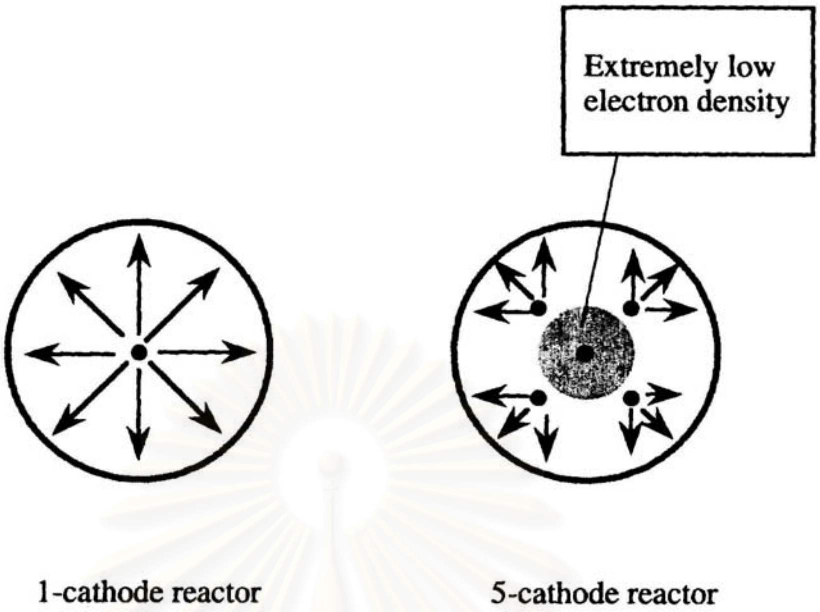

Fig 2.5 Effect of the number of cathode wires

2.4 Effect of coexisting oxygen (ozone effect)

When O_2 is present in a gas mixture, it usually reacts with discharged electrons. Electron attachment on O_2 has been reported in the literature (Morruzzi and Phelps, 1966; Massay, 1976; Rapp and Briglia, 1976; Chantry and Schulz, 1967).

$$O_2 + e^- \longrightarrow O_2^- \qquad (2.4.)$$

$$O_2 + e^- \longrightarrow O + O^- \qquad (2.5)$$

Moruzzi and Phelps (1966) reported that the reaction in **Eq. (2.4)** occurs in the low electron energy range ($E/p < 1.5$ V.m^{-1}.Pa). In contrast, the reaction in **Eq. (2.5)** occurs in the higher electron energy range. Also in the corona-discharge reactor, the closer the electrons are to the cathode wire, the higher their energy level. When an O_2 molecule collides with a high-energy electron near the cathode wire in the corona-discharge reactor, production of O^- is expected as in **Eq. (2.5)**. Next O_3 is produced from the reaction of O^- with O_2 (Loiseau et al., 1994; Hadj-Zaine et al., 1992).

In short, some ozone (O_3) is produced. Since O_3 is very reactive, the ozonation reaction is used in some commercial devices for deodorization and sterilization. The same ozonation reaction is expected to contribute to the removal of gas impurities in the present corona discharge reactor.

2.5 Effect of negative-ion cluster

If a negative ion induces the formation of a cluster of multiple gas molecules, the removal efficiency of the impurities will be improved. This effect is significant because one negative ion and several gas molecules constitute a cluster that drifts to the anode and deposits on it.

2.6 Effect of temperature

The influence of gas or reactor temperature on the relationship between the voltage and the current has been confirmed [Sano et al. (1997)]. As expected, the higher the temperature, the lower the required voltage becomes. Reportedly, several factors may be considered as the reason for the temperature dependency of the voltage-current relationship. They are (1) the positive change in the frequency of the thermal electron emission from the cathode surface to initiate the corona discharge; (2) the positive change in the propagation rate of free electrons in the high electric field region around the wire cathode; (3) the positive change in the ionization rate of the gas molecules; (4) the positive change in the mobility of the ions.

As for the temperature effect on the dissociative electron attachment of O_2, it was reported that the dissociative electron attachment rate increased when the temperature increased. Thus it is logical to consider that the formation of clusters is inhibited by temperature elevation because the ion clusters are thought to be less stable at high temperature condition.

As shown in Table 2.1, past experiments have revealed that many parameters have effect on the removal efficiency such as type of molecules or ions of impurities gas, type of main carrier gas, concentration of gaseous impurities, gas flow rate, and applied voltage and current for corona discharge.

The applicability of the corona-discharge reactor to the removal of various impurities in N_2-O_2 and the removal mechanism are summarized in Table 2.2.

<u>Dissociative electron attachment</u>: Dissociative electron attachment is dominant in the removal of electronegative impurities from N_2-O_2. The observed removal efficiency is not higher than the case of only N_2 because coexisting O_2 consumes electrons. The removal of $C_2F_3Cl_3$ is a typical example. In this case, black particles deposit on the anode. On the other hand, the removal efficiencies of C_6H_6 and p-$C_6H_4Cl_2$ are high. This is because the removal is caused by polycondensation induced by dissociative electron attachment[Tamon et.al., 1998]..

<u>Ozone reaction</u>: Ozone is produced by corona discharge in the air. If impurities react with O_3, the reaction products may be removed by deposition on the anode surface. Sulfur compounds, $C_2F_3Cl_3$, C_6H_6, and p-$C_6H_4Cl_2$ are not removed by O_3 reaction. On the other hand, the O_3 reaction contributes to the removal of I_2,

CH_3I, C_9H_9N, CH_3CHO, and $(CH_3)_3N$. Especially, this effect is dominant in the removal of I_2, C_9H_9N and $(CH_3)_3N$.

Formation of Negative-Ion Clusters: If negative ions induce the formation of clusters with gas molecules, the removal efficiency of impurities will be improved. This effect is significant if one negative ion and many gas molecules constitute a cluster. This effect is important in the removal of sulfur compounds, CH_3CHO, and CH_3I.

Table 2.3 shows the features of deposit obtained on the anode surface during a removal experiment of impurities from N_2-O_2. An analysis of the deposit may be useful to understand the removal mechanism.

Table 2.1. Effect of coexisting oxygen and water vapor with nitrogen on reaction by-products and removal efficiency.

Sample Gas	Experimental conditions [1]				Reaction Byproduct	Removal efficiency								Ref No.
	C_{in} (Sample gas)	C_{O2}	C_{H2O}	SV		Change of removal efficiency when the gas below increases				Maximum efficiency [-]				
	[ppm]	[%]	[ppm]	[hr^{-1}]		C_{in} (in N_2 Only)	O_2	H_2O	O_2 + H_2O	C_{in} (in N_2 Only)	O_2	H_2O	O_2+ H_2O	
SF_6	0.176-298	NI	NI	18.9	NI	↓	NI	NI	NI	A	NI	NI	NI	2,6
H_2S	60	NI	400-1,100	37.8	None	↓	NI	↑	NI	A	NI	A (60ppm)	NI	1,2,6
SO_2	32.7-304	0-18	400-13,000	18.9-37.8	None	↓	↑	↑	↑	C (33ppm)	A	D (122ppm)	A	1,2,6, 12
CS_2	30-65	0-49	300-11,000	18.9-37.8	SO_2 , COS	↓	↑ 5)	↑	↓	A (30ppm)	A	B (48ppm)	A	1,2,6
COS	29-53	0-50	650-10,000	18.9-37.8	SO_2	↓	↑ 5)	↑	NI	B	A	B (53ppm)	NI	1,2,6
CH_3SH	40-69	0-20	1,000-10,000	18.9-37.8	SO_2 , H_2S^* or COS^*	↓	↑	↑	NI	B	A	B (40ppm)	NI	1,2,6
$(CH_3)_2S$	3.88-89	0-22	600-9,100	18.9-52.9	SO_2^{**} , SO_2^{***}	↓	↑	↑	↑	A (4ppm)	A	D (38ppm)	A	1,2,6
CH_3I	75-83	5.6-8.0	5,600-17,800	47.3-50.0	I_2 (in N_2)	↓	↑	↑	↑	C	A	A	A	2,3,4
I_2	40.4-62	0-7	8,500	44-77.9	NI	NI	↑	↓	NI	B 3)	A	A (at I=0)	NI	4,5
$C_2Cl_3F_3$	50-400	0-20	NI	18.9	HCl^* or HF^*	↓	↓	NI	NI	A	A	NI	NI	2,10, 11
CH_3CHO	9.9-35.6	0-20	0-183	80.9	NI	↓	↑	↑	NI	B	A	A	NI	2,7,9, 10
C_9H_9N (skatole)	2.4	0-20	10,000	43.5-189	NI	NI	↑	NI	↑	A	A	NI	A	7
C_6H_6 (benzene)	205-313	29-34	7,500	18.7-28.4	NI	NI	↑	NI	↑	D	A	NI	A	8
p-$C_6H_4Cl_2$ (p-dichloro benzene)	19-57	19-20	NI	20.6-45.5	NI	↓	↑	NI	NI	B	A	NI	NI	8
NH_3	49-143	0-20	3,288-6,418	75.6-189	NI	NI	↑	NI	↑	D	A	NI	A	9,12
$(CH_3)_3N$	58.6-9.4	0-20	NI	58.6-69.4	CH_3CHO, C_2H_5OH, $(CH_3)_2CO$ or CH_3NO_2	NI	↑	NI	NI	D	A	NI	NI	2,9, 12
NO_2	674-747	0-20	NI	75.6	NI	NI	NI	NI	NI	C	NI	NI	NI	9
O_2 4)	1.1-6.3	NI	NI	315-846.3	NI	NI	NI	NI	NI	D 4)	NI	NI	NI	6

Removal efficiency always increases with the discharge current for all of experiment .Unless stated otherwise , the same by-product are observed for the same sample gas.

By-product from observed with coexisting oxygen *

By-product from observed with coexisting water vapor **

By-product from observed with coexisting both oxygen and water vapor***

1) Current , I = 0.05 – 2.0 mA ; Voltage , V = 6.0 - 20.0 kV

2) Removal efficiency ; A > 80% , B 60-80% , C 40-60% ,D< 40 %

3) Removable only with wetted – wall type reactor.

4) Removable only with sweep-out-type type reactor

5) Completed removal at $O_2 > 2\%$

Example for used table : ψ^S for Dimethyl sulfide($(CH_3)_2S$) under the experimental condition decrease with the concentration of Dimethyl sulfide (C_{in}) increase ; ψ^S for Dimethyl sulfide increase with the concentration of O_2 increase ; ψ^S for Dimethyl sulfide increase with the concentration of H_2O increase ; ψ^S for Dimethyl sulfide increase with the concentration of O_2 and H_2O increase

NI not investigated

Table 2.2. Dominant removal mechanism in the presence of O_2

Removal mechanism	Influence of O_2 on removal efficiency	Deposition at anode	Example	Removal efficiency
Reaction with O_3	Increase	Stable	I_2 , CH_3I , C_9H_9N ,CH_3CHO , $(CH_3)_3N$	High
Formation of ion clusters induced by O^-	Increase	Stable	SO_2 , CS_2 , COS , CH_3SH , $(CH_3)_2S$, CH_3CHO , CH_3I	High
Polycondensation by reaction with O^-	Increase	Stable	C_6H_6	High
Polycondensation by dissociative electron attachment	None	Stable	p-$C_6H_4Cl_2$	High
Dissociative electron attachment	Decrease*	Stable	$C_2F_3Cl_3$	Low
Dissociative electron attachment	None	Unstable	F_2 , Cl_3	Low

*Electrons are attached to coexisting oxygen

Table 2.3 Deposit on anode surface in the presence of O_2

Sample gas	Feature of deposit
Sulfur compounds	Solid containing S compound
I_2	Yellow powder (I_4O_9)
CH_3I	Black particles (not identified)
$C_2F_3Cl_3$	Black particles containing F , Cl
C_6H_6 , p-$C_6H_4Cl_2$	Polycyclic aromatic compounds of high boiling point
CH_3CHO	Hard brown coating containing CH_3CHO
$(CH_3)_3N$	Carbon compounds of high boiling point

Reference for table 2.1

1. Tamon, H., Sano, N. and Okazaki, M. " Influence of Oxygen and Water Vapor on Removal of Sulfur Compounds by Electron Attachment," AIChE J., 1996, 42,pp.1481-1486.

2. Tanthapanichakoon, W., Larpsuriyakul, K., Khongprasarnkal, P., Charinpanitkul, T., Tamon, H., and Okazaki, M." Basic Study on the Application of Electron Attachment Reaction to the Treatment of Crematory Emission Gas, " J. National Res. Council of Thailand, 1996, vol 28,pp.282-313.

3. Sano, N., Nagamoto, T., Tamon, H., Suzuki, T. and Okazaki, M." Removal of Methyl Iodide in Gas by Corona-Discharge Reactor," J. Chem. Eng. Japan,1997,vol 30, pp.944-946 .

4. Sano, N., Nagamoto, T., Tamon, H. and Okazaki, M." Removal of Iodine and Methyl Iodide in Gas by Wetted-Wall Reactor Based on Selective Electron Attachment," J. Chem. Eng. Japan, 1996, 29, pp.59-64.

5. Sano, N., Tamon, H. and Okazaki, M." Removal of Iodine in Gas by Corona-Discharge Reactor," J. Chem. Eng. Japan, 1996, 29,pp.59-64.

6. Tamon H., Mizota, H., Sano, N., Schulze, S. and Okazaki, M." New Concept of Gas Purification by Electron Attachment," AIChE J., 1995, 41, pp.1701-1711.

7. Sano, N., Nagamoto, T., Tamon, H., Suzuki, T. and Okazaki, M." Removal of Acetaldehyde and Skatole in Gas by Corona-Discharge," Ind. Eng. Chem. Res., 1997b, 36, pp.3783-3791.

8. Tamon, H., Imanaka, H., Sano, N., Okazaki, M. and Tanthapanichakoon, W.” Removal of Aromatic Compounds in Gas by Electron Attachment,“ Ind. Eng. Chem. Res., 1998, 37, pp.2770-2774.

9. Tanthapanichakoon, W., Larpsuriyakul, K., Charinpanitkul, T., Sano, N., Tamon, H. and Okazaki, M. “ Effect of structure of corona-discharge reactor on removal of dilute gaseous pollutants using selective electron attachment,” J. Chem. Eng. Japan, 1998,vol 31 , pp.7-13

10. Sano ,N.,Tamon ,H and Okazaki , M. “Removal of Chlorofluorocarbon ,1,1,2-Trichloro-1,2,2-Trifluoroethane , in Gas by a Corona-Discharge Reactor,” Ind. Eng. Chem. Res., 1998, 37, pp.1428-1434.

11. Massey, S. H. Negative Ions. Cambridge Univ. Press, Cambridge, England, 1976.

12. Massey, S. H. Atomic and Molecular Collisions. Taylor & Francis, London, 1979.

13. Han S. Uhm et al. “ Influence of chamber temperature on properties of the corona discharge system ” Physics of Plasma , 1999 , 2 , 623-626.

14. Tanthapanichakoon, W., Tamon, H., Khongphasarnkaln , P., Sano, N., Charinpanitkul, T., and Okazaki, M. “ Removal of Trimethylamine and Ammonia Using Electron Attachment Reaction,” Journal of the Science Society of Thailand (Science Asia)., 1999 ,1 ,pp. 57-63.

CHAPTER III

LITERATURE REVIEW

Gas purification involves the removal of vapor-phase impurities from a gas stream. Many methods for gas purification have been proposed, and the primary operation falls into one of the following three categories; 1) absorption into a liquid, 2) adsorption on a porous solid, 3) chemical conversion to another compound. In fact many research works to improve these processes are still going on.

Gas discharge technology is one promising method of achieving ultrahigh purification. Application of gas discharge processes with high-energy electrons has existed for over a hundred years, dating to the first electrostatic precipitator of Lodge (Oglesby and Nichols, 1978) and ozonizer of Simens (Horvath, 1980). The electrostatic precipitator (ESP) is a device-utilizing corona discharge for removing particulate pollutants in the form of either a solid (dust or fumes) or a liquid (mist) from a gas using the electrostatic force. One may realize that the corona-discharge reactor for the gaseous pollutant remover used in this work has the same working principle as ESP. Most information on ESP however focuses on the removal of particulate matter, whereas the reactor proposed in this work, utilizing low-energy electrons in gas discharge to induce electron attachment reaction, aims at separating gaseous impurities from a gas stream. Application of the electron attachment (a reaction of low-energy electrons and gas molecules to produce negative ions), first proposed by Tamon et al. (1989), is still innovative for gas seperation processes nowadays.

Many publications on electron attachment and other reactions of electron with many kinds of gas molecules have appeared but most of them involve only the reaction kinetics (Moruzzi and Phelps, 1966, Caledonia, 1975 and Massay, 1976). In fact basic information on gas purification using electron attachment and the proposed use of the selectivity of electron to remove the electronegative gaseous molecules are still scarce.

Applications of gas discharge technology conducted to date are reviewed as follows.

Castle, Inculet, and Burgess (1969) discussed briefly about surface oxidation of discharge electrodes used in a wire-tube electrostatic precipitator. The rate of ozone generation in the precipitator with both stainless steel and copper wires was clarified. The reaction rate of ozone depended on the intensity of electron flux through the gas. The concentration of ozone generated was a linear function of current but decreased as the gas temperature increased.

Dorsey and Davidson (1994) reported an assessment of the contribution of contaminated wires and plates to ozone production in electrostatic air cleaners. It was found that runaway ozone generation due to contamination of electrode surfaces was a limiting factor in the long-term (7 weeks) effectiveness of electrostatic air cleaners. The corona discharge degraded to streamers after only two weeks, causing increased ozone levels. Wire contamination alone can increase ozone generation. These findings have serious implications for the safe operation of electrostatic air cleaners.

Chemical Vapor Decomposition (CVD) occurring on a discharge wire of an electrostatic air cleaner causes the corona current to decrease more than 95% at the same voltage (after 180 hrs operation). This phenomenon was shown by Jan H. Davidson et al. (1998). Neither current drop nor deposition occurred when operated with clean or dry air (after 2 days).

Tamaki et al. (1979) reported the use of DC and AC coronas for the removal of NO from a flue gas under several discharge conditions. However, the process was energywise inefficient, and the performance was poor. The poor performance was probably due to the small ionization region of DC coronas (small active treatment volume), and the power efficiency was low because a large amount of energy was expended on ion migration, which did not contribute to the production of radicals.

Several types of DC energized point-electrode reactors have been developed and tested for gas chemistry applications. Although designed with different purposes in mind, the configurations could be put to other uses.

Castle, Kanter, Lee, and Kline (1984) tested a narrow-gap, multipoint-to-plane geometry device in which the gas passed through a corona discharge at high velocity (approximately 100 m/s). The upper multipoint electrode (cathode) was separated from the lower flat electrode (anode) by acrylic spacers that electrically isolated the electrodes and allowed visual observation of the corona. The narrow gap spacing ensured that the inter-electrode space was filled with corona induced plasma. However, the lateral spacing of the pins allowed major fractions of the gas flow to bypass the corona zones. A DC current was applied to the multipoint pins through current limiting resistors.

Another type of a multipoint-to-plane device was constructed by Yamamoto, Lawless, and Sparks (1988, 1989). This device was in the form of a narrow-gap, triangle-shaped, DC corona discharge device. The design was intended to reduce the electrical sneakage (bypassing of the corona induced plasma) which was the major problem for the device with multipoint-to-plane geometry. The volumetric filling factor of the corona induced plasma in this device was much higher than in the typical multipoint device.

An experimental investigation has been conducted by Chang, Jen-Shih et al. (1988) to obtain electrode surface temperature profiles of cylindrical hollow electrodes under corona discharges. The result show that a slight temperature increases (about 5 Kelvin within the 10 W input for discharge power level) occurs near the edge of the cylindrical hollow electrodes. Thus, the corona discharge still can be categorized as a cold discharge region.

The pulsed electron technology has also been shown to be capable of generating ozone and active radicals and decomposing several unwanted gases as well as aerosol particles.

Higashi, Sugaya, and Ueki (1985) and Weiss (1985) conducted the reduction of CO_2 the in exhaust gas from a diesel engine vehicle. It was shown that CO_2 concentration in a N_2-CO_2 or even pure CO_2 gas could be reduced by DC and pulsed corona discharges, respectively. Further experiments for soot elimination and NO_x and SO_x reduction in a diesel-engine exhaust by a combination of discharge plasma and oil dynamics have been investigated by Higashi, Uchida, Suzuki, and Fujii (1991, 1992).

Chang (1989) and Chakrabarti et al. (1995) found that the removal of NO_x, SO_x, and aerosol particles could be achieved when NH_3 or H_2O was introduced into a pulsed streamer corona reactor. The pulsed electrons have been shown to cause reactions between oxidizing radicals such as OH, O, and O_3 on the one hand and NO_x and SO_x on the other hand at the concentrations found in flue gases to form several acidic aerosol particles with NH_3 or H_2O injections.

Recent experimental study done by Helfritch (1993) led to the conclusion that H_2S decomposition to hydrogen and sulfur could be directly achieved electronically. A wire-in-tube pulsed corona reactor was energized by short voltage spikes to decompose small concentrations of H_2S contained in nitrogen. Some parameters including the reactor geometry, H_2S concentration, corona power, and the nature of the products were investigated.

Mizuno, Clements, and Davis (1986) compared the performance of the pulsed streamer corona, DC corona, and electron-beam processes. It was found that a pulsed streamer corona discharge produced the radicals instead of a high-energy electron beam. A positive pulsed streamer corona discharge in a nonuniform electrode geometry showed better energy efficiency and higher removal performance than a DC corona discharge. Based on the delivered power, the pulsed streamer corona process removed more than 90% of SO_2 with at least two times better power efficiency than the energetic electron-beam process.

Masuda, Sato, and Seki (1984) developed a high-efficiency ozonizer using traveling wave pulse voltage. The test results relating to the pulse-induced ozone generation showed a great enhancing effect on the speed of reactions by positive pulse corona producing streamers bridging across the entire electrode gap. It was believed that the ozone generated in a corona discharge was a two step process: generation of oxygen free radicals by ionic processes and generation of ozone by free radical reactions. It was found that the ozone generation processes were substantially reduced by increasing the gas temperature, while the ozone loss processes were significantly enhanced by increasing the gas temperature. It was therefore recommended to operate an ozonizer in lower temperature conditions.

High-voltage pulser was used in a pulse-induced plasma chemical processing unit (PPCP unit). This pulser comprised a synchronous rotary spark gap that produced a very sharp negative pulse voltage. High electron energies could be achieved by both units since higher electric fields were allowed in surface-corona and pulse-corona systems than in direct-current systems because of the breakdown limits of the discharge.

Eliasson, Hirth, and Kogelschatz (1987) applied a dielectric-barrier discharge for ozone generation from oxygen. The resulting efficiency of the generation was reported. A value of 1200 g/kWh was the theoretical ozone generation efficiency calculated by thermochemical theory. He also estimated the maximum ozone generation efficiency of 400 g/kWh for pure oxygen by analyzing a Boltzmann equation. The actual ozone generation efficiency was approximately 200 g/kWh for pure oxygen, which was very low compared to the theoretical values. It was because the discharge energy was consumed not only in producing the ozone but was also dissipated in heating the test gas and the electrodes of the ozonizer. Also some of the ozone produced was destroyed by the heat.

After the work of Eliasson et al., there has been attempt to improve the ozone generation efficiency. Ito, Ehara, Sakai, and Miyata (1990) reported that the efficiency in the silent discharge showed a rise of 3-6% by the radiation of ultra-violet ray from the discharge in nitrogen gas. Later, Hattori, Ito, Ehara, and Miyata (1992) reported the superposition effect of two types of discharge in the same discharge space, silent and surface discharges, on ozone generation. Their ozonizer had two power sources with a variable-phase shifter. A 22-30% increase in the efficiency was observed in their ozonizer.

A packed ferroelectric (high-dielectric ceramic) pellet layer used for an electrostatic precipitator was originally developed by Mizuno (1986). Basic performance of the AC energized ferroelectric packed-bed reactor was studied. The effect of the dielectric constant of the packed ferroelectric pellets on the particle collection efficiency was also investigated. In the operation to collect precharged particles, the particle penetration became minimum at a certain voltage V_{aco} and increased when the applied voltage exceeded V_{aco}. The value of V_{aco} became lower with the increase in the dielectric constant value. V_{aco} was always higher than the initiation voltage of partial discharge for all the pellets tested.

Later in 1988, Mizuno and Ito started to apply a packed bed reactor with ferroelectric $BaTiO_3$ pellets to decompose ammonia from dry air. The reactor employed the AC discharge generated inside a pellet layer held within the tube arrangement by two mesh electrodes. An intense electric field was formed around each dielectric pellet contact point, producing high energy free electrons as well as molecular ions throughout the cross section of the reactor.

Yamamoto et al. (1992) constructed a laboratory-scale plasma reactor with a packed ferroelectric (high-dielectric-ceramic) pellet layer and a nanosecond pulsed corona reactor. This study was the first attempt to develop baseline engineering data on the application of these plasma reactors to the destruction of various volatile organic compounds (VOC's) at ppm levels. The conversion rate of VOC's was found to be dependent on the electron energies in the reactor and may also be related to how strongly halogen species were bonded to the carbon.

Mizuno, Chakrabarti, and Okazaki (1993) was the first group that developed the combination of corona and catalyst technology. They reported a corona/catalyst arrangement, which consisted of a needle and a grounded mesh electrode with 40-mm separation. Immediately after the corona section, the 20-mm thick catalyst layer consisting of Al_2O_3 pellets was held in place by the screen. Gas was exposed to the pulsed corona, immediately followed by the catalyst. This was considered a two-stage process.

Yamamoto et al.(1996) demonstrated a new concept--single-stage, catalysis-assisted packed-bed plasma technology, to decompose CCl_4, one of the ozone-depleting substances. The objective of the concept was twofold: to enhance the decomposition efficiency catalytically, and to selectively reduce the by-products. Either $BaTiO_3$ or $SrTiO_3$ pellets were packed in the ferroelectric packed-bed reactor employing an AC power supply. The configuration employed a unique one-stage catalysis/plasma process in which the $BaTiO_3$ pellets were coated or impregnated by active catalysts such as Co, Cu, Cr, Ni, and V. Enhancement of the CCl_4 destruction and the conversion of by-product CO to CO_2 were demonstrated using Ni catalyst in the one-stage plasma reactor.

The so-called non-thermal plasma including corona discharge has been widely studied

A non-thermal plasma chemical process with an AC powered ferroelectric packed-bed reactor was again tested by Zhang, Yamamoto, and Bundy (1996). In this work, the targeted gases to be decomposed were ammonia and odorous compounds gathered from animal houses. The plasma reactor packed with $BaTiO_3$ pellets produced high energy free electrons and radicals, which in turn, decomposed the targeted compounds. Four important parameters affecting the reactor performance were investigated: gas residence time, power voltage, power frequency and initial ammonia concentration.

Tamon, Sano, and Okazaki (1989) proposed a novel method of gas separation based on electron attachment. Two kinds of separation devices using either photocathode or glow discharge as electron source were constructed. They reported high efficiency for the removal from nitrogen of SF_6 at very low concentrations. Recently, Tamon et al. (1995) used two types of corona-discharge reactors, deposition-type and sweep-out-type reactors, to remove from nitrogen dilute sulfur compounds, dilute iodine and oxygen. They also discussed the purification mechanism and presented simulation models for predicting the removal efficiency. Subsequently, Tamon, Sano, and Okazaki (1996) investigated the influence of coexisting oxygen and water vapor on the removal of six sulfur compounds from nitrogen. They discovered that the presence of oxygen and water vapor increased the removal efficiency.

Sano et al. (1996) used a new type of corona-discharge reactor, the wetted-wall reactor, and the conventional deposition-type reactor to remove iodine and methyl iodide from nitrogen. The removal mechanism of I_2 and CH_3I in the reactor was also discussed.

Kittisak Larpsuriyakul et al. (1996) and Wiwut Tanthapanichakoon et al. (1996) reported experimental results regarding the influence of the structure of the corona-discharge reactor on the removal of dilute gases. The effects of the reactor structure, namely the cathode diameter, the anode shape, and the number of cathodes, were investigated. The results revealed that the thicker the cathode diameter, the higher the removal efficiency. In contrast, the smaller the reactor diameter among three equivolume reactors, the higher the removal efficiency. As for the number of cathodes in a single reactor vessel, the single-cathode reactor always exhibited a higher removal efficiency than the 5-cathode one.

Paisarn Khongphasarnkaln (1997) investigated the application of electron attachment to the removal of dilute gaseous pollutants using a corona-discharge deposition-type reactor. It has been found that the presence of O_2 enhanced the removal efficiency of each impurity gas. The enhancement was experimentally shown to be attributable to the ozone reaction in the removal of $(CH_3)_3N$ from O_2-N_2 mixed gas. Water vapor also enhanced the removal efficiency of $(CH_3)_3N$ and CH_3CHO. Furthermore, The high selectivity of electron attachment to electronegative gas molecules was utilized in the simultaneous removal of dilute $(CH_3)_3N$-CH_3CHO, NH_3-CH_3CHO, SO_2-$(CH_3)_3N$, SO_2-CH_3CHO, NO_2-CH_3CHO

and CO_2-CH_3CHO from the air in the single reactor. Compared to single impurity removal, it has been shown that the presence of SO_2 enhanced the removal efficiency but retarded that of CH_3CHO in the single reactor. Some reaction by-products generated could be avoided by using two independently operated reactors in series. In the case of coexisting of NO_2, it was noted that the lower the inlet NO_2 concentration, the lower the discharge current that still yielded beneficial effect. At higher discharge currents, the retarding effect of CO_2 on CH_3CHO removal was obviously significant.

Han S. Uhm (1998) investigated the influence of the chamber temperature on the properties of the corona discharge system. It was found that the critical voltage V_c required for the corona discharge breakdown was inversely proportional to the chamber temperature T. The electrical energy w_c required for corona discharge breakdown was inversely proportional to the square of the chamber temperature T. Thus, the electrical energy consumption for the corona discharge system decreased significantly as the temperature increased. The plasma generation by corona discharge in a hot chamber was much more efficient than that in a cold chamber.

CHAPTER IV

EXPERIMENTAL

4.1 Test Materials and Chemicals

Table 4.1 shows the details of test materials and chemicals in the experiments.

Table 4.1 The specifications of test materials and chemicals

Type	Use	Company	Purity / Grade
Styrene(l)	For preparing styrene vapor (500 ppm)	Fluka	99% (100-42-5)
Styrene(g)	Sample gas	BIG*	Styrene 200 ppm balanced with N_2
Ammonia(g)	Sample gas	TIG	NH_3 500 ppm balanced with N_2
Distilled Water	For preparing water vapor	-	-
Oxygen	Coexisting gas	TIG**	Industrial grade
Nitrogen (g)	Carrier and diluent gas to reactor	TIG	UHP 99.999 % min
Nitrogen (g)	Carrier gas for GC (FID detector)	TIG	HP 99.99 % min
Hydrogen	For flame ignition	TIG	HP, 99.99%
Air Zero	For flame ignition	TIG	N/A
Helium	Carrier gas for GC (TCD detector)	TIG	HP, 99.99%

*Bangkok Industrial Gases Co., Ltd. ** Thai Industrial Gases Co., Ltd.

4.2 Experimental setup

Figure 4.1 shows the actual arrangement of the experimental apparatus of the gaseous pollutant remover used in the present work. Figure 4.2 presents its schematic diagram.

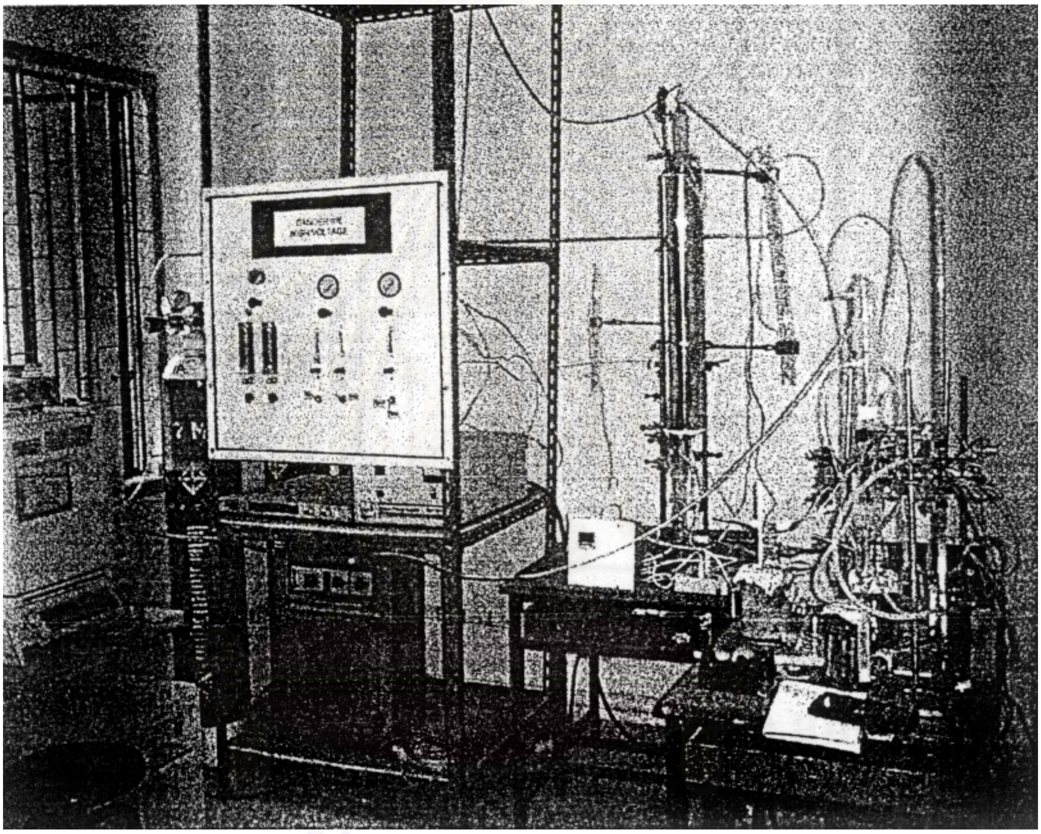

Figure 4.1 Arrangement of present experimental apparatus

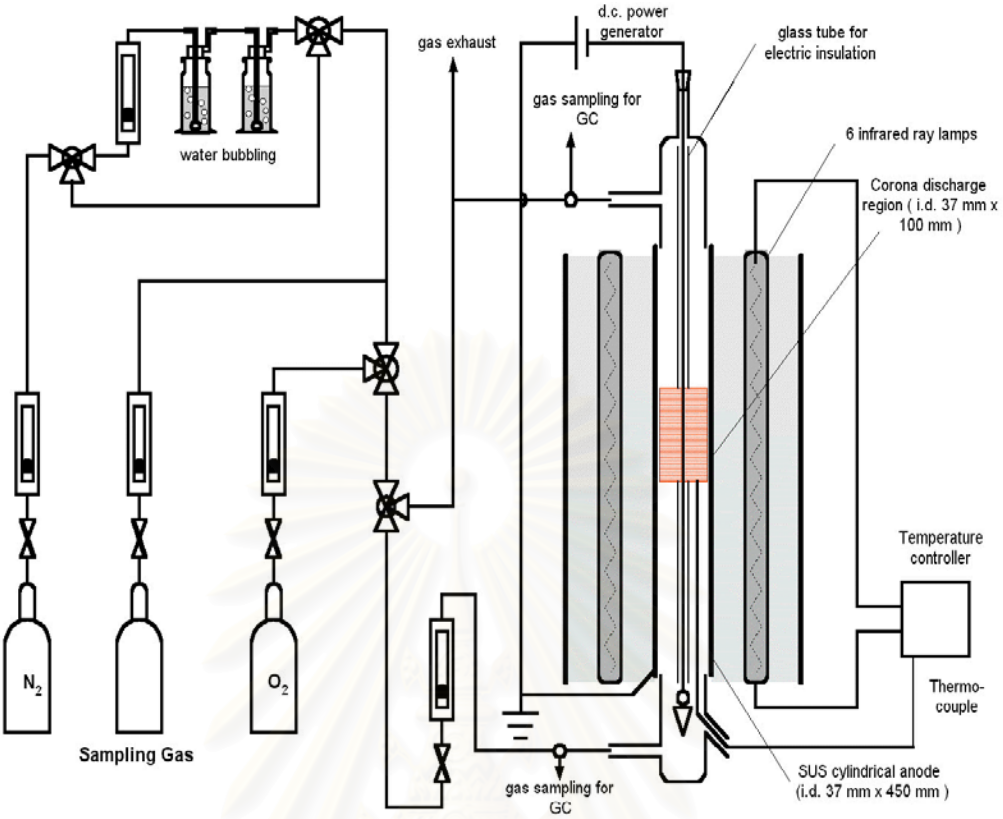

Figure 4.2 Schematic diagram of experimental apparatus

4.2.1 Details of the experimental apparatus

Figure 4.1 and 4.2 show the photograph and the schematic diagram of the experimental setup that consists of a deposition-type corona-discharge reactor, a test gas mixing system, a high-voltage DC generator, a cooling water bath, a temperature controller and a soap film flow meter. The present deposition-type corona-discharge reactor consists of a SUS pipe, 3.7 cm. inner diameter and 80 cm. length, as the anode. The cathode is a stainless-steel wire suspended from a silicone plug at the top of the reactor and straightened along the axis of the anode by a weight. A high-voltage DC generator (Matsusada, HAR-30N5) is connected to the cathode. The high-voltage DC generator whose maximum allowable voltage is 50 kV is utilized to supply a steady stream of energetic electrons to the corona-discharge reactor.

A slim pyrex glass tube is used to cover either end of the cathode in order to limit the corona discharge zone in the middle section of the reactor to 10 cm and the diameter of the cathode wire is 0.5 mm. The discharge zone is restricted to the mid-section of the reactor to achieve a uniform axial temperature distribution within the zone. A type-K thermocouple is inserted into the reactor to measure the gas temperature in the corona discharge zone. To control the reactor temperature, 6-infrared heating lamps (200V, 700W each) are installed lengthwise around the outside perimeter of the reactor. The temperature control unit consists of a temperature controller (FENWAL, AR-24L) and a thyrister power regulator (Shimaden, PAC15C003081-NO). Feed gas mixture with the desired concentration is prepared. To study the influence of water vapor on the removal efficiency, the desired concentration of water vapor is achieved by bubbling nitrogen gas through distilled water in the bottle placed in a temperature–controlled bath.

Figure 4.3 Deposition-type corona discharge reactor

Figure 4.4 High-voltage DC generator

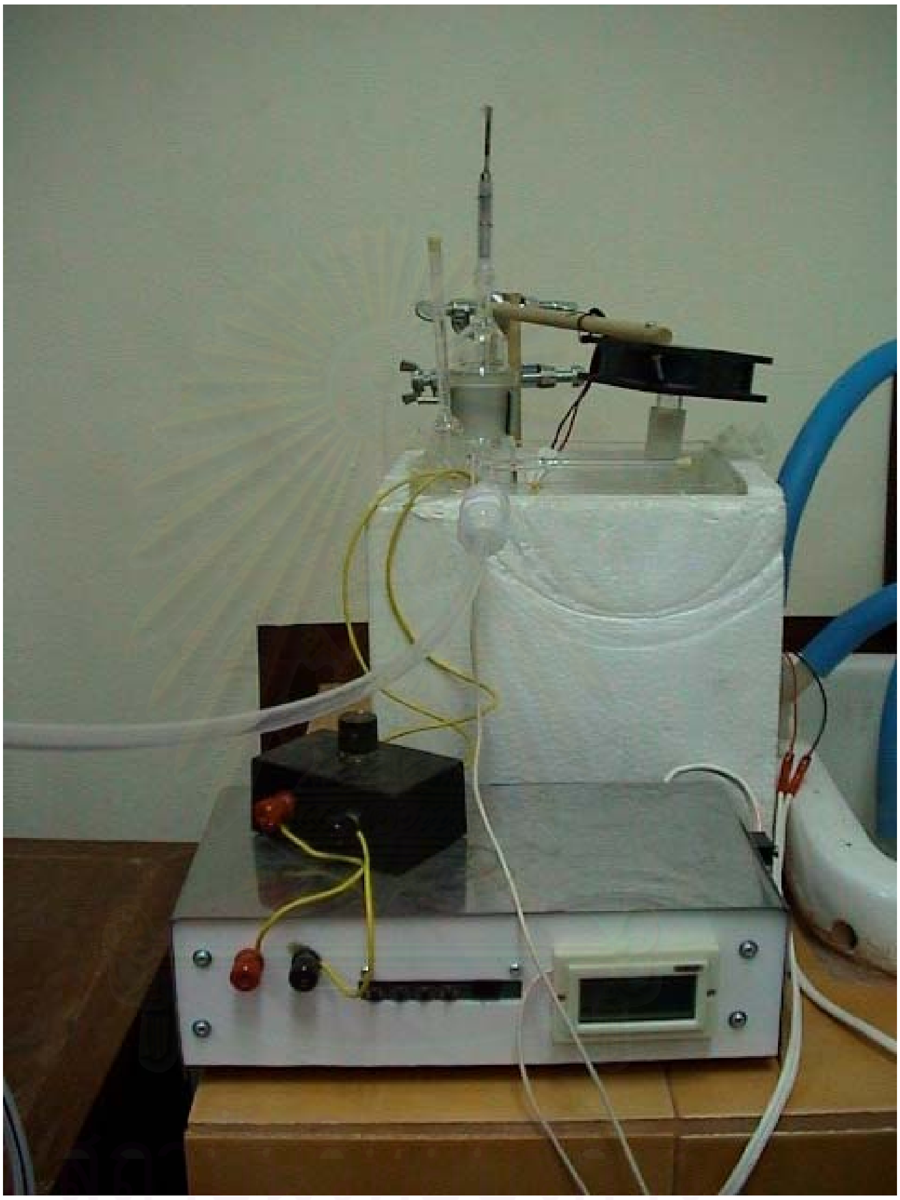

Figure 4.5 Cold water bath

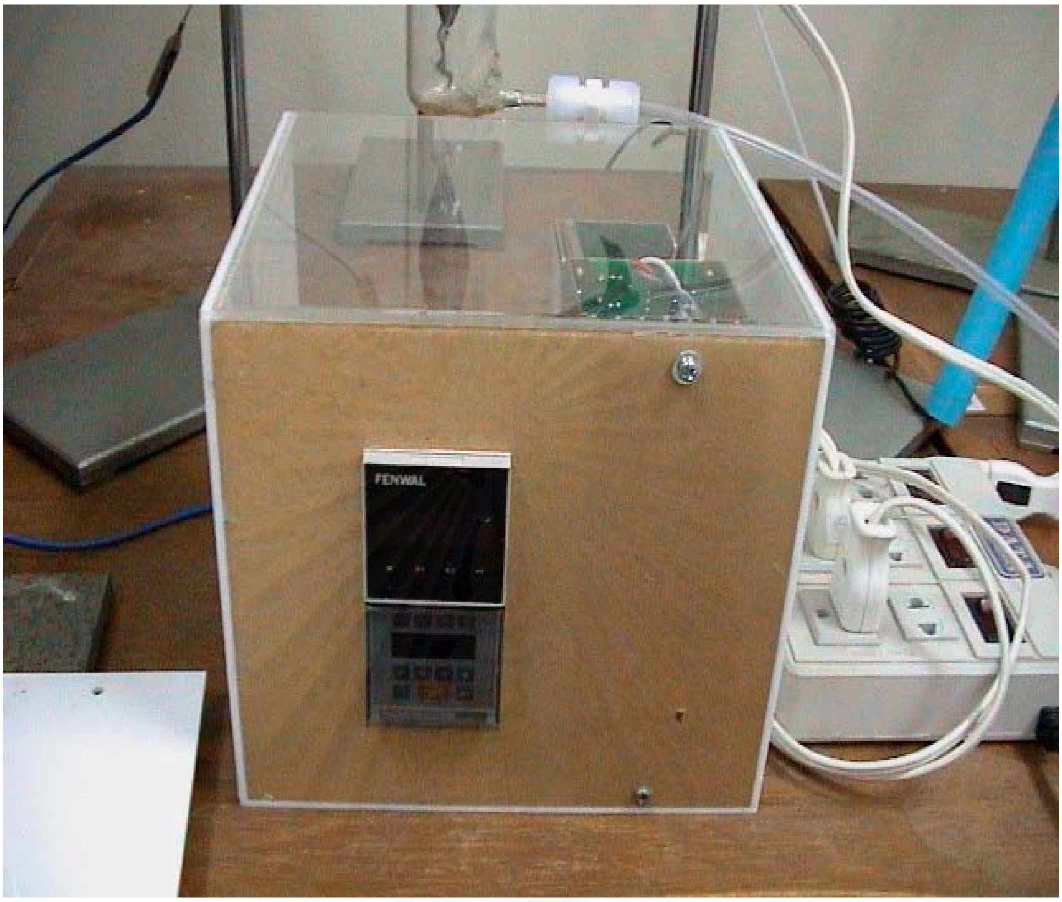

Figure 4.6 Temperature control unit

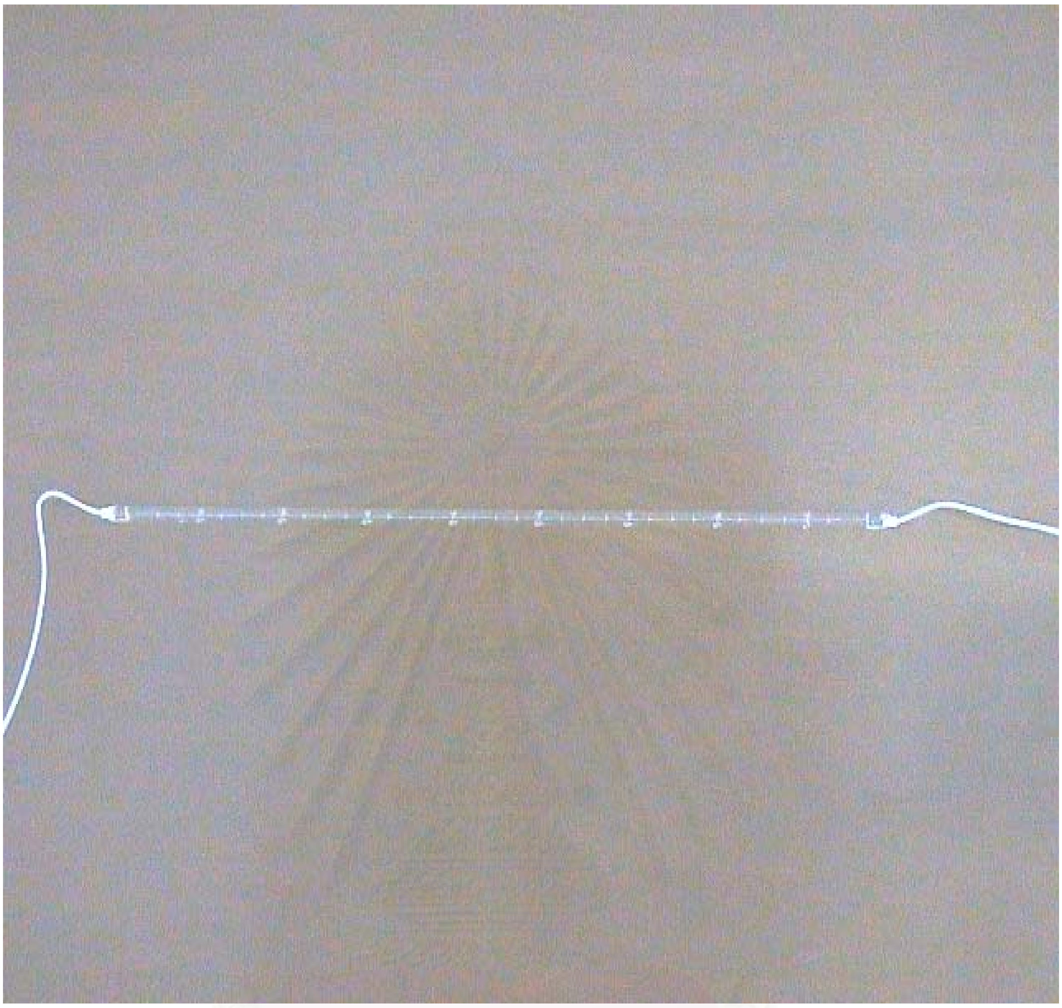

Figure 4.7 Infrared lamp

4.2.2 Analytical Instrument

Inlet and outlet concentrations of styrene are analyzed using a gas chromatograph (Shimadzu Corp., GC 9A) equipped with a flame ionization detector (FID). The packed material in the GC column used for detecting the concentration of styrene is PEG-20M Uniport B (GL Science Inc.) with 60/80 mesh size and usable at maximum temperature of 230ºC. A calibration curve between the FID peak area of the GC and the concentration of styrene is obtained as shown in the Appendix A.

Figure 4.8 FID-Gas chromatograph

Another gas chromatograph (Shimadzu Corp., GC 14A) with a thermal conductivity detector (TCD) is used to analyze the concentration of ammonia. The packed material in the GC column is Chromosorb 103 with 80/100 mesh size and the usable maximum temperature is 230ºC. A calibration curve between the TCD peak area of the GC and the concentration of ammonia is obtained as shown in the Appendix A. Table 4.2 shows the operating conditions of both GC units.

Figure 4.9 TCD-Gas chromatograph

The concentrations of O_3 and NO_x can separately be detected with gas detector tubes. Gas detector tubes from GASTEC Co., Ltd. and Kitagawa Co., Ltd. are used with the desired different range of concentration. Ammonia can be detected by detector tubes too.

Figure 4.10 Gas detector tube

Table4.2 Operating conditions of both GC units.

Sample Gas	Column Temp. (ºC)	Injection Temp. (ºC)	Detector Temp. (ºC)	Retention time (min)
Styrene	120	200	200	4.2
NH_3	50	120	130	3.0

4.3 Experimental Procedure

To carry out the gaseous pollutant removal experiments, the following implementation steps must be carried out carefully because of the high risk of physical injury caused by the high voltage supplied to the reactor.

a. Ensure that the reactor is securely grounded and each unit of the experimental apparatus is also securely connected.
b. Check the gas line for the experiment (feed gas balance nitrogen, O_2 and N_2 for water bubbling)
c. Mix the above streams in the gas mixing device and measure the total flow rate with the soap film flow meter.
d. Feed the gas mixture to the inlet of the reactor and wait until its inlet and outlet concentrations become stable at the reactor temperature of interest.
e. Take gas samples at the reactor inlet and outlet to analyze their concentrations during blank test (zero discharge current).
f. Turn on the high-voltage DC generator, adjust the discharge current as desired, and then keep the current stable throughout each experimental run.
g. Take gas samples at the inlet and outlet of the reactor and analyze their concentrations. Shut off the current after the finish of the experimental run.

h. To study the effect of the reactor temperature, reset the temperature as desired and wait until it becomes stable. Return to step (e) until all reactor temperatures have been investigated.
i. Wait for the reactor temperature to cool down sufficiently, stop the flow of the gas mixture and turn off the DC generator after the completion of the experiment. Be careful that high voltage does not remain in the reactor.

4.4 Experimental Conditions

Table 4.3 Summary of the experimental conditions in the present study.

Gas	Conc. (ppm)	Current (mA)	N_2	N_2-O_2(%)	N_2-H_2O(ppm)	N_2-O_2(%)-H2O(ppm)
Styrene	500	0.50	O(10.0)	very high efficiency	very high efficiency	X
		0.10	unstable	5(11.0)	4050(10.0),13320(10.5),21838(10.3)*	X
		0.05	unstable	5(10.4), 20(10.1), 25(9.8)*;**	unstable	5%:4050(10.2)*,12940(10.7)*,23028(10.2)* 10%:4050(10.1)*, 12940(10.3)*,23028(10.1)* 20% :4050(10.3)*,12940(10.4)*,23028(10.1)*
	100	0.50	O(11.0)	very high efficiency	X	X
	40	0.50	O(10.3)	very high efficiency	X	X
	40	0.10	unstable	5(11.9)	unstable	X
NH_3	400	0.50	O(7.6)	very high efficiency	very high efficiency	can not prepare feed mixture
		0.05	unstable	5(10.3), 10(10.3), 20(10.5)**	unstable	can not prepare feed mixture
	250	0.30	O(8.1)	5(13.1)	5250(8.7), 10500(8.3), 23028(8.7)	5% : 5250(8.2), 10500(12.9)** 10% : 5250(13.0)**, 10500(13.0)** 20% : 5250(13.2), 10500(13.4)
	200	0.10	unstable	5(11.4)	unstable	X
NH_3-Styrene	200-40	0.30	O(9.0)	5(13.6)**,10(13.2)**, 20(13.4)**	5250(9.8)	X
		0.10	unstable	5**(11.5),20(12.1)**	unstable	5% : 5250(11.3)**, 10500(11.1)** 20% : 10500(11.6)**, 24344(11.6)**
	100-40	0.10	unstable	5(11.5)**	unstable	X
	200-80	0.30	O(10.0)	very high efficiency	5250(10.5)	X
		0.10	unstable	5(11.7)	unstable	5% : 5250(11.6), 10500(11.8)

* CO2 detected , ** NOx detected

CHAPTER V

RESULTS AND DISCUSSION

5.1 Data analysis

This section will describe the various definitions of the removal efficiency.

5.1.1 Apparent removal efficiency

$$\psi = \frac{(C_{in} - C_{out,anymA})}{C_{in}} \quad [-] \qquad (5.1)$$

5.1.2 Removal efficiency (by discharge effect only)

$$\psi' = \frac{(C_{out,0\,mA} - C_{out\ at\ any\ mA})}{C_{out,0\,mA}} \quad [-] \qquad (5.2)$$

This removal efficiency excludes from the above ψ any adsorption effect inside the reactor in the absence of corona discharge and thus represents the pure corona discharge effect.

5.1.3 Removal efficiency per unit residence time

$$\psi'' = \frac{\psi' \times residence\ \ time\ \ at\ 25\ {}^{0}C}{residence\ \ time\ \ at\ T\ {}^{0}C}$$

$$= \frac{\dfrac{(C_{out\ at\ 0\ mA} - C_{out\ at\ any\ mA})}{C_{out\ at\ 0\ mA}} \times residence\ \ time\ \ at\ 25\ {}^{0}C}{residence\ \ time\ \ at\ T\ {}^{0}C} \qquad (5.3)$$

At steady state, the equation of continuity requires that $\rho_1\langle\upsilon_1\rangle A_1 = \rho_2\langle\upsilon_2\rangle A_2$. Since $A_1 = A_2$ and ρ is a function of the gas temperature, the gas velocity at temperature T_2 will be faster than its velocity at room temperature T_1. Thus the mean residence time $\theta_2 = \frac{V}{\langle\upsilon_2\rangle}$ of this gas at T_2 will less than $\theta_1 = \frac{V}{\langle\upsilon_1\rangle}$ at room temperature. Here V is the effective volume of the corona discharge reactor. The removal efficiency per unit residence time is defined so as to take into account the effect of shortened residence time on the observed removal efficiency as the reactor temperature is increased.

5.2 Blank tests for the investigation of the effect of temperature on styrene and/or ammonia removal

The experimental results in the Appendix D - G show the results of the blank tests carried out to investigate the temperature effect on styrene and/or ammonia removal. Here the concentration of either styrene or ammonia at the reactor outlet was measured at various temperatures in the absence of the discharge current. There appeared a significant concentration drop at 35^{o}C, which is considered to be due to physical adsorption inside the reactor. As expected, the effect of adsorption inside the reactor gradually decreased as the reactor temperature increased until 200^{o}C. However, at 300^{o}C, the outlet concentration of styrene again decreased. The reverse effect at this highest temperature may be attributed to the thermal decomposition of styrene. In contrast, the outlet concentration of ammonia continued to gradually increase without any effect from thermal decomposition. In both cases, physical adsorption should be insignificant when the temperature was very high. Figure 5.1 shows the results of a blank test on the adsorption of styrene from N_2 stream inside the reactor at room temperature. Figure 5.2 shows the results of a blank test on the desorption of styrene into N_2 stream after the adsorption test at room temperature. From figures 5.1 and 5.2, it is obvious that significant adsorption and desorption of styrene do occur inside the electron attachment reactor even without any application of the corona discharge. In order to exclude the effect of adsorption and/or.

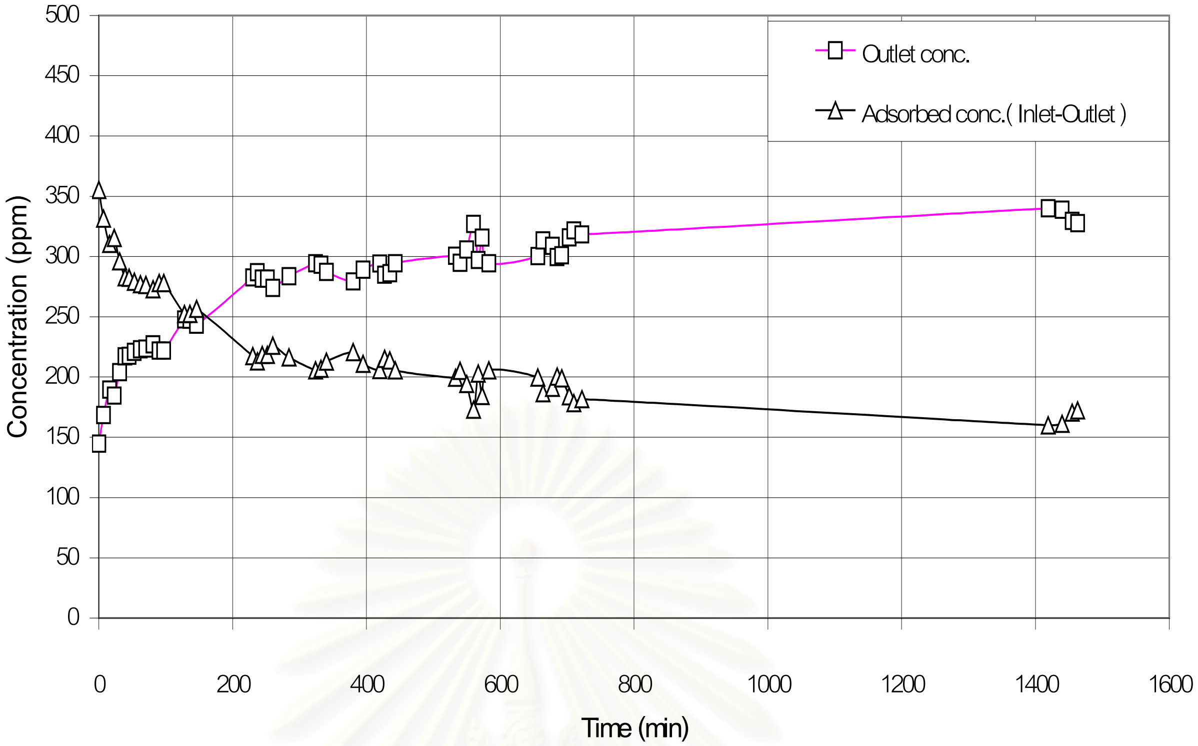

Figure 5.1 Blank test on adsorbtion of styrene from N_2 stream inside the reactor ($C_{styrene}$ = 500 ppm, SV = 55.8 hr^{-1} at room temperature)

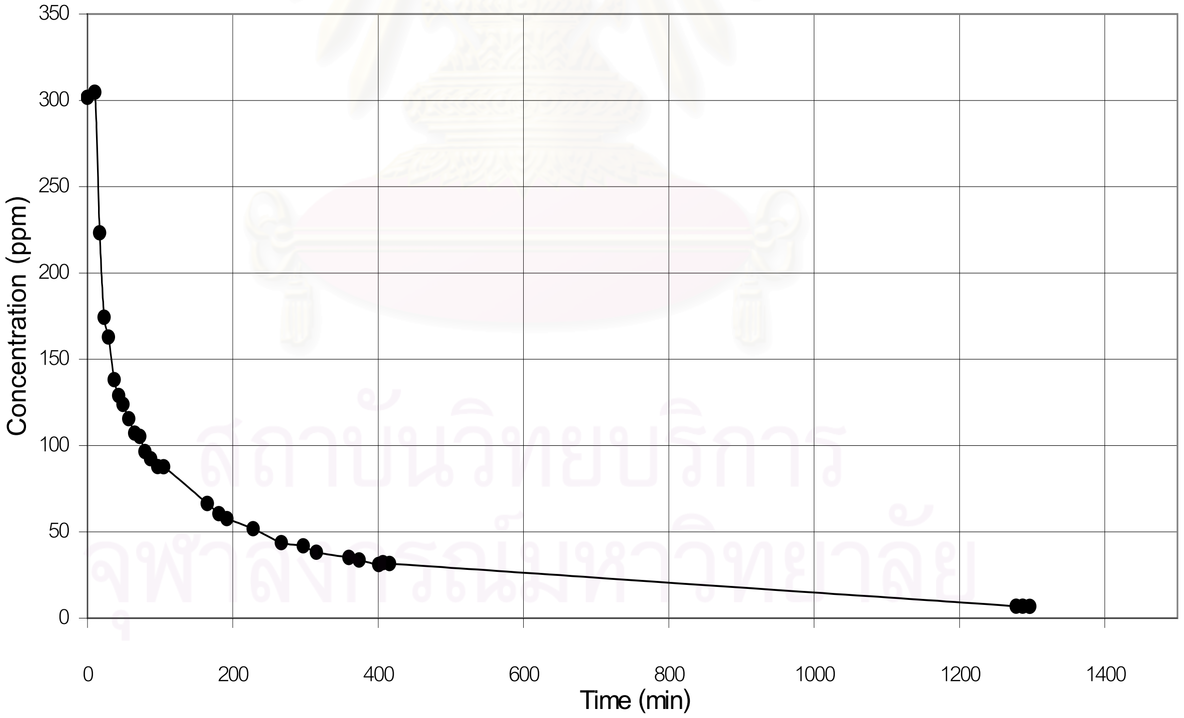

Figure 5.2 Blank test on desorption of styrene into N_2 stream inside the reactor (SV = 55.8 hr^{-1} at room temperature)

desorption on the observed experimental removal efficiency, it is necessary to calculate the removal efficiency ψ' as defined in equation (5.2). In addition, it is crucial to wait until the outlet concentration of the target gas has reached its steady state before obtaining the removal efficiency ψ'.

The obtained experimental data and their analysis are given in details in Appendices D-G. What follows is a discussion of the experimental results.

5.3 Effect of temperature on required voltage to generate corona discharge

The effect of the reactor temperature on the required voltage to generate corona discharge is investigated by supplying either N_2 or N_2-O_2(5%) through the corona-discharge reactor. As shown in Tables 5.1 and 5.2, the reasons for the lower voltage required at a higher temperature are as follows: 1) at the same current, the required voltage is decreased upon increasing the temperature because of the reduced gas density; 2) electrons can be emitted more easily from the cathode at a higher temperature, 3) the rate of the electron propagation process toward the anode $(A+e\rightarrow A^{+}+e+e)$ may increase as the temperature increases, and 4) electron detachment from an electronegative molecule becomes more frequent at

Table 5.1 Relationship between voltage and current from N_2 100 cc/min

Temperature (^{0}C)	Current , mA				
	0.10	0.20	0.30	0.40	0.50
	Voltage , kV				
35	7.5-7.6	9.2	9.2	9.2	9.4
100	7.0-7.1	8.2-8.3	8.2	8.2	8.9
150	6.3-6.5	6.7-6.8	unstable	unstable	6.7
200	4.0-5.4	5.0-5.1	5.4-5.5	5.8-5.9	6.0-6.1
300	unstable	3.9-4.1	3.7-4.0	4.1-4.2	4.3-4.4

a higher temperature, thus resulting in more free electrons to carry the electric current and less resistance. Consequently, the electrons can drift to the anode more easily and the transport requires less voltage drop. Lower applied voltage produces lower energy electrons.

Table 5.2 Relationship between voltage and current from N_2-O_2(5%) 100 cc/min

Temperature (^{0}C)	Current , mA							
	0.05	0.10	0.15	0.20	0.25	0.30	0.35	0.40
	Voltage , kV							
35	10.7	11.9	12.6	13.1	13.6	14	14.4	14.7
100	9.9	10.8	11.2	11.6	12.1	12.5	12.9	13.2
150	8.8	9.5	9.9	10.4	10.8	11.1	11.5	11.7
200	7.6	8.2	8.7	9.3	9.6	10	10.2	10.5
300	5.0-5.1	5.2-5.4	5.2-5.6	5.2-5.3	5.3	5.3	5.4-5.5	5.7

5.4 Effect of reactor temperature on styrene removal

5.4.1 Effect of reactor temperature and concentration on removal of styrene from N_2

Figure 5.3 shows the two kinds of removal efficiency of styrene from pure N_2 versus reactor temperature at different styrene inlet concentrations. Figure 5.3(a) shows the styrene removal efficiency ψ' versus temperature. We see that as the temperature increases, the value of ψ' decreases monotonically starting from room temperature to 300°C. As pointed out above, the mean residence time of the gas mixture inside the reactor decreases as the reactor temperature rises. This phenomenon is attributable to the fact that the gas mixture flows upward more quickly as its volume expands. Above 200 ^{0}C, the rate of detachment of attached styrene molecules on the reactor wall is sufficiently enhanced by the lowered adsorption equilibrium to overcome the effect of electrostatic attraction, thus significantly reducing the net rate of styrene deposition on the wall when the styrene inlet concentration is below 100 ppm. Figure 5.3(b) shows the removal efficiency per residence time ψ'' versus temperature. This figure reveals that when the negative effect of reduced residence time is taken in account, the value of ψ'' actually increases with the temperature up to 200^0C when the styrene inlet concentration is below 100 ppm and up to 300^0C when the concentration is 500 ppm. As explained above, the rate of detachment of styrene from the anode surface becomes significant at high temperature. At sufficiently high concentration (500ppm), this detachment rate is slowed down by the high remaining concentration of styrene in the gas phase.

Tamon et al.(1995) have found that the removal efficiency via electron attachment tends to decrease when the inlet concentration is increased. As expected, the present experimental results on the effect of inlet styrene concentration also exhibit the same tendency. The lower the inlet concentration of styrene, the higher the removal efficiency becomes. To explain the phenomenon, we consider the number ratio of discharge electrons to the incoming styrene molecules. At a higher styrene inlet concentration, there are many more styrene molecules than at a lower inlet concentration of styrene. However, the number of discharge electrons remains more or less constant at the same discharge current. Therefore, the probability of electron attachment onto a styrene molecule becomes lower. This is the reason that the lower the inlet concentration of styrene, the higher the removal efficiency becomes regardless of the same temperature of interest.

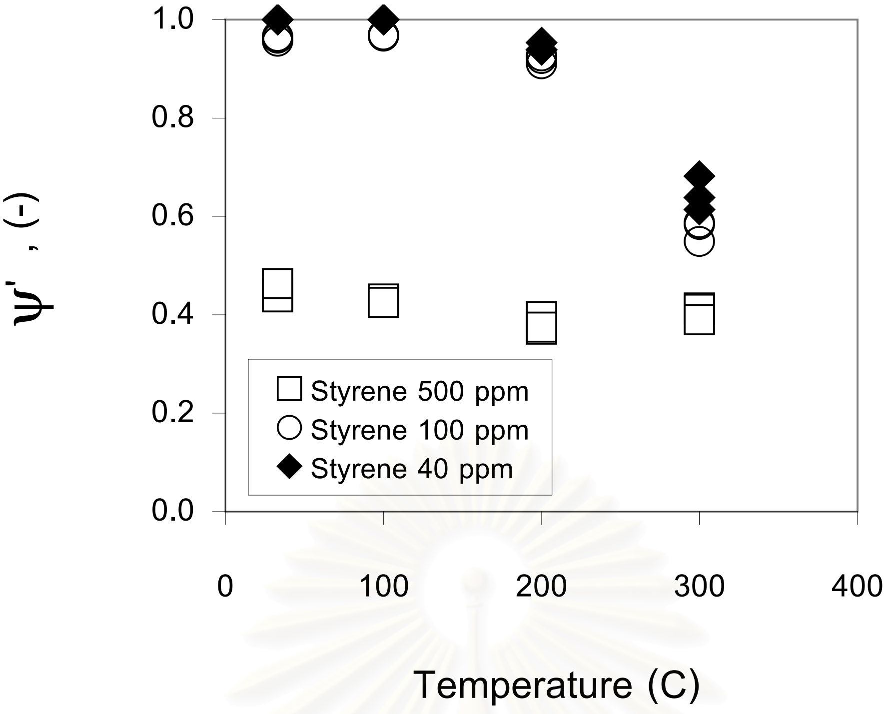

(a)

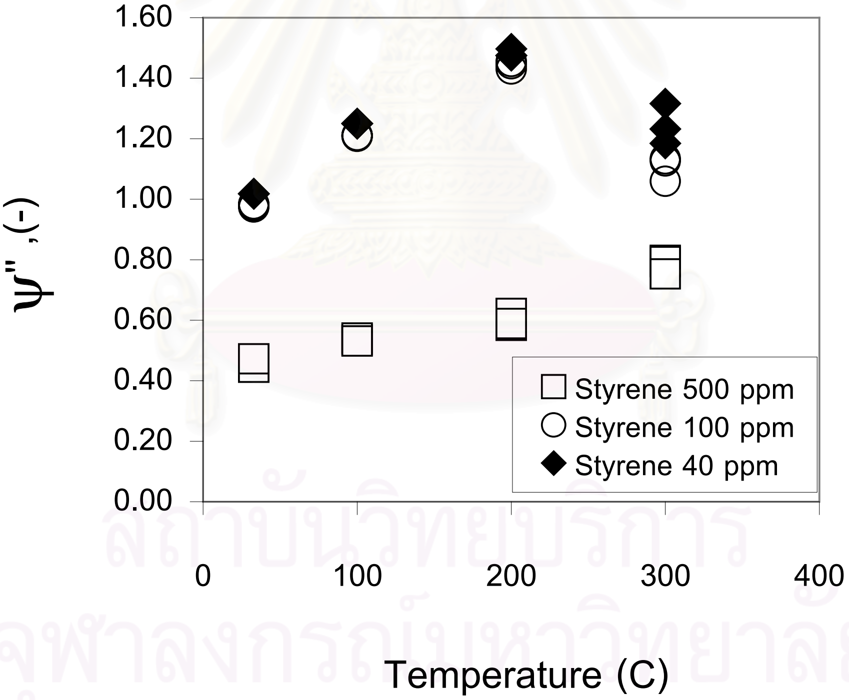

(b)

Figure 5.3 Effect of temperature on the removal of styrene from N_2 ;
I = 0.5 mA , SV = 55.8 hr^{-1} at room temperature

5.4.2 Effect of temperature and coexisting oxygen on removal of styrene from N_2

In most actual applications of gas purification, other kinds of gas components often coexist. Therefore it is necessary to study the influence of common coexisting gases on the removal efficiency.

Figure 5.4 shows the two kinds of removal efficiency of styrene from N_2-O_2 when the styrene inlet concentration is 500 ppm. It is obvious that the presence of O_2 in N_2 greatly enhances the styrene removal efficiency despite the fact that the discharge current has been reduced tenfold to 0.05 mA compared to the case of pure N_2. This can be attributed to the fact that O_3 is produced from O_2 by the corona discharge reaction. At relatively low temperatures, O_3 is quite stable and it enhances the removal of styrene via the formation of ionic ozone-styrene clusters. Part of the ozone might also oxidize or decompose some of the styrene. At high temperatures, the rate of the ozonation reaction increases exponentially and most of the ozone is consumed by the oxidation of the relatively inert but abundant N_2 to NO_x. Coupled with the negative effect of reduced residence time, this explains why the value of ψ' decreases monotonically with the reactor temperature and most abruptly at 300^0C. Figure 5.4(a) shows the removal efficiency ψ' versus temperature. Figure 5.4(b) shows the removal efficiency per residence time ψ'' versus temperature. The value of ψ'' increases up to 200^0C after the effect of residence time is accounted for. Above 200^0C, ozone-styrene clusters not only become less stable but most of the ozone is consumed by the oxidation of N_2 to NO_x. Figure 5.5 shows the measured concentration of O_3 and NO_x under some of the experimental conditions. Recently Nantamas Dhattavorn and Wiwut Tanthapanichakoon et al.(2000) reported experimental results regarding the influence of temperature on O_3 produced in the corona discharge reactor. At high temperature, the ozone concentration decreases because the reaction rate of ozonation effect is very fast. Nitrogen is thus oxidized by ozone to become NO_x. Thus the ozone is found to decrease when the temperature increases. As a result, the styrene removal efficiencies ψ' and ψ'' become lower at 300^0C.

As expected, the removal efficiency is found to increase when not close to 100% as the concentration of coexisting O_2 is increased. This can be attributed to the fact that more ozone is produced and the ozonation effect is the important mechanism to enhance the removal efficiency. The highest effect of coexisting O_2 is found at the highest concentration of 25% O_2

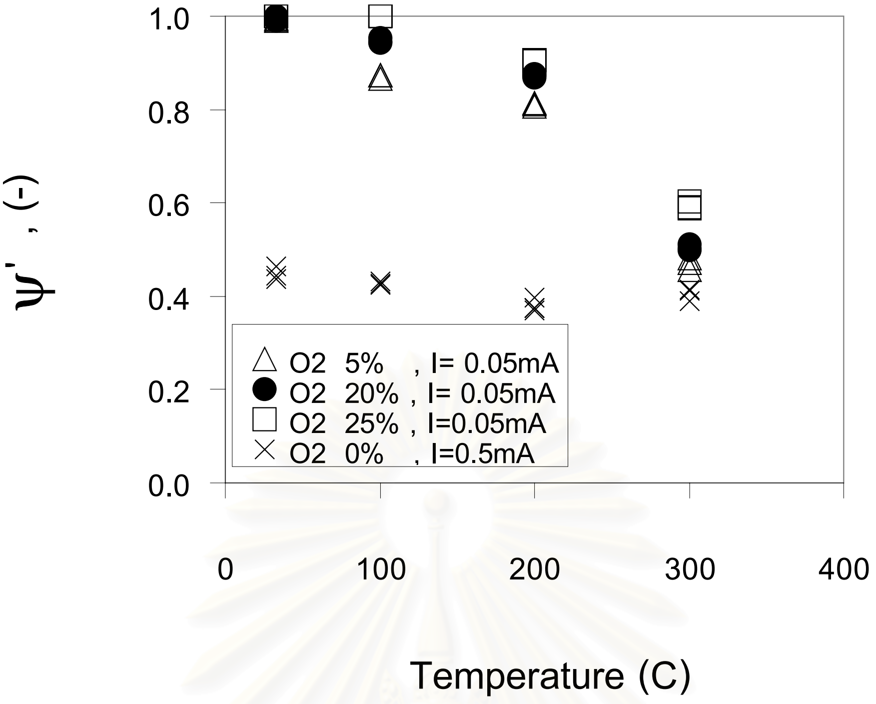

(a)

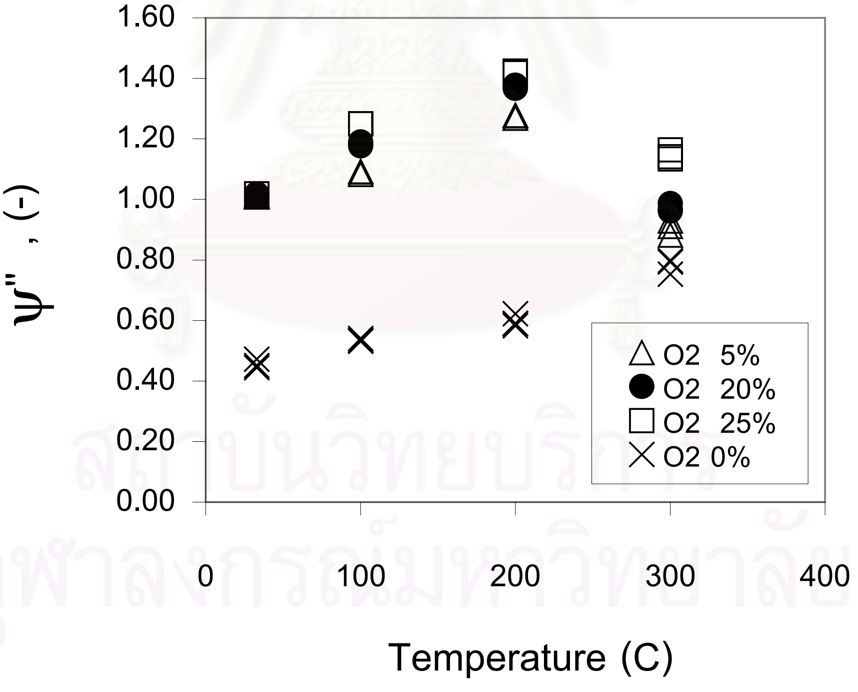

(b)

Figure 5.4 Effect of temperature on the removal of styrene from N_2 –O_2; $C_{in, styrene}$= 500 ppm, I = 0.05 mA, SV = 55.8 hr^{-1} at room temperature

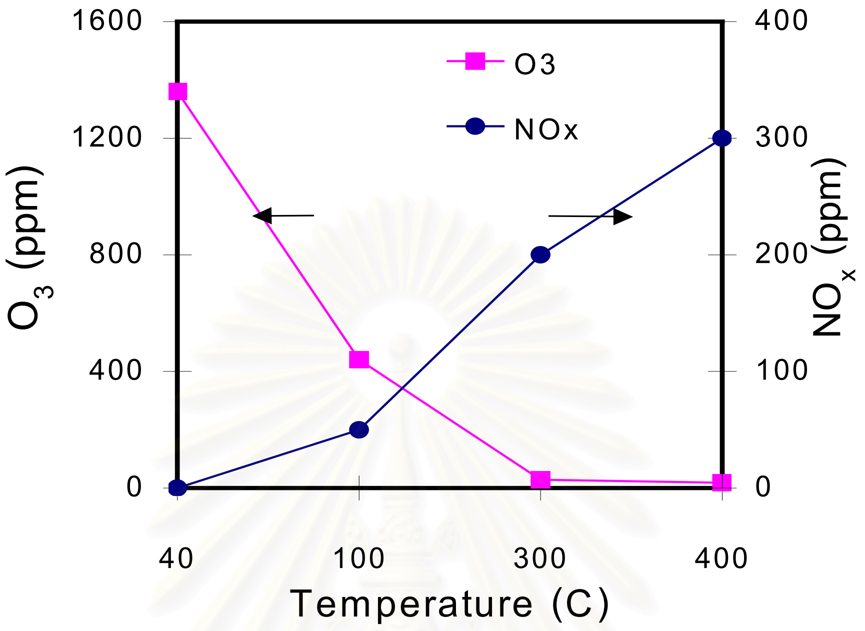

Figure 5.5 Relationship between ozone and NO_x generation at various temperatures for toluene removal from N_2-O_2 (30%); I = 0.5 mA, SV = 55.8 hr^{-1} at room temperature

5.4.3 Influence of water vapor and temperature on removal of styrene from N_2

In actual applications of gas purification, water vapor may be present in the treated gases. Therefore it is necessary to study the influence of water vapor on the removal efficiency. In the previous sections, coexisting oxygen is found to be a significant factor that enhances the removal of styrene.

Figure 5.6 shows the two types of removal efficiency of styrene from N_2-H_2O at various concentrations of water vapor. Figure 5.6(a) shows the removal efficiency ψ' versus temperature. We see that as the temperature increases, the styrene removal efficiency decreases monotonically starting from room temperature to 300^oC because of the reduction in residence time. As for the influence of H_2O, the presence of H_2O significantly raises the removal efficiency compared to the case of pure N_2 despite a 5-fold reduction in the current. Figure 5.6(b) shows the removal efficiency per residence time ψ'' versus temperature. This figure reveals that the value of ψ'' decreases slightly with temperature. It is postulated that styrene is less electronegative than H_2O. In addition the absolute number of water molecules in the experiments are much higher than the styrene molecules. At low discharge currents, only a relatively small number of electrons are available for H_2O molecules to produce O^-, OH^- and H^- via dissociative electron attachment (Moruzzi and Phelps 1966). These negative ions then contribute to styrene removal. When the temperature increases, the required voltage decreases and electron energy level decreases. As a result, the electrons tend to attach to H_2O more than to cause dissociative electron attachment of H_2O. As a result, the styrene removal efficiency ψ'' becomes slightly lower at 300^0C.

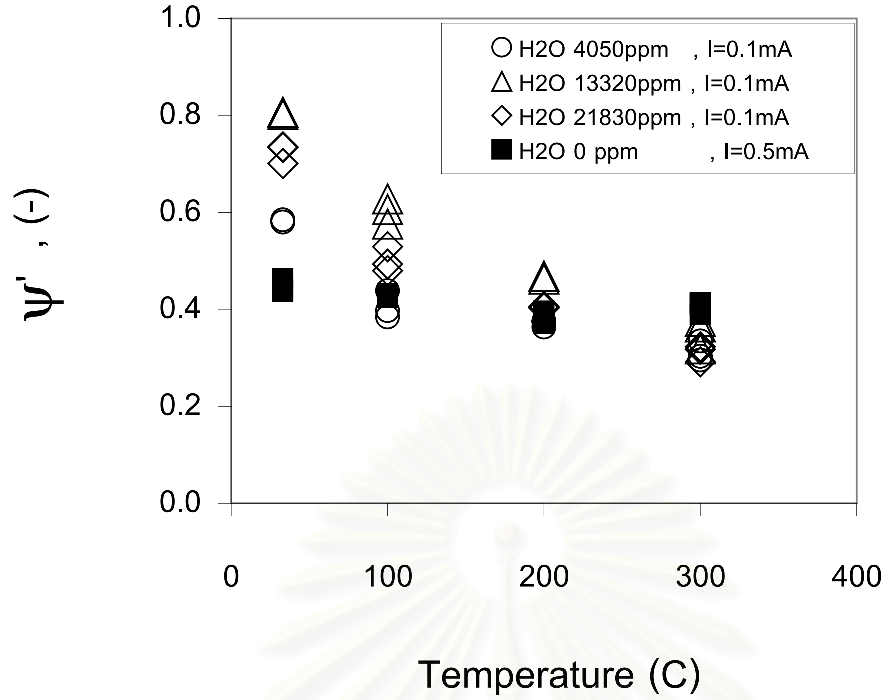

(a)

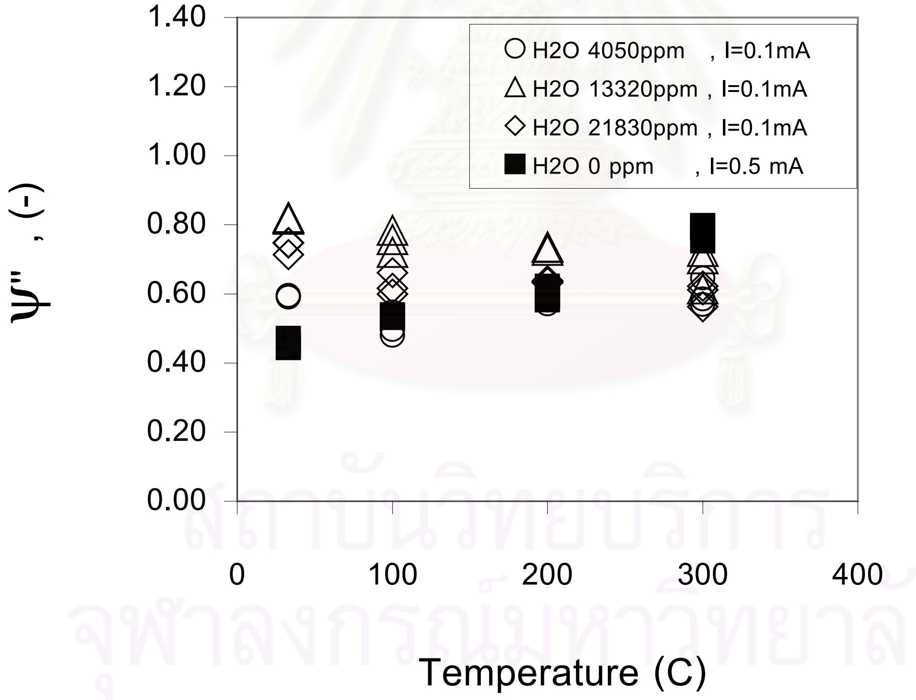

(b)

Figure 5.6 Influence of water vapor on the removal of styrene from N_2 ; $C_{in,\ styrene}$= 500 ppm, I = 0.1 mA , SV = 55.8 hr^{-1} at room temperature

5.4.4 Influence of temperature and water vapor on removal of styrene from N_2-O_2

A number of experiments to observe the influence of H_2O on the removal of styrene from N_2-O_2 mixed gas (5,10,20% O_2) has been carried out. Figure 5.7 shows the influence of water vapor on the two removal efficiencies ψ' and ψ'' of styrene from N_2-O_2 at various temperatures. Figure 5.7(a) shows the removal efficiency ψ' versus temperature. As for the effect of H_2O, the presence of H_2O significantly retards the removal efficiency ψ' of styrene from N_2-O_2 starting from room temperature to 200^0C. On the contrary, at 300^0C the presence of H_2O significantly enhances the removal efficiency compared to the absence of H_2O. Figure 5.7(b) shows the removal efficiency per residence time ψ'' versus temperature. In figure 5.7, the three different concentration of H_2O (4050 ppm, 12940 ppm and 23028 ppm) have considerable effect in the removal efficienciy of styrene from N_2-O_2. The presence of water vapor has enhanced the removal efficiency at 300^oC because O^-, OH^- and H^- from dissociative electron attachment of H_2O may have occurred, thus enhancing the removal efficiency where O_3 is difficult to generate.

Figure 5.8 shows the retarding effect of water vapor on ozone generation at room temperature. It may be concluded the presence of H_2O in N_2-O_2 decreases the removal efficiency at room temperature and up to 200^0C because O_3 generation is progressively retarded.

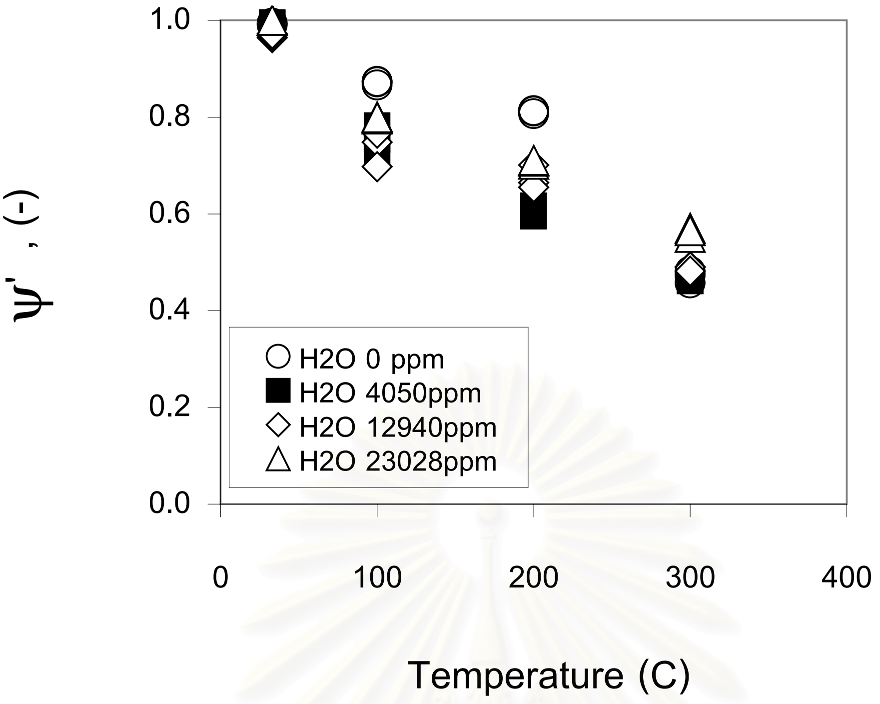

(a)

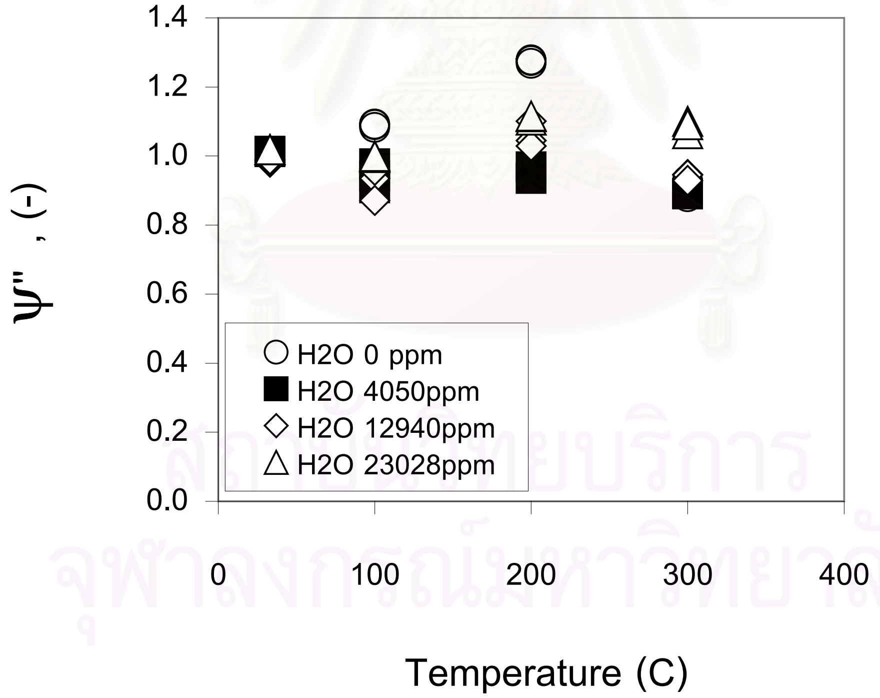

(b)

Figure 5.7 Influence of water vapor on the removal of styrene from N_2-O_2(5%); $C_{in,\ styrene}$= 500 ppm, I = 0.05 mA , SV = 55.8 hr^{-1} at room temperature

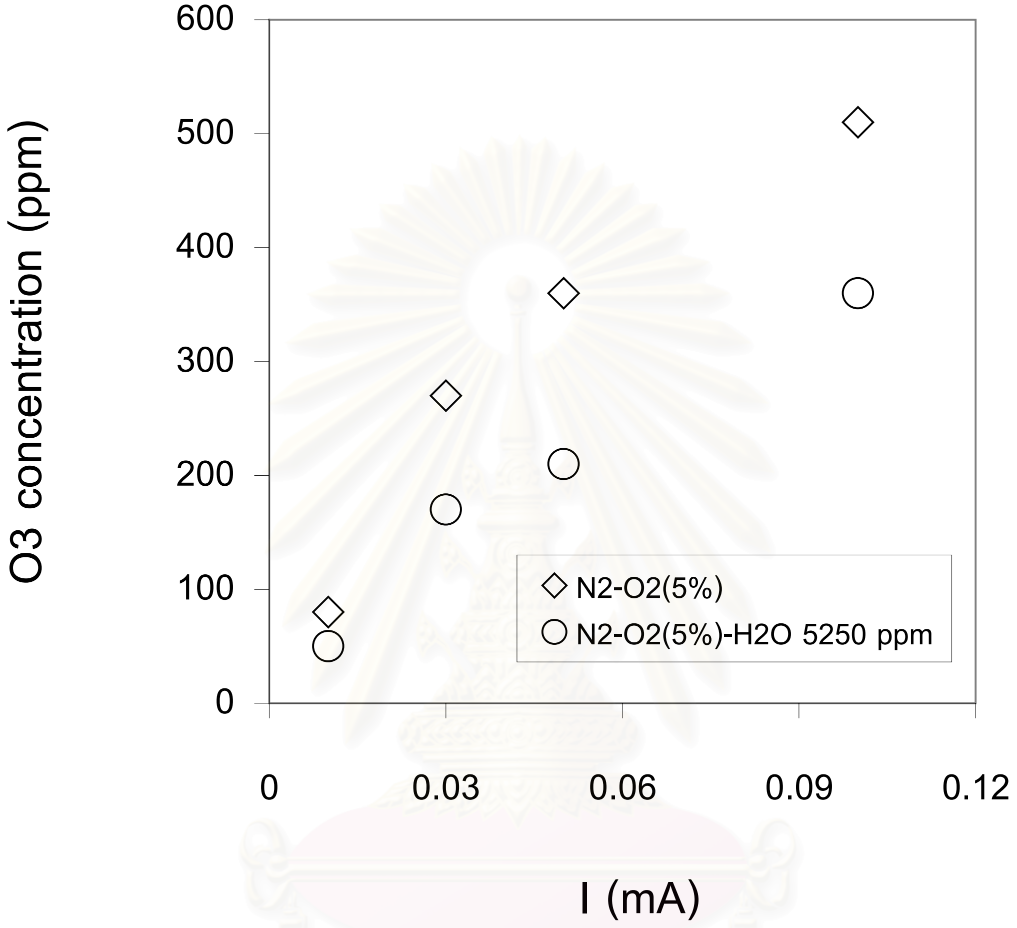

Figure 5.8 Effect of water vapor on O_3 generation from N_2-O_2(5%); SV = 55.8 hr^{-1} at room temperature

5.4.5 Solid deposit in the reactor after removal of styrene from N_2-O_2

After a long period of the removal experiments, there is a gradual buildup of light brown solid deposit on the glass section at the top of the reactor. It is necessary to identify this deposit as well as the gaseous byproducts, if any, in order to understand the removal mechanism of the electron attachment reaction.

A specially designed deposition-type reactor with a detachable anode plate is used to collect deposit from styrene removal (1000 ppm) from N_2-O_2 at room temperature. Similar experiments are not carried out at higher temperatures because the special reactor can only operated at room temperature. The solid deposit has yellowish to brownish color and irregular shape because it consists of agglomerates of nanosized particles formed and growing randomly on the anode plate. Two photos of the deposit on the anode plate are shown in **Appendix I**. Some of the deposit was scraped off and taken for analysis using Fourier-Transform Infrared Spectroscopy (FT-IR). As shown in **Appendix H**, the spectrum shows several prominent peaks and numerous smaller ones around 800-1800 cm^{-1}. However the closely packed peaks can not identified individually. Without any GC-MS analysis of the gaseous byproducts in the effluent stream, there is not sufficient evidence to clearly identify the chemical composition of the solid deposit. In the removal of benzene from N_2-O_2, Tamon et.al.(1998) have identified solid deposit formed from the polymerization and/or polycondensation of benzene. It is postulated here that similar reactions contribute to the formation and growth of the present solid deposit.

5.5 Effect of reactor temperature on ammonia removal

5.5.1 Effect of coexisting oxygen on removal of ammonia from N_2

Figure 5.9 shows the two kinds of removal efficiency of ammonia from N_2 at various concentrations of co-existing O_2 when the ammonia inlet concentration is 400 ppm. It is obvious that the presence of O_2 in N_2 greatly enhances the ammonia removal efficiency despite the fact that the discharge current has been reduced 6-fold to 0.05 mA compared to the case of pure N_2 in the same figure. This can be attributed to the fact that O_3 and O^- radical are produced from O_2 by the corona discharge reaction. Figure 5.9(a) shows the removal efficiency ψ' versus temperature. We see that as the temperature increases, the ammonia removal efficiency in the presence of O_2 drops monotonically starting from room temperature to 300^oC. Figure 5.9(b) shows the removal efficiency per residence time ψ'' versus temperature. In this figure the decreasing tendency of the removal efficiency per residence time ψ'' means that the intrinsic removal rate decreases slightly from room temperature to 300^0C. It is postulated that NH_3 is more electronegative than N2 but less electronegative than O_2. When the discharge current is reduced, a relatively smaller number of electrons is there molecule to produce O_3 from O_2 before, NH_3 is removed via ozone reaction. At high temperatures, the rate of the ozonation reaction increases exponentially and most of the ozone and O^- radical is consumed by the oxidation of the relatively inert but abundant N_2 to NO_x. As a result, the ammonia removal efficiency becomes lower as temperature increases.

The removal efficiency is found to increase appreciably when the concentration of coexisting O_2 is increased. This can readily be ascribed to the ozonation effect which is an important mechanism to enhance the removal efficiency. As expected, the most significant effect of coexisting O_2 is found at the highest 20% O_2.

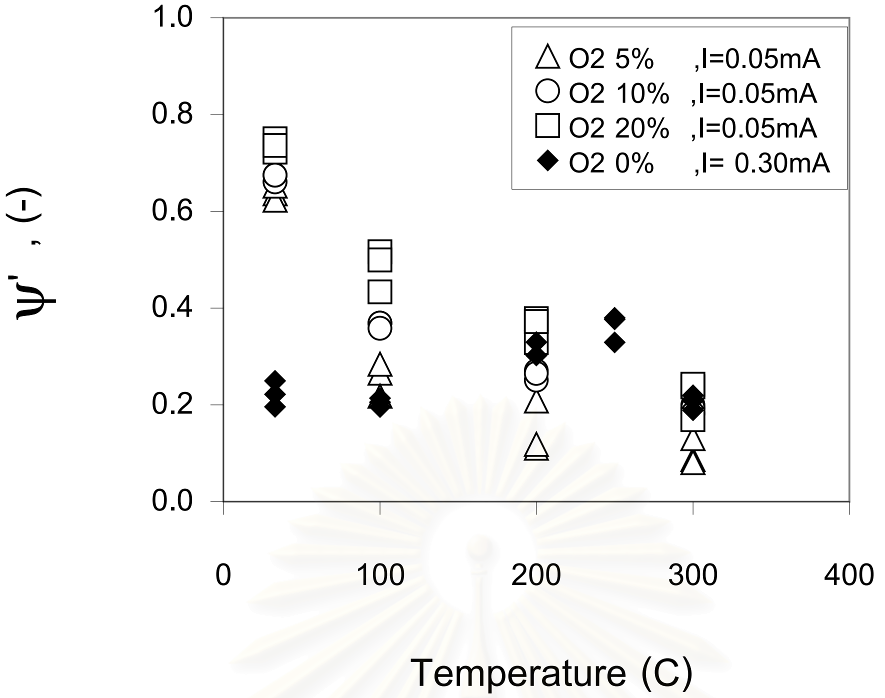

(a)

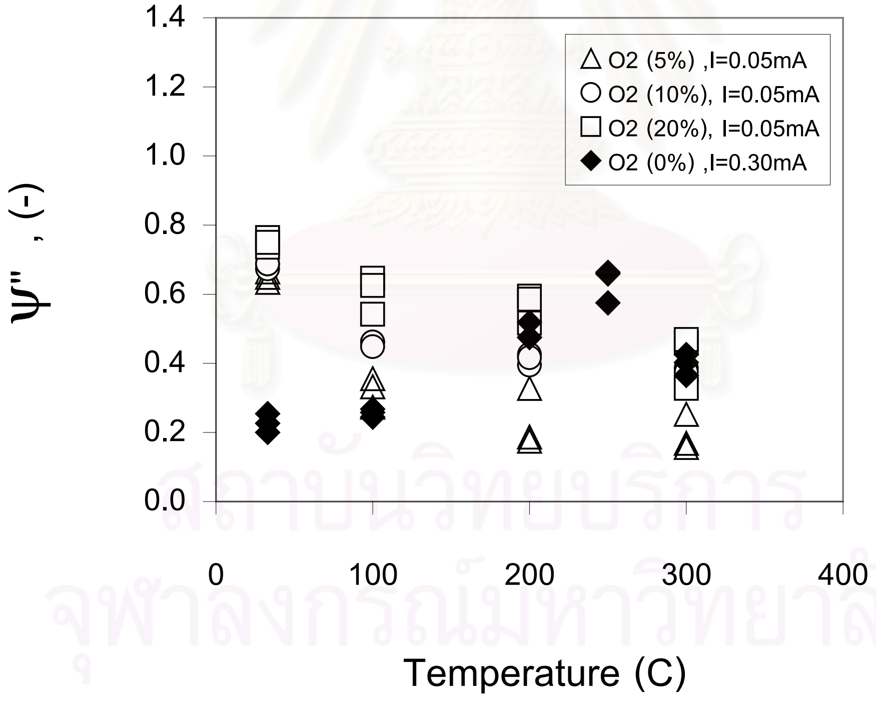

(b)

Figure 5.9 Effect of temperature on the removal of ammonia from N_2 –O_2; $C_{in,\ ammonia}$ = 400 ppm, I = 0.05 mA, SV = 55.8 hr^{-1} at room temperature

5.5.2 Influence of water vapor on removal of ammonia from N_2

Figure 5.10 shows the two types of removal efficiency of ammonia from N_2 at various concentrations of coexisting water vapor. Figure 5.10(a) shows the removal efficiency ψ' versus temperature. We see that as the temperature increases, the ammonia removal efficiency gradually drops starting from room temperature to 300°C. As for the influence of H_2O, the presence of H_2O slightly enhances the removal efficiency compared to the case of pure N_2 when H_2O concentration is less than 10,500 ppm. It is postulated that NH_3 is less electronegative than H_2O. Figure 5.10(b) shows the removal efficiency per residence time ψ'' versus temperature. In this figure, the slightly increasing tendency of the removal efficiency per residence time from room temperature up to 200^0C. Above 200^0C, the slightly positive tendency reverses at 300^0C. When the temperature becomes very high, corona discharge occurs more readily and electron energy level becomes lower and they tend to attach with H_2O more than to cause dissociative electron attachment of H_2O. As the results, the ammonia removal efficiency becomes significantly lower at 300^0C.

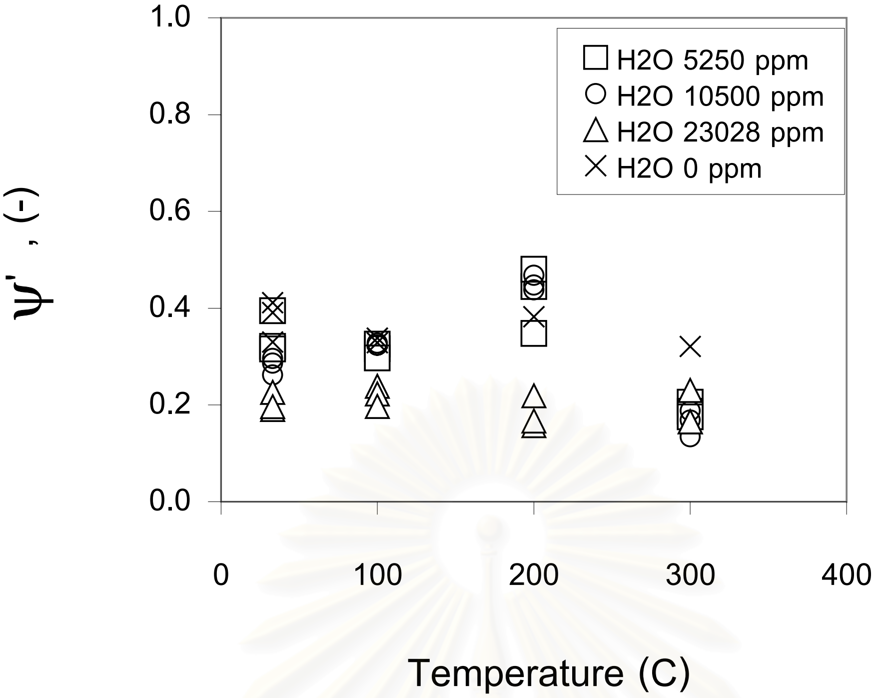

(a)

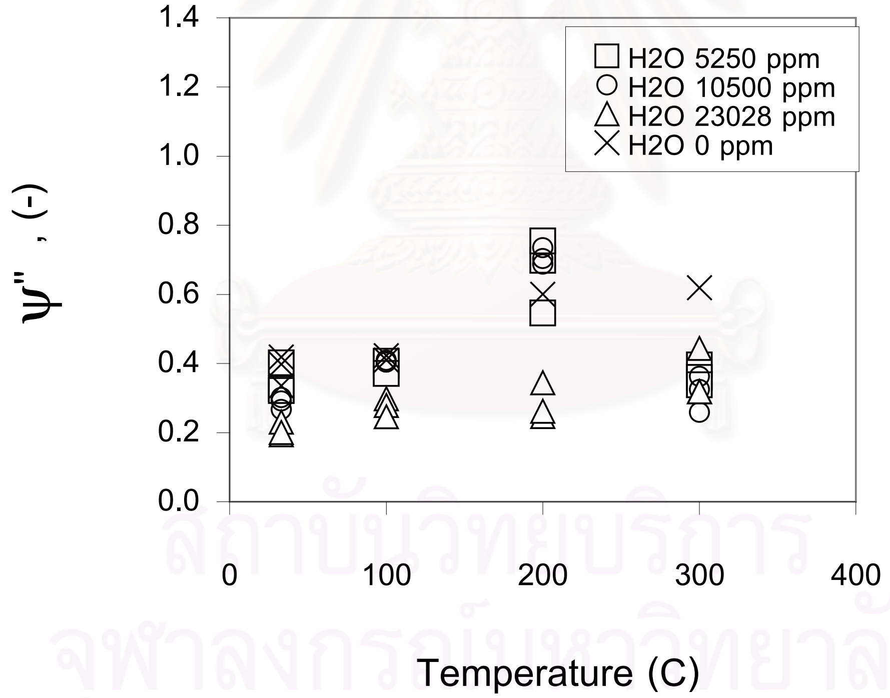

(b)

Figure 5.10 Influence of water vapor on the removal of ammonia from N_2 ; $C_{in,\ ammonia}$ = 250 ppm, I = 0.3 mA , SV = 55.8 hr^{-1} at room temperature

5.5.3 Influence of water vapor on removal of ammonia from N_2-O_2

Some experiments to observe the influence of H_2O on the removal of ammonia from N_2-O_2 mixed gas (5,10,20% O_2) have been carried out. Figure 5.11 shows the influence of water vapor and temperature on the removal efficiency of ammonia from N_2-O_2(5%). Figure 5.11(a) shows the removal efficiency ψ' versus temperature. As for the effect of H_2O, the presence of H_2O significantly retards the removal efficiency ψ' of styrene from N_2-O_2 starting from room temperature to 200^0C. Figure 5.11(b) shows the removal efficiency per residence time ψ'' versus temperature. From this figure a similar trend of the removal efficiency versus temperature is observed. The two different concentration (5250 ppm and 10500 ppm) of H_2O have significant effect on the removal efficiency of NH_3 from N_2-O_2.

In the absence of H_2O and O_2, the removal efficiency of NH_3 from N_2 is relatively low at I=0.3 mA because the electronegativity of NH_3 is not very high (see Figure 5.9). With the presence of O_2 and in the absence of H_2O, the same NH_3 removal efficiency is essentially 100% at I=0.3 mA (except at 300^0C) because the generation of O^- radical and O_3 contributes to the ionic clustering of NH_3 and/or the ozanation reaction that produces NO_x which subsequently reacts with NH_3. With the presence of only H_2O, the NH_3 removal efficiency changes only slightly except when H_2O concentration is very high(see Figure 5.10).

In the presence of O_2 and a relatively low concentration of H_2O (5250 ppm), the NH_3 removal efficiency drops precipitously. It is postulated that H_2O more easily form ionic cluster with $O^\cdot$ than NH_3, thus lowering the NH_3 removal efficiency. H_2O concentration increase twofold to 11500ppm, corona discharge can occur at a lower voltage and the electron energy level becomes too low to generate O^- radical. Meanwhile, the low-energy electrons contributes to the formation of ammonium ions and their clusters, thus enhancing the NH_3 removal efficiency compared with the case of H_2O 5250 ppm.

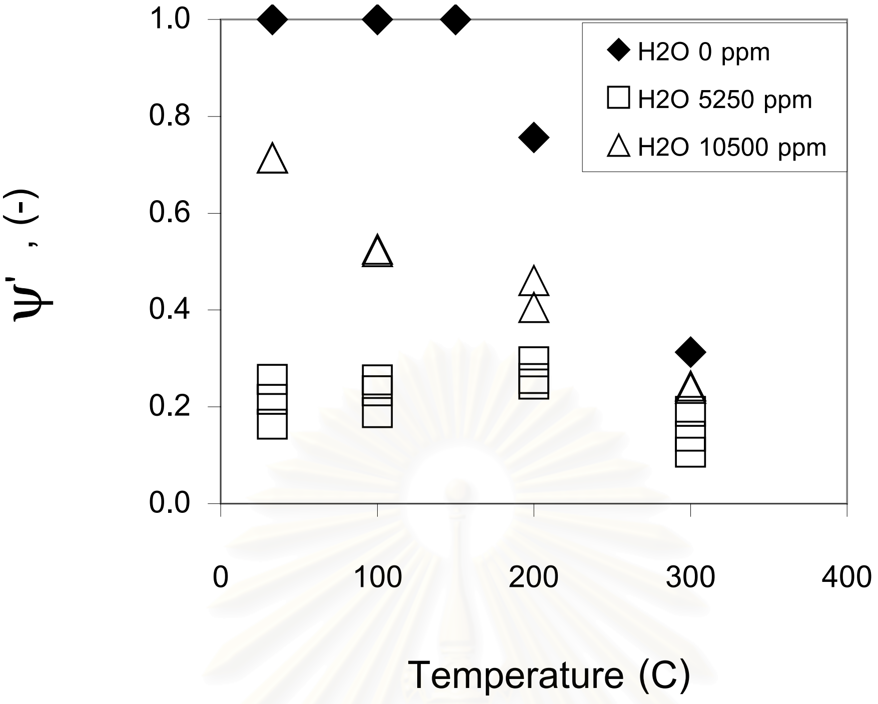

(a)

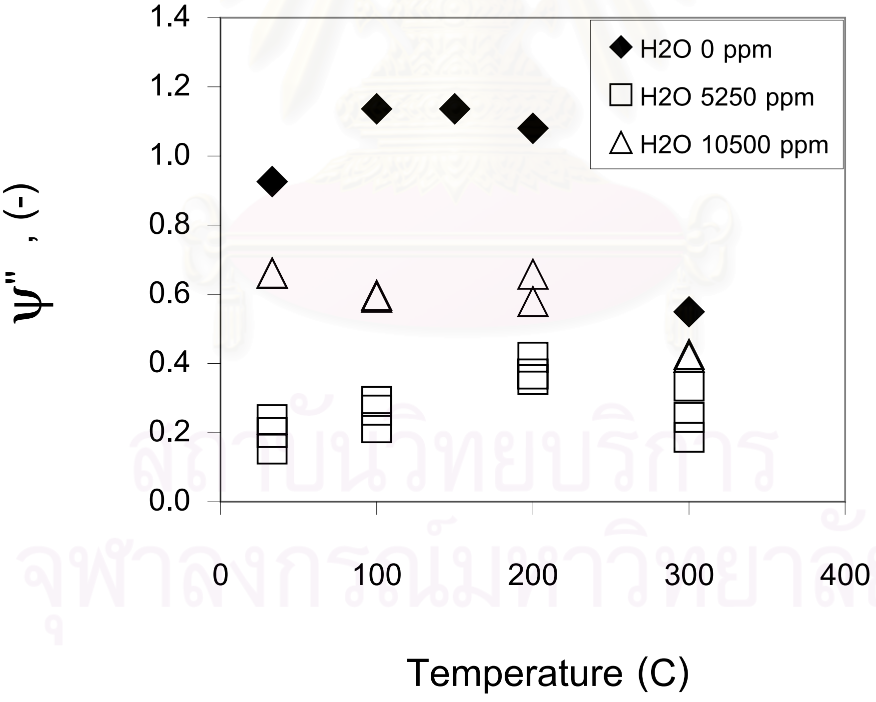

(b)

Figure 5.11 Influence of water vapor on the removal of ammonia from N_2-O_2(5%); $C_{in,\ ammonia}$= 250 ppm, I = 0.30 mA , SV = 55.8 hr^{-1} at room temperature

5.5.4 Solid deposit in the reactor after removal of NH_3 from N_2-O_2

After a long period of the removal experiments, there is a gradual buildup of white solid deposit on the glass section at the top of the reactor. Again it is necessary to identify this deposit as well as the gaseous byproducts in order to understand the removal mechanism of the electron attachment reaction.

A specially designed deposition-type reactor with a detachable anode plate is used to collect deposit from ammonia removal (~500 ppm) from N_2-O_2 at room temperature. Similar experiments are not carried out at higher temperatures because the special reactor can only operated at room temperature. The collected solid particles have white color. Some of the deposit was scraped off and taken for analysis with an FT-IR spectrometer. As shown in **Appendix H** show that the prominent peaks appear at wave number 800, 1450 and 1700 cm^{-1}. It can be considered that the deposit has ammonium ion (NH_4^+) as a functional group and that the deposit consists of ammonium nitrate (NH_4NO_3) produced from the reaction of NH_3 with NO_x since it is known that NO_x can be formed during corona discharge in the air (Dhattavorn, N., 2000).

Table 5.3 shows a list of probable by-products in the effluent stream during removal of NH_3 in N_2-O_2 as reported by Khongphasarnkaln (1998). Since there are not enough detailed data, the reaction by-products can not unambiguously be identified yet. Nevertheless, it can be said that the ozone effect must have played a major role on NH_3 decomposition and removal.

Table 5.3 List of by-products during removal of NH_3 from N_2-O_2 mixture as interpreted from GC-MS data (Khongphasarnkaln, P., 1998)

No.	Retention time(sec)	M/Z	M/Z of fragment	Probable by-product	Change in by-product concentration with discharge current
1	1.8	44	43, 29, 15	H_2N_3	Increase
2	5.5	59	58, 43, 32, 28, 17, 16, 15, 14	HN_3O, N_4H_3	Increase

.

5.6 Effect of temperature on simultaneous removal of styrene and ammonia

5.6.1 Effect of inlet concentration on simultaneous removal of styrene and ammonia from N_2

To investigate possible interaction between styrene and ammonia, two of the reported crematory gas components, several experiments to simultaneously remove styrene and ammonia from N_2 have been carried out. Figure 5.12 shows the influence of concentration and temperature on the simultaneous removal efficiency of styrene and ammonia from N_2. Figure 5.12(a) shows the removal efficiency of styrene versus temperature. As for the effect of ammonia on the styrene removal efficiency, the presence of ammonia only slightly decreases the styrene removal efficiency from room temperature to 300^0C. This is because styrene is much more electronegative than ammonia. Figure 5.12(b) shows the removal efficiency of ammonia versus temperature. As for the effect of styrene on the ammonia removal efficiency, the presence of styrene enhances the ammonia removal efficiency from room temperature to 300^0C. It is may be postulated that styrene is removed by the formation of ionic clusters, and when ammonia is also present, some of the ammonia molecules attach themselves on the styrene clusters, thus raising the ammonia removal efficiency.

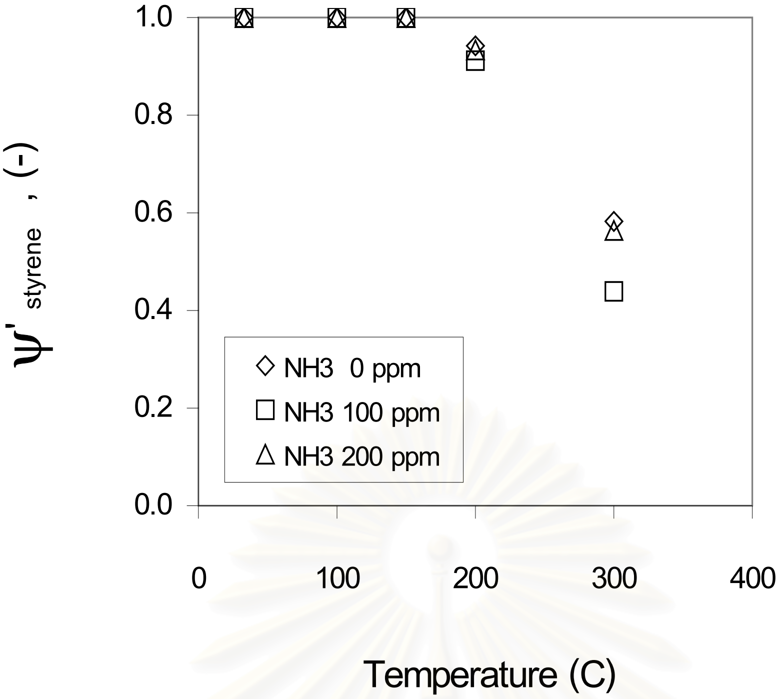

(a)

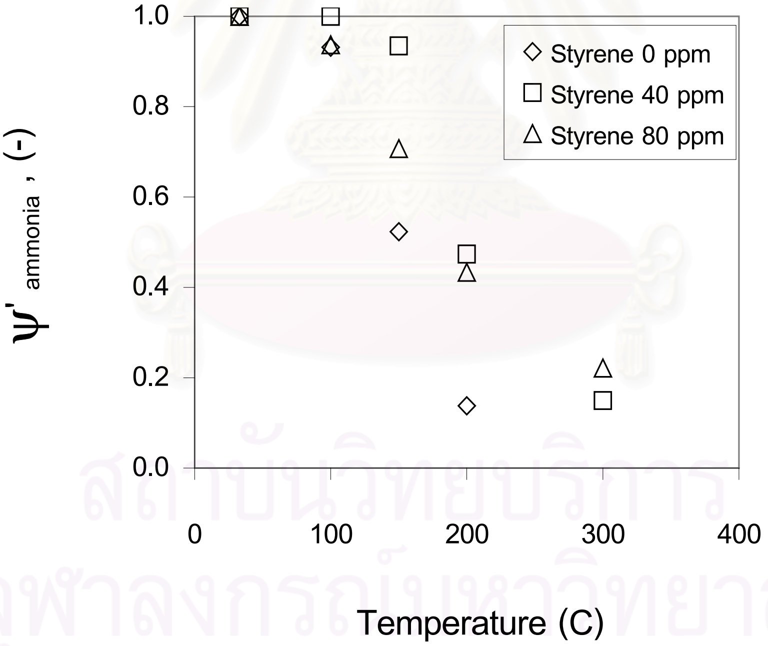

(b)

Figure 5.12 Simultaneous removal of styrene and ammonia from N_2-O_2(5%); $C_{ammonia}$ = 200 ppm, $C_{styrene}$ = 40 ppm, I = 0.10 mA , SV = 55.8 hr^{-1} at room temperature

5.6.2 Effect of coexisting oxygen gas on the simultaneous removal of styrene and ammonia from N_2

Figure 5.13 shows the simultaneous removal efficiency of styrene and ammonia from N_2-O_2. Figure 5.13(a) shows the removal efficiency of styrene versus temperature. Obviously, the presence of O_2 has a significant effect on the stryene removal efficiency. As the temperature increases, the styrene removal efficiency remains essentially 100% from room temperature to 300^0C, except at 5% O_2 and 300^0C. Figure 5.13(b) shows the removal efficiency of ammonia versus temperature. Obviously, the presence of O_2 has a significant effect on the ammonia removal efficiency. As the temperature increases, the ammonia removal efficiency above 200^0C tends to significantly decrease.

The removal efficiency enhancement is found to depend on the concentration of coexisting O_2. Compared to the case of no oxygen, the improved removal efficiency for both styrene and ammonia can be attributed to the ozonation effect. The positive effect of styrene on the removal efficiency of ammonia has been explained in 5.6.1.

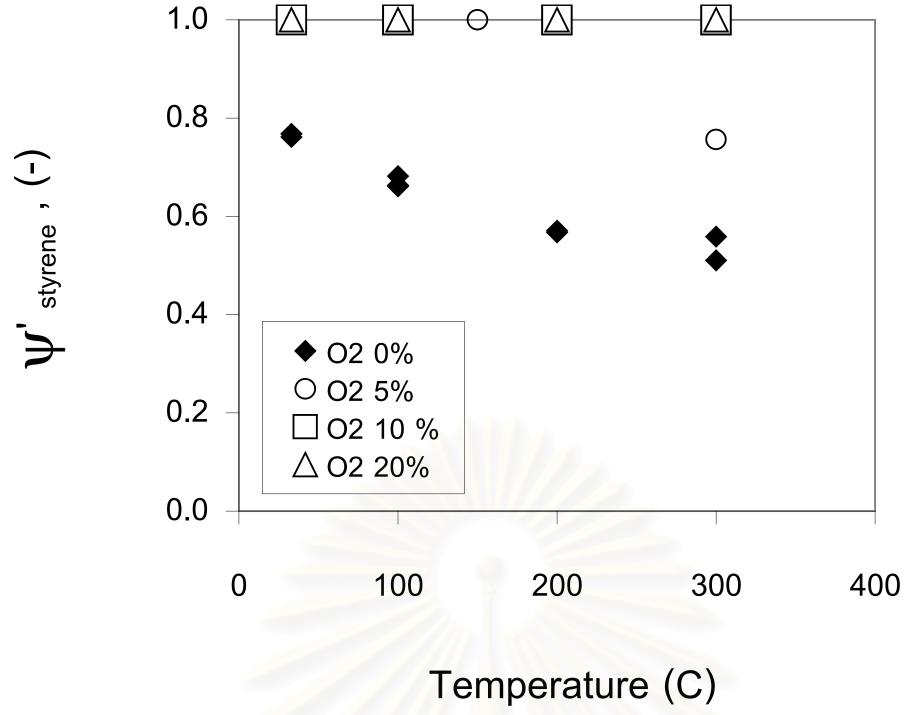

(a)

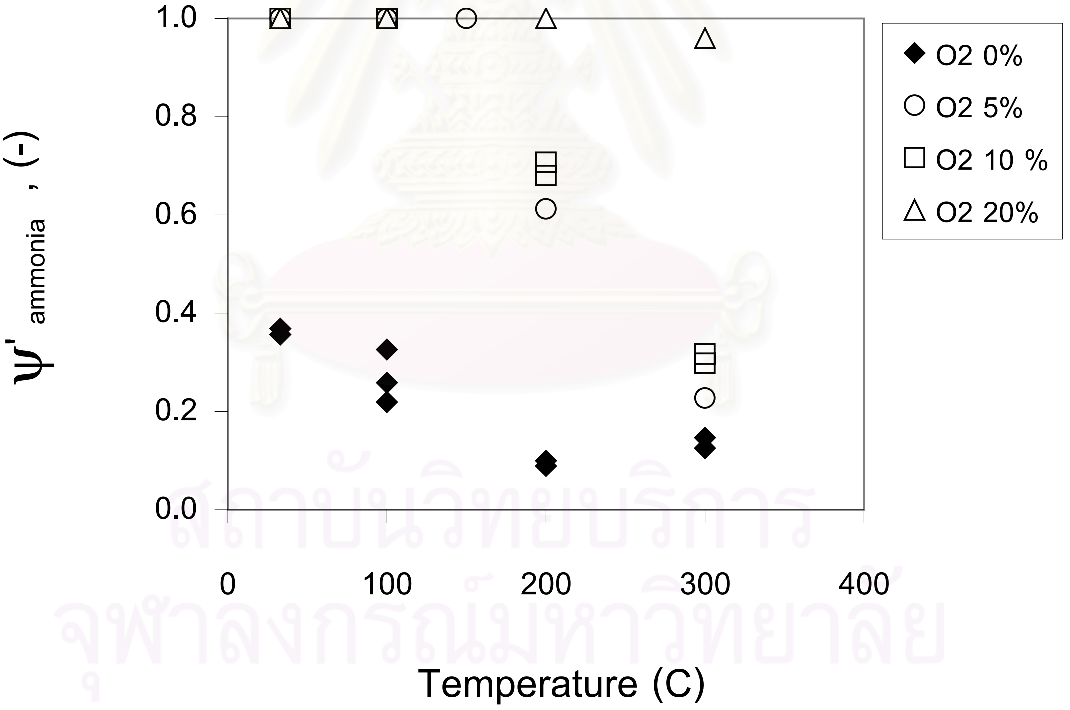

(b)

Figure 5.13 Simultaneous removal of styrene and ammonia from N_2-O_2; $C_{in,\ ammonia}$= 200 ppm , $C_{in,\ styrene}$ = 40 ppm, I = 0.30 mA , SV = 55.8 hr^{-1} at room temperature

5.6.3 Influence of water vapor and temperature on simultaneous removal of styrene and ammonia from N_2-O_2

Figure 5.14 shows the influence of water vapor and temperature on the simultaneous removal efficiency of styrene and ammonia from N_2-O_2(5%). Figure 5.14(a) shows the removal efficiency of styrene versus temperature. As for the influence of H_2O, the presence of H_2O significantly decreases the removal efficiency of styrene only above 200^0C. Figure 5.14(b) shows the removal efficiency of ammonia versus temperature. As for the influence of H_2O, the presence of H_2O significantly decreases the removal efficiency of ammonia from 100^0C onward. Compared to the case of no water vapor, the removal efficiency of both styrene and ammonia is retarded by the presence of water vapor. The negative effect is significant on ammonia removal at 150 ^{0}C and styrene removal at 300^0C. It may be postulated that water vapor slightly effect the formation of O^- radicals and O_3 by lowering the required corona discharge voltage from 11.5 to 11.1 kV and the energy level of the electrons.

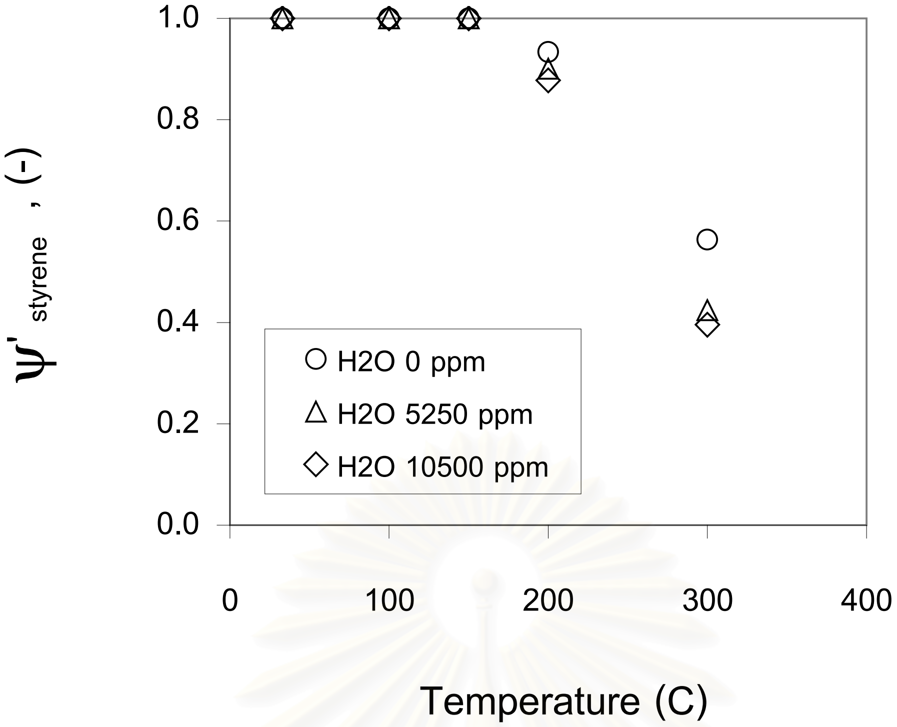

(a)

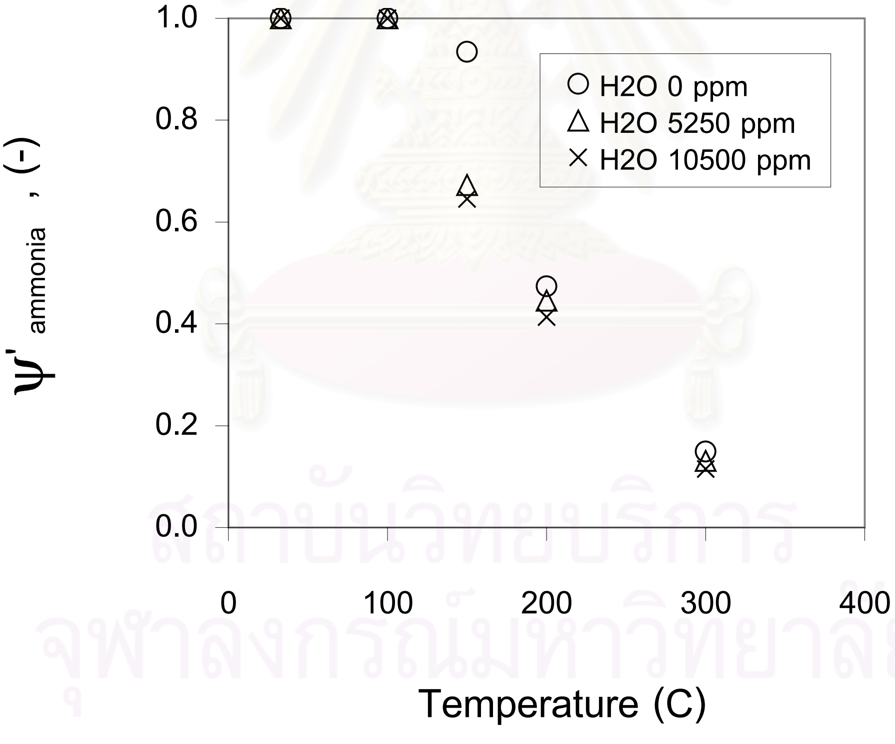

(b)

Figure 5.14 Simultaneous removal of styrene and ammonia from N_2-O_2(5%); $C_{in,\ ammonia}$= 200 ppm , $C_{in,\ styrene}$ = 40 ppm, I = 0.10 mA , SV = 55.8 hr^{-1} at room temperature

5.7 Effect of temperature on the simultaneous removal of styrene and ammonia in two serial reactors.

5.7.1 Complete simultaneous removal of styrene and ammonia in N_2-O_2(5%) at room temperature while minimizing byproduct O_3 and NO_x

In a previous experiment to observe the influence of H_2O on the generation of O_3 from N_2-O_2 mixed gas using a single reactor at room temperature, it is found that the outlet concentration of byproduct O_3 increases with the discharge current. However, it is difficult to effectively remove both styrene and ammonia at a low discharge current through O_3 increases with the discharge current. Lethal at relatively low concentrations and short exposure periods, O_3 must be treated.

A two-reactor system to minimizing undesirable O_3 is proposed for the simultaneous removal of styrene and ammonia from N_2-O_2. In this experiment, the concentration of styrene, ammonia and O_2 are 40 ppm, 200ppm and 5%, respectively. The first reactor mainly aims at the completely removal of styrene and ammonia. Figure 5.15 reveals that the discharge current of the first reactor required for complete removal is about 0.1 mA. In this condition, O_3 is generated and comes out of the first reactor at about 620 ppm. Figure 5.16 shows the operating results of the second reactor. At 190 ^{0}C, the optimum discharge current for O_3 minimization is 0.30 mA. At 300^{0}C, the second reactor with zero discharge current is best because O_3 is unstable at this high temperature and the outlet O_3 concentration is 20 ppm. In contrast, application of the discharge current proportionally increases the generation of undesirable NO_x.

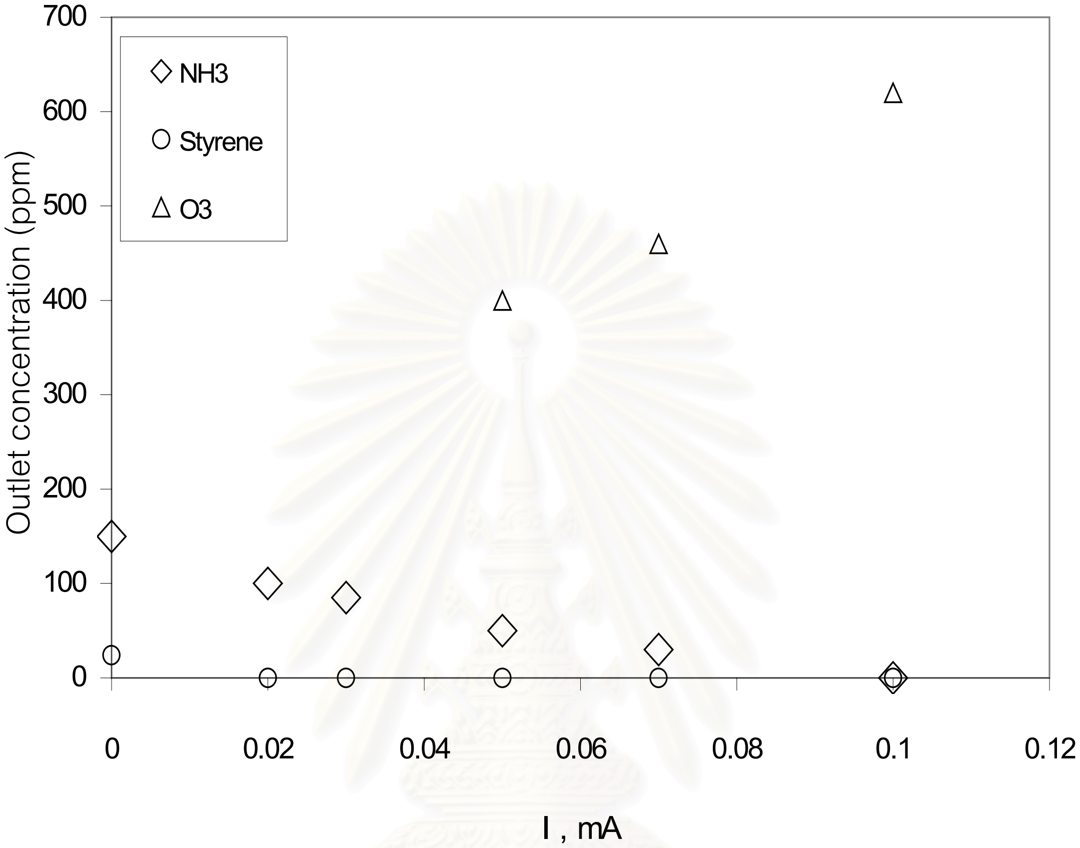

Figure 5.15 First reactor N_2-O_2(5%), $C_{in,\ ammonia}$= 200 ppm, $C_{in,\ styrene}$ = 40 ppm; SV = 55.8 hr^{-1} at room temperature

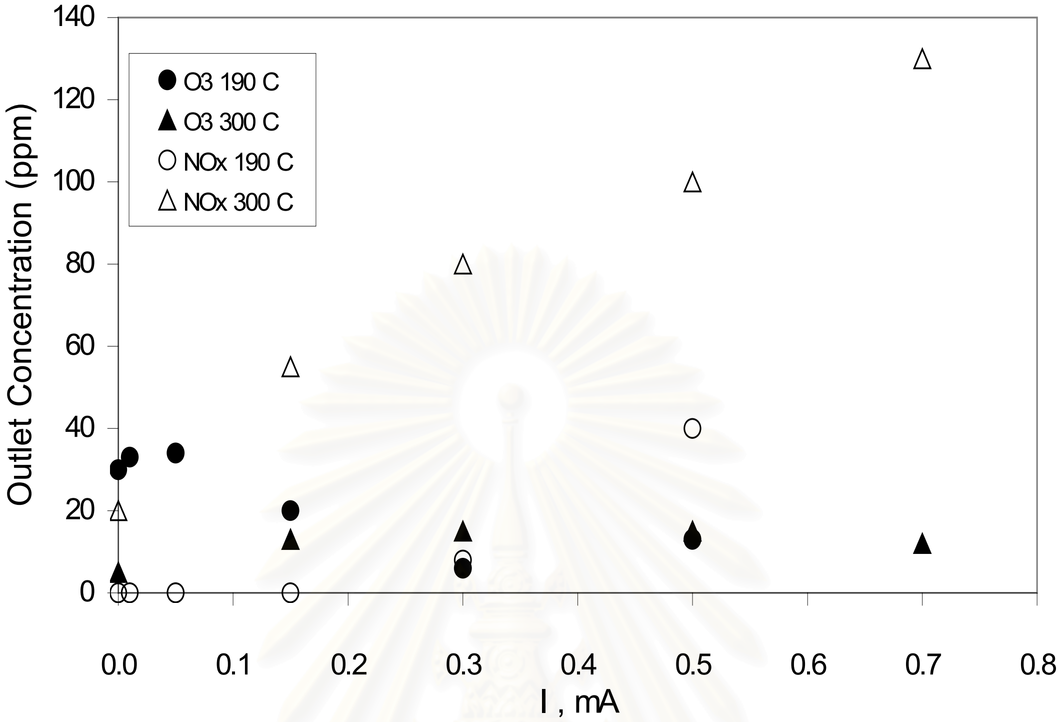

Figure 5.16 O_3 reduction and NO_x production in the second reactor

. First reactor N_2-O_2(5%), $C_{in,\ ammonia}$= 200 ppm , $C_{in,\ styrene}$ = 40 ppm ; I = 0.10 mA , SV = 55.8 hr^{-1} at room temperature ,

$[O_3]$ out from first reactor = 620 ppm,

$[O_3]$out from second reactor ,room temp = 500 ppm

5.7.2 Complete simultaneous removal of styrene and ammonia at high temperatures while minimizing reaction by-products

In the present experiment, the concentrations of styrene, ammonia, water vapor and O_2 are 40 ppm, 200 ppm, 5250 ppm and 5%, respectively. As shown in Figure 5.14(a), complete removal of styrene up to 150^0C can be achieved at the discharge current 0.1 mA in the first reactor and removal of the remaining NH_3 is to be carried out in second reactor. It is found that the remaining NH_3 from the first reactor not only adsorbs in second reactor but is also removed by ozonation reaction. In fact if the second reactor is operated at room temperature, the outlet concentration of NH_3 can even disappear without applying any discharge current but a high concentration of O_3 still remains in the effluent gas.

If the second reactor is operated at a high temperature, the outlet concentration of NH_3 from the second reactor increases because O_3 become less stable and less adsorption of NH_3 also takes place as the temperature increase.

Figure 5.17, 5.18 shows the outlet concentrations of NH_3, O_3 and NO_x from the second reactor at 185^0C and 300^0C, respectively. It can be noticed that at 300^0C high concentrations of reaction by-products are observed in the range of 0.2-0.5mA. At 185^0C the optimum current for complete removal of the residual ammonia is 0.02 mA.

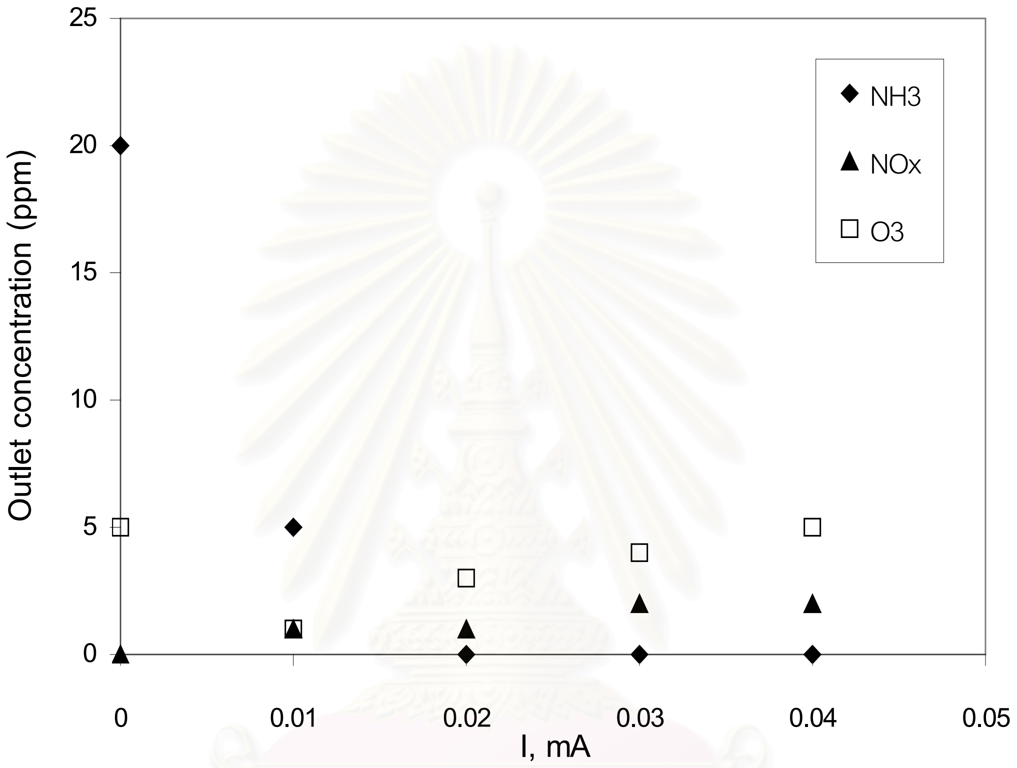

Figure 5.17 Outlet concentration from second reactor temperature at 185 ^{0}C

$C_{in,\ ammonia}$= 200 ppm , $C_{in,\ styrene}$ = 40 ppm in N_2-O_2(5%)-H_2O 5250 ppm is introduced to first reactor at T= 150^{0}C ,

I= 0.10 mA, SV = 55.8 hr^{-1},

[NH_3] out from first reactor 60 ppm

[Styrene] out from first reactor 0 ppm

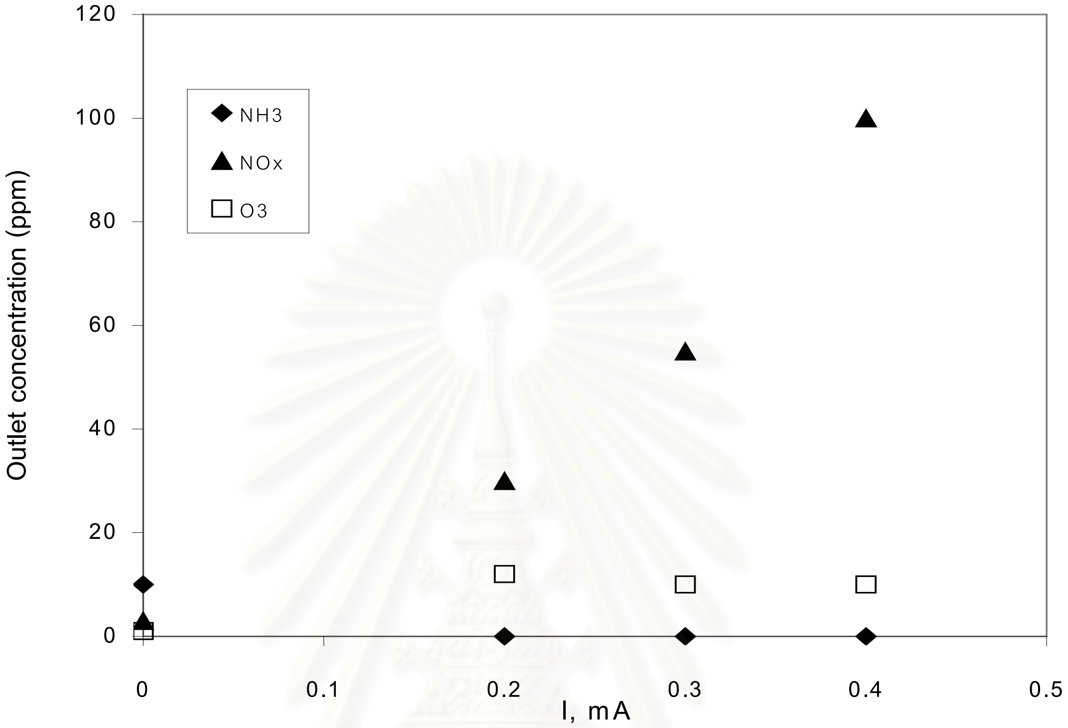

Figure 5.18 Outlet concentration from second reactor temperature at 300 ^{0}C

$C_{in,\ ammonia}$= 200 ppm , $C_{in,\ styrene}$ = 40 ppm in N_2-O_2(5%)-H_2O 5250 ppm is introduced to first reactor at T=150^{0}C ,

I= 0.10 mA, SV = 55.8 hr^{-1},

[NH_3] out from first reactor 60 ppm

[Styrene] out from first reactor 0 ppm

5.7.3 Substantiation of ozone effect

When O_2 is present in N_2 or a gas mixture, it readily reacts with electrons of sufficient energy level. Electron attachment on O_2 has been reported in the literature (Morruzzi and Phelps, 1966; Massay, 1976; Rapp and Briglia, 1976; Chantry and Schulz, 1967)

$$O_2 + e^- \longrightarrow O_2^- \qquad \text{(a)}$$

$$O_2 + e^- \longrightarrow O + O^- \qquad \text{(b)}$$

Moruzzi and Phelps (1966) report that the reaction in Equation (a) occurs in the low electron energy range ($E/p <$ 1.5 $V.m^{-1}.Pa$). In contrast, the reaction in Equation (b) occurs in the higher electron energy range. Also in a corona-discharge reactor, the closer the electrons are to the cathode wire, the higher their energy level. When O_2 collides with a high-energy electron near the cathode wire in the corona-discharge reactor, production of O^- is expected as in Equation (b). Next O_3 is produced from the reaction of O^- with O_2 (Loiseau et al., 1994; HadjZaine et al., 1992).

In short, not only O_2^- and O^- radicals but some ozone (O_3) is also produced. Since O_3 is very reactive, the ozonation reaction is used in some commercial devices for deodorization and sterilization. The same ozonation reaction as well as the oxidation reaction with O^- radicals is expected to contribute to the decomposition and removal of gas impurities in the present corona discharge reactor. The O^- radicals is also expected to contribute to the formation of ionic clusters and removal of the gas impurities.

To substantiate the role of the ozonation, two identical reactors are connected serially. Figure 5.19 shows the experimental setup used to confirm the O_3 effect. N_2-O_2 mixture is supplied to the first reactor to produce O_3 by corona discharge. Then a gas impurity is mixed into the effluent stream from the first reactor, and the resulting mixture is introduced to the second reactor. No voltage is supplied to the second reactor, so there is no corona discharge in the second reactor, which only provides space for the reaction of ozone with the impurity. Then the change in the concentration of the impurity at the outlet of the second reactor is measured. The decrease in the outlet concentration from the second reactor gives the O_3 effect.

In the experiment shows the formation of O_3 from N_2-O_2mixed gas. (N_2 75 cc/min and O_2 5 cc/min.) in first reactor is carried out at the discharge current 0.10 mA and the effluent stream is mixed with N_2 20 cc/min before feeding to the second reactor without discharge current. $[O_3]_{in}$ and $[O_3]_{out}$ of the second reactor are 500ppm and 430ppm, respectively. Next NH_3 (500 ppm balanced with N_2) at 20cc/min is mixed with N_2 80 cc/min before feeding in the second reactor. $[NH_3]_{in}$ and $[NH_3]_{out}$ are 100ppm and 75ppm, respectively. In contrast, when NH_3 (500 ppm balanced with N_2) at 20cc/min is mixed with the N_2-O_2 effluent stream (N_2 75 cc/min and O_2 5 cc/min) from the first reactor at the discharge current 0.10 mA, the outlet concentration of NH_3 at the outlet of the second reactor is reduced from 100ppm to 25 ppm. It can be confirmed that O_3 has an important role on NH_3 removal efficiency.

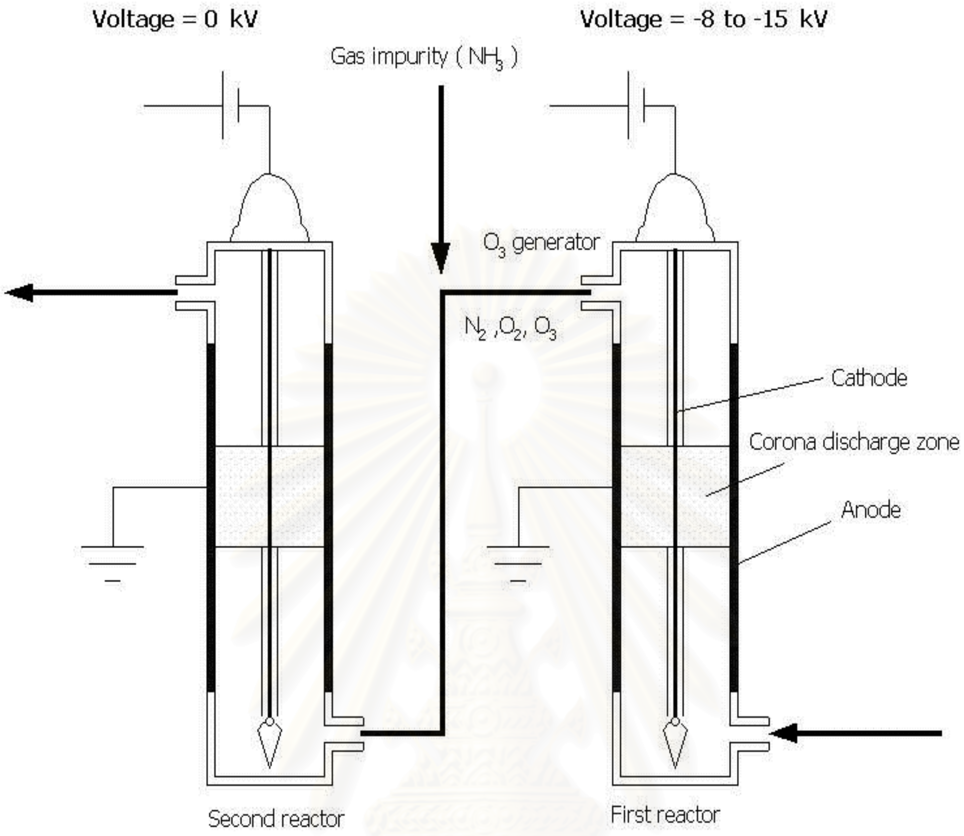

Figure 5.19 Apparatus to substantiate O_3 effect

CHAPTER VI

CONCLUSIONS AND RECOMMENDATION

6.1 Conclusions

One main purpose of the present research is to investigate the effect of temperature on the removal efficiency of styrene and/or ammonia from N_2 using electron attachment reaction. The additional factors investigated are the inlet concentration, coexisting oxygen gas, water vapor and simultaneous removal of styrene and ammonia using two reactors in series. From the results, it can be concluded as follows:

6.1.1 Effect of inlet styrene concentration on styrene removal

In the removal of styrene from nitrogen, the lower the inlet concentration of styrene, the higher the removal efficiency at room temperature to 300 ^{0}C . The removal efficiency of styrene from nitrogen and oxygen mixture is higher than from pure nitrogen because of the ozonation effect.

6.1.2 Effect of oxygen coexisting gas on styrene and/or ammonia removal

In the absence of oxygen, the removal efficiency of styrene and/or ammonia from nitrogen ψ' is a minimum when the temperature is highest at 300^{o}C. With the presence of oxygen, the higher the oxygen content, the higher the removal efficiency. Undoubtedly, the ozonation effect significantly enhances the removal efficiency.

6.1.3 Effect of water vapor on the removal of styrene and/or ammonia

The presence of water vapor in nitrogen enhances the removal efficiency of styrene but slightly retards that of ammonia. The presence of water vapor in N_2-O_2 mixed gas generally has adverse effect on the removal efficiency of styrene and/or ammonia.

6.1.4 Two corona-discharge reactors in series for removing reaction by-products

Ozone plays an important role in electron attachment reaction, but it has pungent odor and is lethal at relatively low concentrations. Increasing the temperature in the second reactor reduces ozone concentration because it becomes less stable. At 185 ^{o}C, an appropriate discharge current can minisize $O_{3,}$ whereas NO_x monotonically increases with the discharge current. At 300^{o}C, NO_x concentration increases rapidly when the discharge current is increased.

6.2 Recommendation for future work

Investigation on the other types of malodorous gas components emitted from a crematory furnace and their simultaneous removal should be carried out at various temperatures.

REFERENCES

Abouaf R., Paineau R. and Fiquet-Fayard F. Phys. B.: At Mol. Phys. 9 (1976): 303-314

Caledonia, G. E. A survey of the gas-phase negative ion kinetics of inorganic molecules - Electron Attachment Reactions. Chem. Rev. 75 (1975): 333-351.

Castle, G. S. P., Inculet, I. I., and Burgess, K. I. Ozone generation in positive corona electrostatic precipitators. IEEE Trans. Ind. and Gen. Appl. IGA-5 (1969): 489-496.

Castle, P. M., Kanter, I. E., Lee, P. K., and Kline, L. E. Corona glow detoxification study. Final Rep., Westinghouse Co., Contract No. DAAA 09-82-C-5396, 1984.

Chakarbarti, A., et al. Gas cleaning with semi-wet type plasma reactor. IEEE Trans. Ind. Appl. 31 (1995): 500-506.

Chang, J. S., and Masuda S. Mechanism of pulse corona induced plasma chemical processes for removal of NO_x and SO_x from combustion gases. Conf. Rec. IEEE/IAS 1988 Meeting (1988): 1599-1635.

Chang, J. S., and Maezono I. The electrode surface temperature profile in a corona discharge. J. Phys. D: Appl. Phys. 21 (1988): 1023-1024.

Chang, J. S., Lawless, P. A., and Yamamoto, T. Corona discharge processes. IEEE Trans. Plasma Sci. 19 (December 1991): 1152-1166.

Chang, M. B., Kushner, M. J., and Rood, M. J. Gas-phase removal of NO from gas streams via dielectric barrier discharges. Envir. Sci. and Tech. 26 (1992): 777-781.

Chang, M. B. Removal of SO_2 and NO from gas streams with combined plasma photolysis. J. Envir. Eng. ASCE, 119 (1993): 414-423.

Chang, M. B., and Tseng, T. D. Gas-phase removal of H_2S and NH_3 with dielectric barrier discharges. J. Envir. Eng. 122 (January 1996): 41-46.

Chantry, P.J. and G.J. Schulz, Phys. Rev., 156 (1967): 134

Clements, J. S., Mizuno, A., Finney, W. C., and Davis, R. H. Combined removal of SO_2, NO_x and fly ash from flue gas using pulsed streamer corona. IEEE Trans. Ind. Appl. 25 (1989): 62-69.

Davidson, J.H. and Mckinney, P.J. Chemical vapor deposition in the corona discharge of electrostatic air cleaners. Aerosol Science and Technology. 29(2) 1998.

David R. Lide. Handbook of Chemistry and Physics. 73rd ed. 1992-1993.

Dhattavorn, N. Effect of temperature on removal of toluene vapor using the electron attachment reaction. Master's degree thesis. Chulalongkorn University 2000.

Divers, E.; Ogawa, M. Ammonia amidosulphite. J. Chem. Society, Trans. 77 (1990): 327-335.

Dorsey, J. A., and Davidson, J. H. Ozone production in electrostatic air cleaners with contaminated electrodes. IEEE Trans. Ind. Appl. 30 (1994): 370-376.

Duecker, W. W., and J. R. West manufacture of sulfuric acid. ACS Monograph 144. Reinhold (1959)

Eliasson, B., Hirth, M., and Kogelschatz, U. Ozone synthesis from oxygen in dielectric barrier discharges. J. Phys. D: Applied Phys. 20 (1987): 1421-1437.

Hadj-Ziane, S., B. Held, P. Pignoleet, R. Peyrous and C. Coste, J. Phys. D: Appl. Phys. 25 (1992): 677.

Hattori, H., Ito, T., Ehara, Y., and Miyata, Y. Superposition effect on ozone synthesis by two types of discharges. Trans. IEE Japan 112A (1992): 41-46.

Helfritch, D. J., and Feldman, P. L. A pilot scale study of electron beam removal of SO_2 and NO_x from flue gas. Cottrel Envir. Sci. Somerville, N. J., Final Rep. to US DOE under Contract No. DE-FC22-81PC15079, 1985.

Helfritch, D. J. Pulsed corona discharge for hydrogen sulfide decomposition. IEEE Trans. Ind. Appl. 29, 1993.

Hickman, W. M., and R. E. Fox Electron Attachment in Sulfur Hexafluoride Usinf Monoenergetic Electron. J. Chem. Phys. 25 (1956): 642

Higashi, M., Sugaya, M., Ueki, K., and Fujii, K. Plasma processing of exhaust gas from a diesel engine vehicle. Proc. Int. Conf. on Plasma Chem. 2 (1985): 366-371.

Horvath, M. Ozone. Amsterdam, The Netherlands: Elsevier Sci., 1980.

Hsunling Bai, Fundamental Study of Ammonia-Sulfur Dioxide Reactions to Form Solid Particles. Doctoral Dissertation, Univ. of Cincinnati, USA, 1992.

Ito, T., Ehara, Y., Sakai, T., and Miyata, Y. Superposition effect on ozone synthesis by discharge. J. Jpn. Res. Group Elec. Discharges no. 127 (1990): 113-118.

Jordan, S., and Schikarski, W. Simultaneous $DeSO_x$ and $DeNO_x$ of flue gases by the EB-process in the agate pilot plant. Electron Beam Processing of Combustion Gases IAEA-TECDOC-428, (1987): 135-150.

Kamase, Y., Nagahama, T., and Mizuno, A. Removal of ethylene by streamer corona discharge. Rec. 1991 IEEE/IAS Ann. Meet. (1991): 747-751.

Kawamura, K., et al. Flue gas treatment of electron-beam irradiation. J. Atomic Energy Soc. Japan 20 (1978): 359-367.

Kohl, A. L., and Riesenfeld, F. C. Gas Purification. 3rd ed., Gulf Pub., Houston, 1979.

Khongphasarnkaln, P., Removal of Trimethylamine Acetaldehyde and Ammonia using electron attachment reaction. Master's degree thesis. Chulalongkorn University 1998.

Lagarias, J. S. Discharge electrodes and electrostatic precipitors. JAPCA 10 (1960): 271-274.

Lakdawala V. K. and Moruzzi J. L. Attachment, detachment and ion-molecule reactions in SO_2 and SO_2- O_2 mixtures. J. Phys. D: Appl. Phys., 14 (1981): 2015-26.

Landreeth, R., de Pena, R.G., Heicklen, J. Thermodynamics of the Reactions $(NH_3)_nSO_{2(g)} = nNH_{3(g)} + SO_2$. J. Phys. Chem., 78 (1974): 1378-1380.

Larpsuriyakul, K., Sano, N., Tamon, H., Tanthapanichakoon, W., and Okazaki, M. Influence of structure of corona-discharge reactor on removal of dilute gases using electron attachment. Proc. Himeji Conf. Soc. Chem. Engrs. Japan (1996): 270-271.

Larpsuriyakul, K., Charinpanitkul, T., Tanthapanichakoon, W., Sano, N., Tamon, H., and Okazaki, M. Removal of dilute gaseous impurities by electron attachment reaction using corona-discharge reactors of different structures. 7th National Conf. Chem. Eng. and Appl. Chemistry 24-25 October 1997.

Lawless, P. A., McLean, K. J., Sparks, L. E., and Ramsey, G. H. Negative corona in wire-plate electrostatic precipitators. Part I: Characteristics of individual tuft-corona discharge. J. Electrostatics 18 (1986): 199-217.

Loiseau, J.F., F. Lacassie, C. Monge, R. Peyrous, B. Held and C. Coste, J., Phys, D, 29 (1994): 63

Massay, S. H. Negative Ions. Cambridge Univ. Press, Cambridge, England, 1976.

Massay, S. H. Atomic and Molecular Collisions. Taylor & Francis, London, 1979.

Masuda, S., Hirano, M., and Akutsu, K. Enhancement of electron beam denitrization process by means of electric field. Radiat. Phys. Chem. 17 (1981): 223-228.

Masuda, S., Sato, M., and Seki, T. High efficiency ozonizer using traveling wave pulse voltage. Conf. Rec. IEEE/IAS 1984 Ann. Meet. Chicago, IL, (1984): 978-985.

Masuda, S., and Nakao, H. Control of NO_x by positive and negative pulsed corona discharges. Conf. Rec. IEEE/IAS Ann. Meet. (1986): 1173-1182.

Masuda, S., Akutsu, K., Kuroda, M., Awatsu, Y., and Shibuya, Y. A ceramic-based ozonizer using high-frequency surface discharge. IEEE Trans. Ind. Appl. IA-24 (1988): 223-231.

Masuda, S., Pulse corona induced plasma chemical process. Pure Applied Chem. 60 (1988): 727-731.

Masuda, S., and Nakao, H. Control of NO_x by positive and negative pulsed corona discharges. IEEE Trans. Ind. Appl. 26 (1990): 374-383.

Masuda, S., et al. Destruction of gaseous pollutants by surface-induced plasma chemical process (SPCP). IEEE Trans. Ind. Appl. 29 (1993): 781-786.

Mizuno, A., Clements, J. S., and Davis, R. H. The use of energetic electrons in a particle precharger and in a sulfur dioxide reactor. <u>Proc. 2nd Int. Conf. on Electrostatic Precipitation</u> (1984): 498-512.

Mizuno, A. An electrostatic precipitator using a ferroelectric pellet layer for particle collection. <u>Proc. IEEE/IES 1986 Ann. Conf</u>. (Denver, Co.) (October 1986): 1106-1112.

Mizuno, A., Clements, J. S., and Davis, R. H. A method for the removal of sulfur dioxide from exhaust gas utilizing pulsed streamer corona for electron energization. <u>IEEE Trans. Ind. Appl</u>. IA-22 (1986): 516-522.

Mizuno, A., and Ito, H. An electrostatic precipitator using a ferroelectric pellet layer for particle collection. <u>Proc. 3rd Int. Conf. on Electrostatic Precipitation</u> (1988): 617-624.

Mizuno, A., Chakrabarti, A., and Okazaki, K. Application of corona technology in the reduction of greenhouse gases and other gaseous pollutants. <u>Nonthermal Plasma Tech. Pollution Contr</u>. B. M. Penetrante and S. E. Schultheis, Ed., Berlin: Springer-Verlag, NATO ASI Series, 34 (1993): 165-185.

Mizuno, A., et al. NO_x removal process using pulsed discharge plasma. <u>IEEE Trans. Ind. Appl</u>. 3 (1995): 957-963.

Moruzzi, J. L., and Phelps, A. V. Survey of negative-ion-molecule reactions in O_2, CO_2, H_2O, CO, and mixtures of these gases at high pressures. <u>J. Chem. Phys</u>. 45 (December 1966): 4617-4627.

Nashimoto, K. The effect of electrode materials on O_3 and NO_x emissions by corona discharging. <u>J. Imaging Sci</u>. 32 (1988): 205-210.

Oda, T., et al. Decomposition of gaseous organic contaminants by surface discharge induced plasma chemical process-SPCP. <u>IEEE Trans. Ind. Appl</u>. 32 (1996): 118-124.

Oda, T., Yamashita, R., Takahashi, T., and Masuda, S. Atmospheric pressure discharge plasma decomposition for gaseous air contaminants-Trichlorotrifluoroethane and Trichloroethylene. <u>IEEE Trans. Ind. Appl</u>. 32 (1996): 227-232.

Oglesby, S., and Nichols, G. B. Electrostatic Precipitation. Marcel Dekker, New York, 1978.

Palumbo, F. J., and Fraas, F. The removal of sulfur from stack gases by an electric discharge. J. Air Pollution Contr. Assoc. 21 (1971): 143-144.

Penny, G. W., and Craig, S. E. Sparkover as influenced by surface conditions in dc corona. AIEE (1960): 112-118.

Perry, R.H., and Green, D. W. Perry's Chemical Engineers' handbook. 7th ed. New York: McGraw-Hill, 1997.

Rapp, D. And D. D. Brriglia, J. Chem. Phys., 43 (1965): 1480

Sano, N., Nagamoto, T., Tamon, H., and Okazaki, M. Removal of iodine and methyl iodide in gas by wetted-wall reactor based on selective electron attachment. J. Chem. Eng. Japan 29 (1996): 59-64.

Sano, N. Development of Gas Purification Technology by Selective Electron Attachment. Doctoral Dissertation, Kyoto Univ., Japan, 1997.

Sima-Aldrich Co. Ltd. The Aldrich Library of FT-IR Spectra 2nd ed. 1997.

Tamaki, K., et al. Oxidation of nitrogen monoxide by corona discharge - Effect of discharge conditions. Proc. Chem. Soc. Japan 11 (1979): 1582.

Tamon, H., Yano, H., and Okazaki, M. A new method of gas mixture separation based on selective electron attachment. Kagaku Kogaku Ronbunshu 15 (1989): 663-668.

Tamon, H., et al. New concept of gas purification by electron attachment. AIChE J. 41 (1995): 1701-1711.

Tanthapanichakoon, W., Larpsuriyakul, K., Sano, N., Tamon, H., and Okazaki, M. Effect of reactor structure on removal of methyl iodide and chlorofluorocarbon in gas using selective electron attachment. Proc. Regional Sym. Chem. Eng. 1996 Jakarta, Indonesia, (October 1996): 3.2.1-3.2.14.

Tanthapanichakoon, W., Larpsuriyakul, K., Charinpanitkul, T., Sano, N., Tamon, H., and Okazaki, M. Effect of structure of corona-discharge reactor on removal of dilute gaseous pollutants using selective electron attachment. J. Chem. Eng. Japan (in press).

Uhm, H.S., Influence of chamber temperature on properties of the corona discharge system. Physics of Plasmas 6(2) 1999: 623-626.

Urabe, T., et al. Removal of Hg vapor by the pulse energization. Proc. Chem. Eng. Conf. Japan (in Japanese) July 1986.

Viner, A. S., Lawless, P. A., and Ensor, D. S. Ozone generation in dc-energized electrostatic precipitators. Proc. 1989 IEEE/IAS (1989): 2167-2174.

Waddams, A. L., Acetylene derivatives Chemicals from Petroleum (1980): 58.

Weiss, H. R. Plasma induced dissociation of carbon dioxide. Proc. Int. Conf. on Plasma Chem. 2 (1985): 383-388.

White, H. J., and Cole, W. H. Design and performance of high-velocity, high-efficiency air cleaning precipitators. JAPCA 10 (1960): 239-245.

Yamamoto, T., Lawless, P. A., and Sparks, L. E. Narrow-gap point-to-plane corona with high velocity flows. IEEE Trans. Ind. Appl. 24 (1988): 934-939.

Yamamoto, T., et al. Control of volatile organic compounds by an ac energized ferroelectric pellet reactor and a pulsed corona reactor. IEEE Trans. Ind. Appl. 28 (1992): 528-534.

Yamamoto, T., Shioji, S., and Masuda, S. Synthesis of ultra-fine particles by surface discharge induced plasma chemical process (SPCP) and its application. IEEE Trans. Ind. Appl. 28 (1992): 1189-1193.

Yamamoto, T., et al. Catalysis-assisted plasma technology for carbon tetrachloride destruction. IEEE Trans. Ind. Appl. 32 (1996): 100-105.

Zhang, R., Yamamoto, T., and Bundy, D. S. Control of ammonia and odors in animal house by a ferroelectric plasma reactor. IEEE Trans. Ind. Appl. 32 (1996): 113-117.

APPENDICES

APPENDIX A
CALIBRATION CURVE OF STYRENE AND AMMONIA

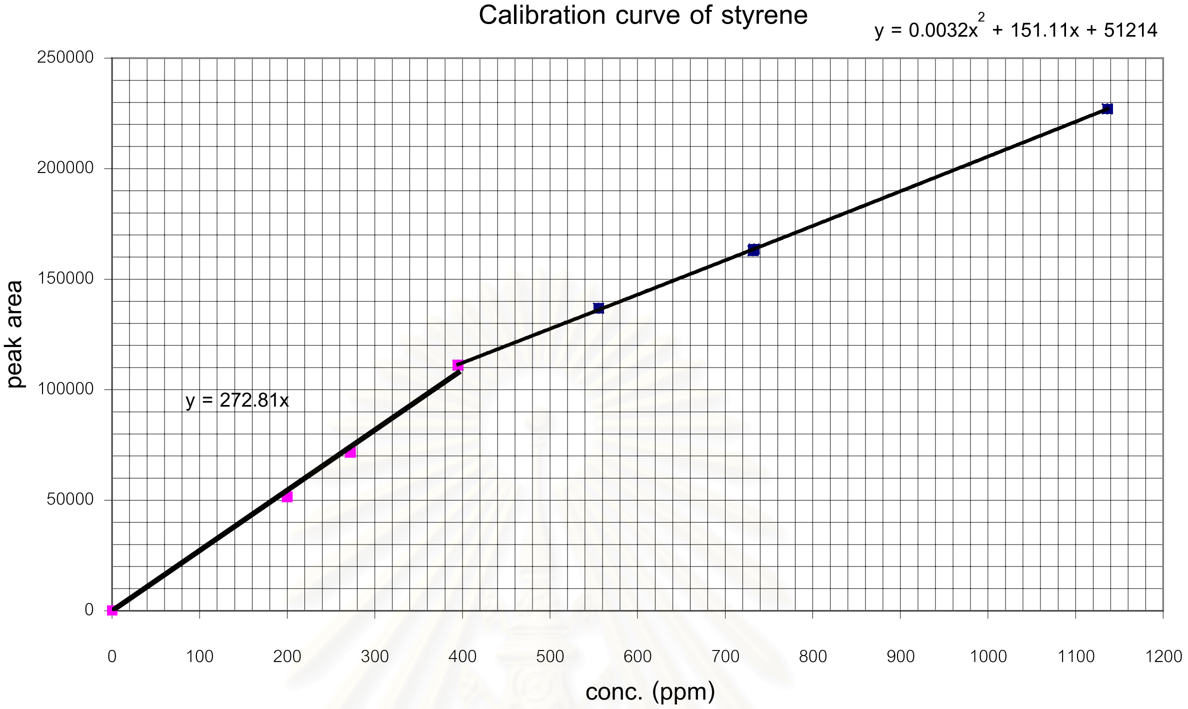

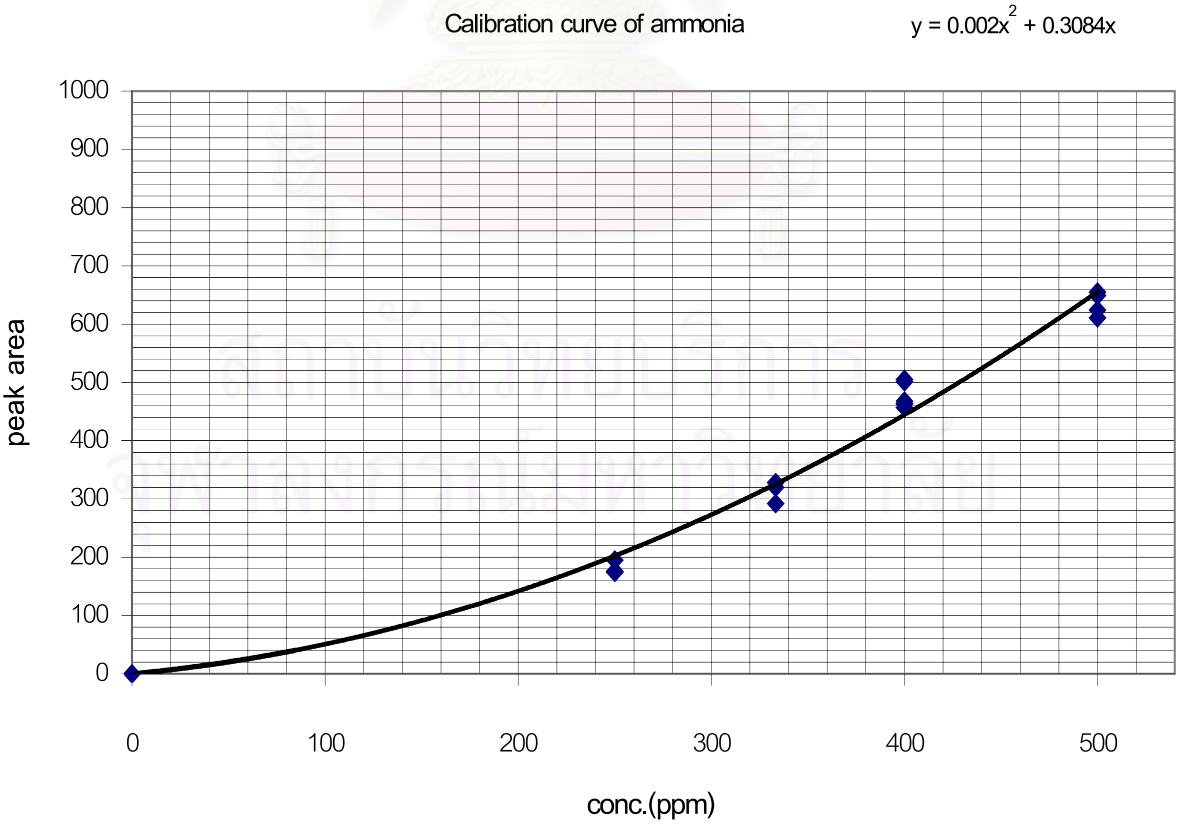

APPENDIX B
CALCULATION OF WATER VAPOR CONCENTRATION

Vapor pressure of liquid water from "PERRY'S CHEMICAL ENGINEER'S HANDBOOK" Seven Edition

Page 2-49

			N2 bubbling water flow rate (cc/min) : total flow rate (cc/min)		
T(C)	Vapor pressure (mmHg)	conc. (ppm)	10/100	20/100	30/100
0	4.579	6025	603	1205	1808
2	5.294	6966	697	1393	2090
4	6.101	8028	803	1606	2408
6	7.013	9228	923	1846	2768
8	8.045	10586	1059	2117	3176
10	9.209	12117	1212	2423	3635
12	10.518	13839	1384	2768	4152
14	11.987	15772	1577	3154	4732
16	13.634	17939	1794	3588	5382
18	15.477	20364	2036	4073	6109
20	17.535	23072	2307	4614	6922
22	19.827	26088	2609	5218	7826
24	22.377	29443	2944	5889	8833
26	25.209	33170	3317	6634	9951
28	28.349	37301	3730	7460	11190
30	31.824	41874	4187	8375	12562
32	35.663	46925	4693	9385	14078
34	39.898	52497	5250	10499	15749
36	44.563	58636	5864	11727	17591
38	49.692	65384	6538	13077	19615
40	55.324	72795	7279	14559	21838
41	58.338	76761	7676	15352	23028

APPENDIX C
CALCULATION OF RESIDENCE TIME AND SPACE VELOCITY

$$\text{Effective residence time} = \frac{\text{Volume of corona discharge region}}{\text{Volumetric flow rate}}$$

Corona discharge region (i.d. 37 mm x 100 mm)

$$= \pi \times 3.7^2 \times 10 / 4 = 107.535 \quad cm^3$$

Volumetric flow rate (at 33 ^{0}C)

$$= 100 \quad cm^3 / min$$

Volumetric flow rate (at 100 ^{0}C)

From PV = nRT ; P,n,R constant

$$= 100 \times (373/306) = 121.9 \ cm^3 / min$$

Temperature (^{0}C)	Volumetric flow rate (cc/min)	Residence time (min)	Space velocity (hr^{-1})
25	97.39	1.10	54.34
33	100.00	1.08	55.80
100	121.90	0.88	68.01
200	154.58	0.70	86.25
300	187.25	0.57	104.48

APPENDIX D
STYRENE REMOVAL

Date:	7/4/44		
Subject:	Removal of Styrene from N2		
Gas flow rate:	Styrene balanced N2 200 ppm	20	cc/min
	N2 dilute flow rate	80	cc/min
	total flow rate	100	cc/min

Inlet concentration	40	ppm	peak area(avg)	5794
Current:	0.5	mA	SV 55.8	hr^{-1}

			Peak Area		Concentration		Efficiency		
T, (^{0}C)	V(kV)	P(W)	Cout, 0 mA(avg)	Cout	Cout, 0 mA(avg)	Cout	ψ,(-)	ψ',(-)	ψ'',(-)
33	10.3	5.15	3374	-	23	0	1.00	1.00	1.02
33	10.3	5.15	3374	-	23	0	1.00	1.00	1.02
100	8.4	4.20	5187	-	36	0	1.00	1.00	1.25
100	8.4	4.20	5187	-	36	0	1.00	1.00	1.25
100	8.4	4.20	5187	-	36	0	1.00	1.00	1.25
200	6.9	3.45	5482	338	38	2	0.94	0.94	1.47
200	6.9	3.45	5482	334	38	2	0.94	0.94	1.48
200	6.9	3.45	5482	258	38	2	0.96	0.95	1.50
300	4.0	2.00	5130	1981	35	14	0.66	0.61	1.18
300	4.0	2.00	5130	1855	35	13	0.68	0.64	1.23
300	4.0	2.00	5130	1631	35	11	0.72	0.68	1.32

Date: 1/6/44

Subject: Removal of Styrene from N2

Gas flow rate:	Styrene balanced N2 200 ppm	50	cc/min
	N2 dilute flow rate	50	cc/min
	total flow rate	100	cc/min

Inlet concentration	100	ppm	peak area(avg)		14614
Current:	0.5	mA	SV	55.8	hr^{-1}

			Peak Area		Concentration		Efficiency		
T, (^{0}C)	V(kV)	P(W)	Cout, 0 mA(avg)	Cout	Cout, 0 mA(avg)	Cout	ψ,(-)	ψ',(-)	ψ'',(-)
33	11.0	5.50	10597	467	73	3	0.97	0.96	0.97
33	11.0	5.00	10597	403	73	3	0.97	0.96	0.98
33	11.0	5.00	10597	362	73	2	0.98	0.97	0.98
100	12.3	6.15	12673	408	87	3	0.97	0.97	1.21
100	12.3	6.15	12673	424	87	3	0.97	0.97	1.21
100	12.3	6.15	12673	397	87	3	0.97	0.97	1.21
200	8.5	4.25	13341	985	91	7	0.93	0.93	1.46
200	8.5	4.25	13341	1052	91	7	0.93	0.92	1.45
200	8.5	4.25	13341	1197	91	8	0.92	0.91	1.43
300	5.4	2.70	10372	4676	71	32	0.68	0.55	1.06
300	5.4	2.70	10372	4317	71	30	0.70	0.58	1.13
300	5.4	2.70	10372	4282	71	29	0.71	0.59	1.13

Date:	31/1/44		
Subject:	Removal of Styrene from N2		
Gas flow rate:	N2 bubbling flow rate	15	cc/min (cooling bath 11.6 ^{0}C)
	N2 dilute flow rate	85	cc/min
	total flow rate	100	cc/min

Inlet concentration 500 ppm

Current: 0.5 mA SV 55.8 hr^{-1}

			Peak Area		Concentration		Efficiency		
T, (^{0}C)	V(kV)	P(W)	Cout, 0 mA(avg)	Cout	Cout, 0 mA(avg)	Cout	ψ,(-)	ψ',(-)	ψ'',(-)
33	10.0	5.00	76253	42466	280	156	0.69	0.44	0.45
33	10.0	5.00	76253	42984	280	158	0.68	0.44	0.44
33	10.0	5.00	76253	40930	280	150	0.70	0.46	0.47
100	9.3	4.65	105634	60429	387	222	0.56	0.43	0.53
100	9.3	4.65	105634	59981	387	220	0.56	0.43	0.54
100	9.3	4.65	105634	60753	387	223	0.55	0.42	0.53
200	8.5	4.25	104978	65515	385	240	0.52	0.38	0.59
200	8.5	4.25	104978	66074	385	242	0.52	0.37	0.58
200	8.5	4.25	104978	65623	385	241	0.52	0.37	0.59
300	8.0	4.00	91831	53840	337	197	0.61	0.41	0.80
300	8.0	4.00	91831	54063	337	198	0.60	0.41	0.79
300	8.0	4.00	91831	56012	337	205	0.59	0.39	0.75

Date:	7/2/44			
Subject:	Removal of Styrene from N2-O2(5%)			
Gas flow rate:	N2 bubbling flow rate (styrene)	15	cc/min (cooling bath 11.6C)	
	O2 dilute flow rate	5	cc/min	
	N2 dilute flow rate	80	cc/min	
	total flow rate	100	cc/min	

Inlet concentration	500	ppm		
Current:	0.05	mA	SV	55.8 hr^{-1}

			Peak Area		Concentration		Efficiency		
T, (^{0}C)	V(kV)	P(W)	Cout, 0 mA(avg)	Cout	Cout, 0 mA(avg)	Cout	ψ,(-)	ψ',(-)	ψ'',(-)
33	10.4	0.52	57596	586	211	2	1.00	0.99	1.01
33	10.4	0.52	57596	428	211	2	1.00	0.99	1.01
33	10.4	0.52	57596	325	211	1	1.00	0.99	1.01
100	9.0	0.45	79668	10659	292	39	0.92	0.87	1.08
100	9.0	0.45	79668	10058	292	37	0.93	0.87	1.09
100	9.0	0.45	79668	10142	292	37	0.93	0.87	1.09
200	8.1	0.41	86553	16240	317	60	0.88	0.81	1.28
200	8.1	0.41	86553	16149	317	59	0.88	0.81	1.28
200	8.1	0.41	86553	16683	317	61	0.88	0.81	1.27
300	6.6	0.33	85635	46487	314	170	0.66	0.46	0.88
300	6.6	0.33	85635	44418	314	163	0.67	0.48	0.93
300	6.6	0.33	85635	45233	314	166	0.67	0.47	0.91

Date:	23/4/44		
Subject:	Removal of Styrene from N2-O2(5%)		
Gas flow rate:	N2 bubbling flow rate (styrene)	15	cc/min (cooling bath 11.6C)
	O2 dilute flow rate	5	cc/min
	N2 dilute flow rate	80	cc/min
	total flow rate	100	cc/min

Inlet concentration	500	ppm		
Current:	0.1	mA	SV	55.8 hr^{-1}

			Peak Area		Concentration		Efficiency		
T, (^{0}C)	V(kV)	P(W)	Cout, 0 mA(avg)	Cout	Cout, 0 mA(avg)	Cout	ψ,(-)	ψ',(-)	ψ'',(-)
33	11.0	1.10	57596	0	211	0	1.00	1.00	1.02
33	11.0	1.10	57596	0	211	0	1.00	1.00	1.02
33	11.0	1.10	57596	0	211	0	1.00	1.00	1.02
100	9.6	0.96	79668	514	292	2	1.00	0.99	1.24
100	9.6	0.96	79668	492	292	2	1.00	0.99	1.24
100	9.6	0.96	79668	457	292	2	1.00	0.99	1.24
200	8.7	0.87	86553	12453	317	46	0.91	0.86	1.35
200	8.7	0.87	86553	11747	317	43	0.91	0.86	1.36
200	8.7	0.87	86553	12165	317	45	0.91	0.86	1.35
300	6.9	0.69	85635	21540	314	79	0.84	0.75	1.44
300	6.9	0.69	85635	22315	314	82	0.84	0.74	1.43
300	6.9	0.69	85635	22412	314	82	0.84	0.74	1.42

Date:	9/2/44		
Subject:	Removal of Styrene from N2-O2(20%)		
Gas flow rate:	N2 bubbling flow rate (styrene)	15	cc/min (cooling bath 11.6C)
	O2 dilute flow rate	20	cc/min
	N2 dilute flow rate	65	cc/min
	total flow rate	100	cc/min

Inlet concentration 500 ppm

Current: 0.05 mA SV 55.8 hr^{-1}

			Peak Area		Concentration		Efficiency		
T, (^{0}C)	V(kV)	P(W)	Cout, 0 mA(avg)	Cout	Cout, 0 mA(avg)	Cout	ψ,(-)	ψ',(-)	ψ'',(-)
33	10.1	0.51	78466	776	288	3	0.99	0.99	1.01
33	10.1	0.51	78466	500	288	2	1.00	0.99	1.01
33	10.1	0.51	78466	200	288	1	1.00	1.00	1.02
100	9.2	0.46	78104	4180	286	15	0.97	0.95	1.18
100	9.2	0.46	78104	3760	286	14	0.97	0.95	1.19
100	9.2	0.46	78104	4550	286	17	0.97	0.94	1.18
200	7.5	0.38	82471	10537	302	39	0.92	0.87	1.37
200	7.5	0.38	82471	10186	302	37	0.93	0.88	1.38
200	7.5	0.38	82471	10749	302	39	0.92	0.87	1.37
300	6.4	0.32	84386	42341	309	155	0.69	0.50	0.96
300	6.4	0.32	84386	42034	309	154	0.69	0.50	0.97
300	6.4	0.32	84386	41263	309	151	0.70	0.51	0.99

Date:	7/4/44		
Subject:	Removal of Styrene from N2-O2(25%)		
Gas flow rate:	N2 bubbling flow rate (styrene)	15	cc/min (cooling bath 11.6C)
	O2 dilute flow rate	25	cc/min
	N2 dilute flow rate	60	cc/min
	total flow rate	100	cc/min

Inlet concentration 500 ppm

Current: 0.05 mA SV 55.8 hr^{-1}

			Peak Area		Concentration		Efficiency		
T, (^{0}C)	V(kV)	P(W)	Cout, 0 mA(avg)	Cout	Cout, 0 mA(avg)	Cout	ψ,(-)	ψ',(-)	ψ'',(-)
33	9.8	0.49	75214	0	276	0	1.00	1.00	1.02
33	9.8	0.49	75214	0	276	0	1.00	1.00	1.02
33	9.8	0.49	75214	0	276	0	1.00	1.00	1.02
100	8.7	0.44	78253	0	287	0	1.00	1.00	1.25
100	8.7	0.44	78253	0	287	0	1.00	1.00	1.25
100	8.7	0.44	78253	0	287	0	1.00	1.00	1.25
200	7.5	0.38	86958	8278	319	30	0.94	0.90	1.42
200	7.5	0.38	86958	8491	319	31	0.94	0.90	1.42
200	7.5	0.38	86958	8152	319	30	0.94	0.91	1.42
300	6.0	0.30	88828	35266	326	129	0.74	0.60	1.16
300	6.0	0.30	88828	36289	326	133	0.73	0.59	1.14
300	6.0	0.30	88828	36664	326	134	0.73	0.59	1.13

Date: 12/2/44

Subject: Removal of Styrene from N2 -H2O 4050 ppm

Gas flow rate:	N2 bubbling flow rate (styrene)	15	cc/min (cooling bath 11.6 ^{0}C)
	N2 bubbling flow rate (water)	30	cc/min (cooling bath 11.6 ^{0}C)
	N2 dilute flow rate	55	cc/min
	total flow rate	100	cc/min

Inlet concentration	styrene	500	ppm			
	H_2O	4050	ppm			
Current:	0.05	mA		SV	55.8	hr^{-1}

			Peak Area		Concentration		Efficiency		
T, (^{0}C)	V(kV)	P(W)	Cout, 0 mA(avg)	Cout	Cout, 0 mA(avg)	Cout	ψ,(-)	ψ',(-)	ψ'',(-)
33	9.4	0.47	91264	54375	335	199	0.60	0.40	0.41
33	9.4	0.47	91264	54130	335	198	0.60	0.41	0.41
100	8.2	0.41	100635	68080	369	250	0.50	0.32	0.40
100	8.2	0.41	100635	67618	369	248	0.50	0.33	0.41
100	8.2	0.41	100635	70417	369	258	0.48	0.30	0.38
100	8.2	0.41	100635	66509	369	244	0.51	0.34	0.42
200	6.2	0.31	107778	81593	395	299	0.40	0.24	0.38
200	6.2	0.31	107778	82639	395	303	0.39	0.23	0.37
200	6.2	0.31	107778	81025	395	297	0.41	0.25	0.39
300	5.6	0.28	105921	91556	388	336	0.33	0.14	0.26
300	5.6	0.28	105921	93265	388	342	0.32	0.12	0.23

Date: 14/2/44

Subject: Removal of Styrene from N2 -H2O 4050 ppm

Gas flow rate:	N2 bubbling flow rate (styrene)	15	cc/min (cooling bath 11.6 ^{0}C)
	N2 bubbling flow rate (water)	30	cc/min (cooling bath 11.6 ^{0}C)
	N2 dilute flow rate	55	cc/min
	total flow rate	100	cc/min

Inlet concentration	styrene	500	ppm		
	H_2O	4050	ppm		
Current:	0.1	mA	SV	55.8	hr^{-1}

			Peak Area		Concentration		Efficiency		
T, (^{0}C)	V(kV)	P(W)	Cout, 0 mA(avg)	Cout	Cout, 0 mA(avg)	Cout	ψ,(-)	ψ',(-)	ψ'',(-)
33	10.0	1.00	65806	27338	241	100	0.80	0.58	0.60
33	10.0	1.00	65806	27658	241	101	0.80	0.58	0.59
100	9.4	0.94	75895	42640	278	156	0.69	0.44	0.55
100	9.4	0.94	75895	45731	278	168	0.66	0.40	0.50
100	9.4	0.94	75895	46741	278	171	0.66	0.38	0.48
200	7.0	0.70	92573	58932	339	216	0.57	0.36	0.57
200	7.0	0.70	92573	57932	339	212	0.58	0.37	0.59
200	7.0	0.70	92573	57788	339	212	0.58	0.38	0.59
300	6.4	0.64	98723	68781	362	252	0.50	0.30	0.59
300	6.4	0.64	98723	65669	362	241	0.52	0.33	0.65
300	6.4	0.64	98723	69580	362	255	0.49	0.30	0.57

Date:	13/2/44		
Subject:	Removal of Styrene from N2 -H2O 13320 ppm		
Gas flow rate:	N2 bubbling flow rate (styrene)	15	cc/min (cooling bath 11.6 ^{0}C)
	N2 bubbling flow rate (water)	30	cc/min (water bath 31.0 ^{0}C)
	N2 dilute flow rate	55	cc/min
	total flow rate	100	cc/min

Inlet concentration	styrene	500	ppm		
	H_2O	13320	ppm		
Current:	0.1	mA	SV	55.8	hr^{-1}

			Peak Area		Concentration		Efficiency		
T, (^{0}C)	V(kV)	P(W)	Cout, 0 mA(avg)	Cout	Cout, 0 mA(avg)	Cout	ψ,(-)	ψ',(-)	ψ'',(-)
33	10.5	1.05	63853	12361	234	45	0.91	0.81	0.82
33	10.5	1.05	63853	12404	234	45	0.91	0.81	0.82
33	10.5	1.05	63853	12661	234	46	0.91	0.80	0.82
100	8.9	0.89	91011	38567	334	141	0.72	0.58	0.72
100	8.9	0.89	91011	35878	334	132	0.74	0.61	0.76
100	8.9	0.89	91011	33893	334	124	0.75	0.63	0.78
200	6.9	0.69	95083	50626	349	186	0.63	0.47	0.73
200	6.9	0.69	95083	51134	349	187	0.63	0.46	0.73
200	6.9	0.69	95083	50545	349	185	0.63	0.47	0.74
300	5.6	0.56	97806	62241	359	228	0.54	0.36	0.70
300	5.6	0.56	97806	61161	359	224	0.55	0.37	0.72
300	5.6	0.56	97806	66652	359	244	0.51	0.32	0.61

Date:	13/2/44		
Subject:	Removal of Styrene from N2 -H2O 13320 ppm		
Gas flow rate:	N2 bubbling flow rate (styrene)	15	cc/min (cooling bath 11.6 ^{0}C)
	N2 bubbling flow rate (water)	30	cc/min (water bath 31.0 ^{0}C)
	N2 dilute flow rate	55	cc/min
	total flow rate	100	cc/min

Inlet concentration	styrene	500	ppm		
	H_2O	13320	ppm		
Current:	0.15	mA	SV	55.8	hr^{-1}

			Peak Area		Concentration		Efficiency		
T, (^{0}C)	V(kV)	P(W)	Cout, 0 mA(avg)	Cout	Cout, 0 mA(avg)	Cout	ψ,(-)	ψ',(-)	ψ'',(-)
33	10.8	1.62	63853	8529	234	31	0.94	0.87	0.88
33	10.8	1.62	63853	8190	234	30	0.94	0.87	0.89
33	10.8	1.62	63853	8860	234	32	0.94	0.86	0.88
100	9.3	1.40	91011	28864	334	106	0.79	0.68	0.85
100	9.3	1.40	91011	32141	334	118	0.77	0.65	0.81
100	9.3	1.40	91011	32401	334	119	0.76	0.64	0.80
200	7.6	1.14	93583	45243	343	166	0.67	0.52	0.81
200	7.6	1.14	93583	45693	343	167	0.67	0.51	0.80
200	7.6	1.14	93583	45980	343	169	0.67	0.51	0.80
300	6.4	0.96	97806	51232	359	188	0.63	0.48	0.92
300	6.4	0.96	97806	51435	359	189	0.63	0.47	0.91
300	6.4	0.96	97806	53215	359	195	0.61	0.46	0.88

Date: 17/2/44

Subject: Removal of Styrene from N2 -H2O 21838 ppm

Gas flow rate:	N2 bubbling flow rate (styrene)	15	cc/min (cooling bath 11.6 ^{0}C)
	N2 bubbling flow rate (water)	30	cc/min (water bath 44.0 ^{0}C)
	N2 dilute flow rate	55	cc/min
	total flow rate	100	cc/min

Inlet concentration styrene 500 ppm

H_2O 21838 ppm

Current: 0.1 mA SV 55.8 hr^{-1}

			Peak Area		Concentration		Efficiency		
T, (^{0}C)	V(kV)	P(W)	Cout, 0 mA(avg)	Cout	Cout, 0 mA(avg)	Cout	ψ,(-)	ψ',(-)	ψ'',(-)
33	10.3	1.03	60708	18164	223	67	0.87	0.70	0.71
33	10.3	1.03	60708	16086	223	59	0.88	0.74	0.75
33	10.3	1.03	60708	16169	223	59	0.88	0.73	0.75
100	8.8	0.88	89913	46771	330	171	0.66	0.48	0.60
100	8.8	0.88	89913	45565	330	167	0.67	0.49	0.62
100	8.8	0.88	89913	42315	330	155	0.69	0.53	0.66
200	7.1	0.71	93646	55879	343	205	0.59	0.40	0.63
200	7.1	0.71	93646	55943	343	205	0.59	0.40	0.63
200	7.1	0.71	93646	55615	343	204	0.59	0.41	0.64
300	4.9	0.49	94487	63995	346	235	0.53	0.32	0.62
300	4.9	0.49	94487	66928	346	245	0.51	0.29	0.56
300	4.9	0.49	94487	64517	346	236	0.53	0.32	0.61

Date: 19/2 /44

Subject: Removal of Styrene from N2 -O2(5%)-H2O 4050 ppm

Gas flow rate: N2 bubbling flow rate (styrene) 15 cc/min (cooling bath 11.6 ^{0}C)
N2 bubbling flow rate (water) 30 cc/min (cooling bath 11.6 ^{0}C)
O2 flow rate 5 cc/min
N2 dilute flow rate 50 cc/min
total flow rate 100 cc/min

Inlet concentration styrene 500 ppm
H_2O 4050 ppm
Current: 0.05 mA SV 55.8 hr^{-1}

			Peak Area		Concentration		Efficiency		
T, (^{0}C)	V(kV)	P(W)	Cout, 0 mA(avg)	Cout	Cout, 0 mA(avg)	Cout	ψ,(-)	ψ',(-)	ψ'',(-)
33	10.2	0.51	59884	366	220	1	1.00	0.99	1.01
33	10.2	0.51	59884	284	220	1	1.00	1.00	1.01
33	10.2	0.51	59884	325	220	1	1.00	0.99	1.01
100	9.1	0.46	86515	21318	317	78	0.84	0.75	0.94
100	9.1	0.46	86515	18841	317	69	0.86	0.78	0.98
100	9.1	0.46	86515	23705	317	87	0.83	0.73	0.91
200	7.3	0.37	90918	36808	333	135	0.73	0.60	0.94
200	7.3	0.37	90918	34878	333	128	0.74	0.62	0.97
300	6.0	0.30	91242	49095	334	180	0.64	0.46	0.89
300	6.0	0.30	91242	49156	334	180	0.64	0.46	0.89
300	6.0	0.30	91242	49118	334	180	0.64	0.46	0.89

Date: 20/2/44

Subject: Removal of Styrene from N2 -O2(5%)-H2O 12940 ppm

Gas flow rate:	N2 bubbling flow rate (styrene)	15	cc/min (cooling bath 11.6 ^{0}C)
	N2 bubbling flow rate (water)	30	cc/min (water bath 30.5 ^{0}C)
	O2 flow rate	5	cc/min
	N2 dilute flow rate	50	cc/min
	total flow rate	100	cc/min

Inlet concentration	styrene	500	ppm
	H_2O	12940	ppm

Current: 0.05 mA SV 55.8 hr^{-1}

			Peak Area		Concentration		Efficiency		
T, (^{0}C)	V(kV)	P(W)	Cout, 0 mA(avg)	Cout	Cout, 0 mA(avg)	Cout	ψ,(-)	ψ',(-)	ψ'',(-)
33	10.7	0.54	66107	2372	242	9	0.98	0.96	0.98
33	10.7	0.54	66107	2055	242	8	0.98	0.97	0.99
33	10.7	0.54	66107	1827	242	7	0.99	0.97	0.99
100	9.0	0.45	79593	20030	292	73	0.85	0.75	0.94
100	9.0	0.45	79593	18547	292	68	0.86	0.77	0.96
100	9.0	0.45	79593	24095	292	88	0.82	0.70	0.87
200	7.4	0.37	86088	28877	316	106	0.79	0.66	1.04
200	7.4	0.37	86088	25766	316	94	0.81	0.70	1.10
200	7.4	0.37	86088	29713	316	109	0.78	0.65	1.03
300	6.0	0.30	86383	44005	317	161	0.68	0.49	0.95
300	6.0	0.30	86383	44070	317	162	0.68	0.49	0.95
300	6.0	0.30	86383	44782	317	164	0.67	0.48	0.93

Date: 22/2/44

Subject: Removal of Styrene from N2 -O2(5%)-H2O 23028 ppm

Gas flow rate:	N2 bubbling flow rate (styrene)	15	cc/min (cooling bath 11.6 ^{0}C)
	N2 bubbling flow rate (water)	30	cc/min (water bath 41.0 ^{0}C)
	O2 flow rate	5	cc/min
	N2 dilute flow rate	50	cc/min
	total flow rate	100	cc/min

Inlet concentration	styrene	500	ppm
	H_2O	23028	ppm

Current: 0.05 mA SV 55.8 hr^{-1}

			Peak Area		Concentration		Efficiency		
T, (^{0}C)	V(kV)	P(W)	Cout, 0 mA(avg)	Cout	Cout, 0 mA(avg)	Cout	ψ,(-)	ψ',(-)	ψ'',(-)
33	10.2	0.51	67572	0	248	0	1.00	1.00	1.02
33	10.2	0.51	67572	0	248	0	1.00	1.00	1.02
33	10.2	0.51	67572	0	248	0	1.00	1.00	1.02
100	8.9	0.45	87768	17881	322	66	0.87	0.80	1.00
100	8.9	0.45	87768	17515	322	64	0.87	0.80	1.00
100	8.9	0.45	87768	17631	322	65	0.87	0.80	1.00
200	7.3	0.37	88372	26251	324	96	0.81	0.70	1.10
200	7.3	0.37	88372	25732	324	94	0.81	0.71	1.11
200	7.3	0.37	88372	25614	324	94	0.81	0.71	1.12
300	6.0	0.30	90871	40745	333	149	0.70	0.55	1.06
300	6.0	0.30	90871	39044	333	143	0.71	0.57	1.10
300	6.0	0.30	90871	39514	333	145	0.71	0.57	1.09

Date: 19/2 /44

Subject: Removal of Styrene from N2 -O2(10%)-H2O 4050 ppm

Gas flow rate: N2 bubbling flow rate (styrene) 15 cc/min (cooling bath 11.6 ^{0}C)
N2 bubbling flow rate (water) 30 cc/min (cooling bath 11.6 ^{0}C)
O2 flow rate 10 cc/min
N2 dilute flow rate 45 cc/min
total flow rate 100 cc/min

Inlet concentration styrene 500 ppm
H_2O 4050 ppm

Current: 0.05 mA SV 55.8 hr^{-1}

			Peak Area		Concentration		Efficiency		
T, (^{0}C)	V(kV)	P(W)	Cout, 0 mA(avg)	Cout	Cout, 0 mA(avg)	Cout	ψ,(-)	ψ',(-)	ψ'',(-)
33	10.1	0.51	64758	0	237	0	1.00	1.00	1.02
33	10.1	0.51	64758	0	237	0	1.00	1.00	1.02
33	10.1	0.51	64758	0	237	0	1.00	1.00	1.02
100	8.9	0.45	86231	18393	316	67	0.87	0.79	0.98
100	8.9	0.45	86231	19577	316	72	0.86	0.77	0.97
100	8.9	0.45	86231	20964	316	77	0.85	0.76	0.95
200	7.1	0.36	89211	30309	327	111	0.78	0.66	1.04
200	7.1	0.36	89211	27159	327	100	0.80	0.70	1.09
200	7.1	0.36	89211	30108	327	110	0.78	0.66	1.04
300	5.9	0.30	90187	48076	331	176	0.65	0.47	0.90
300	5.9	0.30	90187	45762	331	168	0.66	0.49	0.95
300	5.9	0.30	90187	46944	331	172	0.66	0.48	0.93

Date: 20/2/44

Subject: Removal of Styrene from N2 -O2(10%)-H2O 12940 ppm

Gas flow rate:	N2 bubbling flow rate (styrene)	15	cc/min (cooling bath 11.6 ^{0}C)
	N2 bubbling flow rate (water)	30	cc/min (water bath 30.5 ^{0}C)
	O2 flow rate	10	cc/min
	N2 dilute flow rate	45	cc/min
	total flow rate	100	cc/min

Inlet concentration	styrene	500	ppm		
	H_2O	12940	ppm		
Current:	0.05	mA	SV	55.8	hr^{-1}

			Peak Area		Concentration		Efficiency		
T, (^{0}C)	V(kV)	P(W)	Cout, 0 mA(avg)	Cout	Cout, 0 mA(avg)	Cout	ψ,(-)	ψ',(-)	ψ'',(-)
33	10.3	0.52	67325	0	247	0	1.00	1.00	1.02
33	10.3	0.52	67325	0	247	0	1.00	1.00	1.02
33	10.3	0.52	67325	0	247	0	1.00	1.00	1.02
100	9.0	0.45	86049	16395	315	60	0.88	0.81	1.01
100	9.0	0.45	86049	20316	315	74	0.85	0.76	0.95
100	9.0	0.45	86049	20031	315	73	0.85	0.77	0.96
200	7.3	0.37	90899	30624	333	112	0.78	0.66	1.04
200	7.3	0.37	90899	26588	333	97	0.81	0.71	1.11
200	7.3	0.37	90899	26443	333	97	0.81	0.71	1.11
300	6.2	0.31	90875	42727	333	157	0.69	0.53	1.02
300	6.2	0.31	90875	42258	333	155	0.69	0.53	1.03
300	6.2	0.31	90875	42535	333	156	0.69	0.53	1.03

Date:	22/2/44			
Subject:	Removal of Styrene from N2 -O2(10%)-H2O 23028 ppm			
Gas flow rate:	N2 bubbling flow rate (styrene)	15	cc/min	(cooling bath 11.6 ^{0}C)
	N2 bubbling flow rate (water)	30	cc/min	(water bath 41.0 ^{0}C)
	O2 flow rate	10	cc/min	
	N2 dilute flow rate	45	cc/min	
	total flow rate	100	cc/min	

Inlet concentration	styrene	500	ppm		
	H_2O	23028	ppm		
Current:	0.05	mA	SV	55.8	hr^{-1}

			Peak Area		Concentration		Efficiency		
T, (^{0}C)	V(kV)	P(W)	Cout, 0 mA(avg)	Cout	Cout, 0 mA(avg)	Cout	ψ,(-)	ψ',(-)	ψ'',(-)
33	10.1	0.51	67857	0	249	0	1.00	1.00	1.02
33	10.1	0.51	67857	0	249	0	1.00	1.00	1.02
33	10.1	0.51	67857	0	249	0	1.00	1.00	1.02
100	9.0	0.45	86324	14895	316	55	0.89	0.83	1.03
100	9.0	0.45	86324	15316	316	56	0.89	0.82	1.03
100	9.0	0.45	86324	15031	316	55	0.89	0.83	1.03
200	7.4	0.37	89760	22643	329	83	0.83	0.75	1.18
200	7.4	0.37	89760	21874	329	80	0.84	0.76	1.19
200	7.4	0.37	89760	22445	329	82	0.84	0.75	1.18
300	5.9	0.30	89875	34841	329	128	0.74	0.61	1.18
300	5.9	0.30	89875	34922	329	128	0.74	0.61	1.18
300	5.9	0.30	89875	36196	329	133	0.73	0.60	1.15

Date:	19/2 /44			
Subject:	Removal of Styrene from N2 -O2(20%)-H2O 4050 ppm			
Gas flow rate:	N2 bubbling flow rate (styrene)	15	cc/min	(cooling bath 11.6 ^{0}C)
	N2 bubbling flow rate (water)	30	cc/min	(cooling bath 11.6 ^{0}C)
	O2 flow rate	20	cc/min	
	N2 dilute flow rate	35	cc/min	
	total flow rate	100	cc/min	

Inlet concentration	styrene	500	ppm		
	H_2O	4050	ppm		
Current:	0.05	mA	SV	55.8	hr^{-1}

			Peak Area		Concentration		Efficiency		
T, (^{0}C)	V(kV)	P(W)	Cout, 0 mA(avg)	Cout	Cout, 0 mA(avg)	Cout	ψ,(-)	ψ',(-)	ψ'',(-)
33	10.3	0.52	62415	0	229	0	1.00	1.00	1.02
100	9.0	0.45	84436	5381	310	20	0.96	0.94	1.17
100	9.0	0.45	84436	6432	310	24	0.95	0.92	1.15
100	9.0	0.45	84436	4832	310	18	0.96	0.94	1.18
200	7.4	0.37	87572	19696	321	72	0.86	0.78	1.22
200	7.4	0.37	87572	18945	321	69	0.86	0.78	1.23
200	7.4	0.37	87572	19375	321	71	0.86	0.78	1.22
300	6.0	0.30	90735	29614	333	109	0.78	0.67	1.30
300	6.0	0.30	90735	32920	333	121	0.76	0.64	1.23
300	6.0	0.30	90735	27660	333	101	0.80	0.70	1.34

Date:	20/2/44			
Subject:	Removal of Styrene from N2 -O2(20%)-H2O 12940 ppm			
Gas flow rate:	N2 bubbling flow rate (styrene)	15	cc/min	(cooling bath 11.6 ^{0}C)
	N2 bubbling flow rate (water)	30	cc/min	(water bath 30.5 ^{0}C)
	O2 flow rate	20	cc/min	
	N2 dilute flow rate	35	cc/min	
	total flow rate	100	cc/min	

Inlet concentration	styrene	500	ppm		
	H_2O	12940	ppm		
Current:	0.05	mA	SV	55.8	hr^{-1}

			Peak Area		Concentration		Efficiency		
T, (^{0}C)	V(kV)	P(W)	Cout, 0 mA(avg)	Cout	Cout, 0 mA(avg)	Cout	ψ,(-)	ψ',(-)	ψ'',(-)
33	10.4	0.52	67535	0	248	0	1.00	1.00	1.02
33	10.4	0.52	67535	0	248	0	1.00	1.00	1.02
33	10.4	0.52	67535	0	248	0	1.00	1.00	1.02
100	9.1	0.46	86476	4321	317	16	0.97	0.95	1.19
100	9.1	0.46	86476	3586	317	13	0.97	0.96	1.20
100	9.1	0.46	86476	5213	317	19	0.96	0.94	1.17
200	7.3	0.37	87558	17681	321	65	0.87	0.80	1.25
200	7.3	0.37	87558	18547	321	68	0.86	0.79	1.24
200	7.3	0.37	87558	17965	321	66	0.87	0.79	1.25
300	5.9	0.30	91025	28763	334	105	0.79	0.68	1.32
300	5.9	0.30	91025	27524	334	101	0.80	0.70	1.35
300	5.9	0.30	91025	31067	334	114	0.77	0.66	1.27

Date:	22/2/44			
Subject:	Removal of Styrene from N2 -O2(20%)-H2O 23028 ppm			
Gas flow rate:	N2 bubbling flow rate (styrene)	15	cc/min	(cooling bath 11.6 ^{0}C)
	N2 bubbling flow rate (water)	30	cc/min	(water bath 41.0 ^{0}C)
	O2 flow rate	20	cc/min	
	N2 dilute flow rate	35	cc/min	
	total flow rate	100	cc/min	

Inlet concentration	styrene	500	ppm			
	H_2O	23028	ppm			
Current:	0.05	mA		SV	55.8	hr^{-1}

			Peak Area		Concentration		Efficiency		
T, (^{0}C)	V(kV)	P(W)	Cout, 0 mA(avg)	Cout	Cout, 0 mA(avg)	Cout	ψ,(-)	ψ',(-)	ψ'',(-)
33	10.1	0.51	67658	0	248	0	1.00	1.00	1.02
33	10.1	0.51	67658	0	248	0	1.00	1.00	1.02
33	10.1	0.51	67658	0	248	0	1.00	1.00	1.02
100	8.9	0.45	70369	3576	258	13	0.97	0.95	1.19
100	8.9	0.45	70369	2846	258	10	0.98	0.96	1.20
100	8.9	0.45	70369	4132	258	15	0.97	0.94	1.18
200	7.3	0.37	70155	16730	257	61	0.88	0.76	1.20
200	7.3	0.37	70155	15950	257	58	0.88	0.77	1.21
200	7.3	0.37	70155	16120	257	59	0.88	0.77	1.21
300	6.0	0.30	75461	40581	277	149	0.70	0.46	0.89
300	6.0	0.30	75461	47099	277	173	0.65	0.38	0.73
300	6.0	0.30	75461	45022	277	165	0.67	0.40	0.78

APPENDIX E
AMMONIA REMOVAL

Date:	4/4/44		
Subject:	Removal of NH_3 from N_2		
Gas flow rate:	NH_3 balanced N_2 500 ppm	50	cc/min
	N_2 dilute flow rate	50	cc/min
	total flow rate	100	cc/min

Inlet concentration	250	ppm	peak area(avg)		215
Current:	0.3	mA	SV	55.8	hr^{-1}

			Peak Area		Concentration		Efficiency		
T, (^{0}C)	V(kV)	P(W)	Cout, 0 mA(avg)	Cout	Cout, 0 mA(avg)	Cout	ψ,(-)	ψ',(-)	ψ'',(-)
33	8.1	2.43	197	120	229	140	0.44	0.39	0.40
33	8.1	2.43	197	132	229	153	0.39	0.33	0.34
33	8.1	5.00	197	116	229	135	0.46	0.41	0.42
100	6.9	2.07	201	135	234	157	0.37	0.33	0.41
100	6.9	2.07	201	133	234	155	0.38	0.34	0.42
200	5.1	1.53	212	131	247	152	0.39	0.38	0.60
300	3.5	1.05	215	146	250	170	0.32	0.32	0.62

Date:	7/3/44		
Subject:	Removal of NH3 from N2-H2O(5250ppm)		
Gas flow rate:	NH3 balance N2 500ppm	50	cc/min
	N2 bubbling flow rate (water)	10	cc/min (water bath 34^{0}C)
	N2 dilute flow rate	40	cc/min
	total flow rate	100	cc/min

Inlet concentration	NH3	250	ppm		
	H2O	5250	ppm		
Current:	0.3	mA	SV	55.8	hr^{-1}

			Peak Area		Concentration		Efficiency		
T, (^{0}C)	V(kV)	P(W)	Cout, 0 mA(avg)	Cout	Cout, 0 mA(avg)	Cout	ψ,(-)	ψ',(-)	ψ'',(-)
33	8.7	2.61	210	118	190	115	0.54	0.39	0.40
33	8.7	2.61	210	135	190	129	0.48	0.32	0.33
33	8.7	2.61	210	136	190	130	0.48	0.32	0.32
100	7.2	2.16	238	154	212	145	0.42	0.32	0.40
100	7.2	2.16	238	151	212	143	0.43	0.33	0.41
100	7.2	2.16	238	158	212	149	0.40	0.30	0.37
200	5.1	1.53	332	166	279	155	0.38	0.44	0.70
200	5.1	1.53	332	154	279	145	0.42	0.48	0.75
200	5.1	1.53	332	200	279	182	0.27	0.35	0.55
300	3.6	1.08	317	240	268	213	0.15	0.21	0.40
300	3.6	1.08	317	246	268	218	0.13	0.19	0.36
300	3.6	1.08	317	251	268	221	0.12	0.18	0.34

Date: 5/3/44

Subject: Removal of NH_3 from N_2-H_2O(10500ppm)

Gas flow rate:	NH_3 balance N_2 500ppm	50	cc/min
	N_2 bubbling flow rate (water)	20	cc/min (water bath 34°C)
	N_2 dilute flow rate	30	cc/min
	total flow rate	100	cc/min

Inlet concentration	NH_3	250	ppm		
	H_2O	10500	ppm		
Current:	0.3	mA	SV	55.8	hr^{-1}

			Peak Area		Concentration		Efficiency		
T, (°C)	V(kV)	P(W)	Cout, 0 mA(avg)	Cout	Cout, 0 mA(avg)	Cout	ψ,(-)	ψ',(-)	ψ'',(-)
33	8.3	2.49	231	162	206	152	0.39	0.26	0.27
33	8.3	2.49	231	154	206	145	0.42	0.30	0.30
33	8.3	2.49	231	156	206	147	0.41	0.29	0.29
100	6.8	2.04	262	166	229	155	0.38	0.32	0.40
100	6.8	2.04	262	164	229	154	0.38	0.33	0.41
100	6.8	2.04	262	165	229	155	0.38	0.32	0.40
200	5.1	1.53	359	177	297	164	0.34	0.45	0.70
200	5.1	1.53	359	169	297	158	0.37	0.47	0.74
200	5.1	1.53	359	181	297	167	0.33	0.44	0.69
300	3.7	1.11	306	239	261	212	0.15	0.19	0.36
300	3.7	1.11	306	257	261	226	0.10	0.13	0.26
300	3.7	1.11	306	245	261	217	0.13	0.17	0.33

Date:	10/3/44		
Subject:	Removal of NH_3 from N_2-H_2O(23028ppm)		
Gas flow rate:	NH_3 balance N_2 500ppm	50	cc/min
	N_2 bubbling flow rate (water)	20	cc/min (water bath 41^{0}C)
	N_2 dilute flow rate	30	cc/min
	total flow rate	100	cc/min

Inlet concentration	250	ppm			
Current:	0.3	mA	SV	55.8	hr^{-1}

			Peak Area		Concentration		Efficiency		
T, (^{0}C)	V(kV)	P(W)	Cout, 0 mA(avg)	Cout	Cout, 0 mA(avg)	Cout	ψ,(-)	ψ',(-)	ψ'',(-)
33	8.7	2.61	182	143	168	136	0.46	0.19	0.19
33	8.7	2.61	182	136	168	130	0.48	0.23	0.23
33	8.7	2.61	182	141	168	135	0.46	0.20	0.20
100	6.6	1.98	213	156	193	147	0.41	0.24	0.30
100	6.6	1.98	213	159	193	150	0.40	0.22	0.28
100	6.6	1.98	213	165	193	155	0.38	0.20	0.25
200	5.2	1.56	236	193	210	177	0.29	0.16	0.25
200	5.2	1.56	236	177	210	164	0.34	0.22	0.34
200	5.2	1.56	236	191	210	175	0.30	0.17	0.26
300	4.1	1.23	222	164	200	154	0.38	0.23	0.44
300	4.1	1.23	222	180	200	167	0.33	0.17	0.32
300	4.1	1.23	222	181	200	167	0.33	0.17	0.32

Date: 27/2/44

Subject: Removal of NH_3 from N_2

Gas flow rate: NH_3 balanced N_2 500 ppm 80 cc/min

N2 dilute flow rate 20 cc/min

total flow rate 100 cc/min

Inlet concentration 400 ppm

Current: 0.5 mA SV 55.8 hr^{-1}

			Peak Area		Concentration		Efficiency		
T, (^{0}C)	V(kV)	P(W)	Cout, 0 mA(avg)	Cout	Cout, 0 mA(avg)	Cout	ψ,(-)	ψ',(-)	ψ'',(-)
33	7.6	3.80	433	299	395	317	0.21	0.20	0.20
33	7.6	5.00	433	283	395	307	0.23	0.22	0.23
33	7.6	5.00	433	266	395	296	0.26	0.25	0.25
100	6.2	3.10	409	277	382	303	0.24	0.21	0.26
100	6.2	3.10	409	283	382	307	0.23	0.20	0.24
100	6.2	3.10	409	272	382	300	0.25	0.21	0.27
200	5.3	2.65	380	209	366	255	0.36	0.30	0.48
200	5.3	2.65	380	196	366	245	0.39	0.33	0.52
200	5.3	2.65	380	208	366	255	0.36	0.30	0.48
250	4.3	2.15	361	165	355	220	0.45	0.38	0.66
250	4.3	2.15	361	186	355	238	0.41	0.33	0.58
250	4.3	2.15	361	166	355	221	0.45	0.38	0.66
300	3.9	1.95	209	141	255	199	0.50	0.22	0.43
300	3.9	1.95	209	149	255	207	0.48	0.19	0.36
300	3.9	1.95	209	144	255	202	0.50	0.21	0.40

Date:	28/2/44		
Subject:	Removal of NH_3 from N_2-O_2 (5%)		
Gas flow rate:	NH_3 balanced N_2 500 ppm	80	cc/min
	N_2 dilute flow rate	15	cc/min
	O_2 flow rate	5	cc/min
	total flow rate	100	cc/min

Inlet concentration	400	ppm		
Current:	0.05	mA	SV	55.8 hr^{-1}

			Peak Area		Concentration		Efficiency		
T, (^0C)	V(kV)	P(W)	Cout, 0 mA(avg)	Cout	Cout, 0 mA(avg)	Cout	ψ,(-)	ψ',(-)	ψ'',(-)
33	10.3	0.52	401	80	377	137	0.66	0.64	0.65
33	10.3	0.52	401	84	377	142	0.65	0.62	0.63
33	10.3	0.52	401	75	377	131	0.67	0.65	0.66
100	7.6	0.38	406	242	380	279	0.30	0.27	0.33
100	7.6	0.38	406	232	380	272	0.32	0.28	0.36
100	7.6	0.38	406	268	380	297	0.26	0.22	0.27
200	5.5	0.28	404	331	379	337	0.16	0.11	0.17
200	5.5	0.28	404	273	379	300	0.25	0.21	0.33
200	5.5	0.28	404	326	379	334	0.17	0.12	0.19
300	4.6	0.23	305	262	321	293	0.27	0.09	0.17
300	4.6	0.23	305	265	321	295	0.26	0.08	0.16
300	4.6	0.23	305	241	321	279	0.30	0.13	0.25

Date:	3/3/44		
Subject:	Removal of NH_3 from N_2-O_2 (10%)		
Gas flow rate:	NH_3 balanced N_2 500 ppm	80	cc/min
	N_2 dilute flow rate	10	cc/min
	O_2 flow rate	10	cc/min
	total flow rate	100	cc/min

Inlet concentration	400	ppm			
Current:	0.05	mA	SV	55.8	hr^{-1}

			Peak Area		Concentration		Efficiency		
T, (^{0}C)	V(kV)	P(W)	Cout, 0 mA(avg)	Cout	Cout, 0 mA(avg)	Cout	ψ,(-)	ψ',(-)	ψ'',(-)
33	10.3	0.52	385	-	369	125	0.69	0.66	0.67
33	10.3	0.52	385	-	369	120	0.70	0.67	0.69
33	10.3	0.52	385	-	369	120	0.70	0.67	0.69
100	7.6	0.38	390	181	371	234	0.42	0.37	0.46
100	7.6	0.38	390	182	371	234	0.42	0.37	0.46
100	7.6	0.38	390	187	371	238	0.41	0.36	0.45
200	5.5	0.28	380	225	366	267	0.33	0.27	0.43
200	5.5	0.28	380	234	366	274	0.32	0.25	0.40
200	5.5	0.28	380	227	366	269	0.33	0.27	0.42
300	4.6	0.23	335	231	340	272	0.32	0.20	0.39
300	4.6	0.23	335	235	340	274	0.32	0.19	0.37
300	4.6	0.23	335	240	340	278	0.31	0.18	0.35

Date: 1/3/44

Subject: Removal of NH3 from N2-O2 (20%)

Gas flow rate: NH3 balanced N2 500 ppm 80 cc/min

O2 flow rate 20 cc/min

total flow rate 100 cc/min

Inlet concentration 400 ppm

Current: 0.05 mA SV 55.8 hr^{-1}

			Peak Area		Concentration		Efficiency		
T, (^{0}C)	V(kV)	P(W)	Cout, 0 mA(avg)	Cout	Cout, 0 mA(avg)	Cout	ψ,(-)	ψ',(-)	ψ'',(-)
33	10.5	0.53	370	-	360	90	0.78	0.75	0.76
33	10.5	0.53	370	-	360	100	0.75	0.72	0.74
33	10.5	0.53	370	-	360	95	0.76	0.74	0.75
100	9.0	0.45	374	115	362	175	0.56	0.52	0.65
100	9.0	0.45	374	121	362	181	0.55	0.50	0.63
100	9.0	0.45	374	147	362	205	0.49	0.43	0.54
200	7.0	0.35	378	173	365	227	0.43	0.38	0.59
200	7.0	0.35	378	195	365	245	0.39	0.33	0.52
200	7.0	0.35	378	176	365	229	0.43	0.37	0.59
300	5.9	0.30	359	229	354	270	0.33	0.24	0.46
300	5.9	0.30	359	226	354	268	0.33	0.24	0.47
300	5.9	0.30	359	264	354	294	0.27	0.17	0.33

Date:	24/4/44			
Subject:	Removal of NH_3 from N2-O2 (5%)			
Gas flow rate:	NH3 balanced N2 500 ppm	50	cc/min	
	N2 dilute flow rate	45	cc/min	
	O2 flow rate	5	cc/min	
	total flow rate	100	cc/min	

Inlet concentration	250	ppm	peak area(avg)		198
Current:	0.3	mA	SV	55.8	hr^{-1}

			Peak Area		Concentration		Efficiency		
T, (^{0}C)	V(kV)	P(W)	Cout, 0 mA(avg)	Cout	Cout, 0 mA(avg)	Cout	ψ,(-)	ψ',(-)	ψ'',(-)
33	13.1	3.93	159	-	201	0	1.00	1.00	1.02
100	11.8	3.54	171	-	216	0	1.00	1.00	1.25
150	10.9	3.27	183	-	231	0	1.00	1.00	1.41
200	8.3	2.49	195	166	246	60	0.76	0.76	1.19
300	5.4	1.62	196	240	247	170	0.32	0.31	0.60

Date:	8/3/44		
Subject:	Removal of NH3 from N2-O2 (5%)-H2O 5250 ppm		
Gas flow rate:	NH3 balance N2 500ppm	50	cc/min
	N2 bubbling flow rate (water)	10	cc/min (water bath 34^{0}C)
	O2 flow rate	5	cc/min
	N2 dilute flow rate	35	cc/min
	total flow rate	100	cc/min

Inlet concentration	250	ppm			
Current:	0.3	mA	SV	55.8	hr^{-1}

			Peak Area		Concentration		Efficiency		
T, (^{0}C)	V(kV)	P(W)	Cout, 0 mA(avg)	Cout	Cout, 0 mA(avg)	Cout	ψ,(-)	ψ',(-)	ψ'',(-)
33	8.2	2.46	217	163	195	153	0.39	0.22	0.22
33	8.2	2.46	217	154	195	145	0.42	0.26	0.26
33	8.2	2.46	217	176	195	163	0.35	0.16	0.17
100	6.7	2.01	253	179	223	166	0.34	0.26	0.32
100	6.7	2.01	253	198	223	181	0.28	0.19	0.24
100	6.7	2.01	253	185	223	171	0.32	0.23	0.29
200	5.0	1.50	309	215	263	195	0.22	0.26	0.41
200	5.0	1.50	309	220	263	198	0.21	0.25	0.39
200	5.0	1.50	309	204	263	186	0.26	0.29	0.46
300	3.7	1.11	324	250	273	221	0.12	0.19	0.37
300	3.7	1.11	324	282	273	244	0.02	0.11	0.20
300	3.7	1.11	324	270	273	235	0.06	0.14	0.27

Date:	13/3/44		
Subject:	Removal of NH_3 from N_2-O_2 (5%)-H_2O 10500 ppm		
Gas flow rate:	NH_3 balance N_2 500ppm	50	cc/min
	N_2 bubbling flow rate (water)	20	cc/min (water bath 34^{0}C)
	O_2 flow rate	5	cc/min
	N_2 dilute flow rate	25	cc/min
	total flow rate	100	cc/min

Inlet concentration 250 ppm

Current: 0.3 mA SV 55.8 hr^{-1}

			Peak Area		Concentration		Efficiency		
T, (^{0}C)	V(kV)	P(W)	Cout, 0 mA(avg)	Cout	Cout, 0 mA(avg)	Cout	ψ,(-)	ψ',(-)	ψ'',(-)
33	12.9	3.87	195	-	210	60	0.76	0.71	0.73
33	12.9	3.87	195	-	210	60	0.76	0.71	0.73
100	9.0	2.70	201	78	215	102	0.59	0.53	0.66
100	9.0	2.70	201	79	215	103	0.59	0.52	0.65
200	6.8	2.04	204	104	217	129	0.48	0.41	0.64
200	6.8	2.04	204	92	217	117	0.53	0.46	0.72
300	5.3	1.59	205	110	218	165	0.34	0.24	0.47
300	5.3	1.59	205	111	218	166	0.34	0.24	0.46

Date:	9/3/44		
Subject:	Removal of NH_3 from N_2-O_2 (10%)-H_2O 5250 ppm		
Gas flow rate:	NH_3 balance N_2 500ppm	50	cc/min
	N_2 bubbling flow rate (water)	10	cc/min (water bath 34^{0}C)
	O_2 flow rate	10	cc/min
	N_2 dilute flow rate	30	cc/min
	total flow rate	100	cc/min

Inlet concentration	250	ppm			
Current:	0.3	mA	SV	55.8	hr^{-1}

			Peak Area		Concentration		Efficiency		
T, (^{0}C)	V(kV)	P(W)	Cout, 0 mA(avg)	Cout	Cout, 0 mA(avg)	Cout	ψ,(-)	ψ',(-)	ψ'',(-)
33	13.0	3.90	188	-	239	0	1.00	1.00	1.02
33	13.0	3.90	188	-	239	0	1.00	1.00	1.02
100	11.7	3.51	178	-	231	0	1.00	1.00	1.25
100	11.7	3.51	178	-	231	0	1.00	1.00	1.25
200	8.6	2.58	195	65	245	119	0.52	0.51	0.81
200	8.6	2.58	195	71	245	126	0.50	0.49	0.76
300	6.0	1.80	214	127	259	186	0.26	0.28	0.54
300	6.0	1.80	214	105	259	165	0.34	0.36	0.70

Date:	10/3/44		
Subject:	Removal of NH_3 from N_2-O_2 (20%)-H_2O 5250 ppm		
Gas flow rate:	NH_3 balance N_2 500ppm	50	cc/min
	N_2 bubbling flow rate (water)	10	cc/min (water bath 34^{0}C)
	O_2 flow rate	20	cc/min
	N_2 dilute flow rate	20	cc/min
	total flow rate	100	cc/min

Inlet concentration	250	ppm		
Current:	0.3	mA	SV	55.8 hr^{-1}

			Peak Area		Concentration		Efficiency		
T, (^{0}C)	V(kV)	P(W)	Cout, 0 mA(avg)	Cout	Cout, 0 mA(avg)	Cout	ψ,(-)	ψ',(-)	ψ'',(-)
33	13.2	3.96	201	-	183	0	1.00	1.00	1.02
33	13.2	3.96	201	-	183	0	1.00	1.00	1.02
100	11.8	3.54	215	-	194	0	1.00	1.00	1.25
100	11.8	3.54	215	-	194	0	1.00	1.00	1.25
200	9.2	2.76	231	66	206	65	0.74	0.68	1.08
200	9.2	2.76	231	72	206	71	0.72	0.66	1.03
200	9.2	2.76	231	64	206	63	0.75	0.69	1.09
300	6.4	1.92	221	117	199	121	0.52	0.39	0.76
300	6.4	1.92	221	112	199	115	0.54	0.42	0.81
300	6.4	1.92	221	115	199	118	0.53	0.41	0.79

APPENDIX F
SIMULTANEOUS REMOVAL OF STYRENE AND AMMONIA

Date:	26/3/44		
Subject:	Removal of NH3-Styrene from N2		
Gas flow rate:	NH3 balanced N2 500 ppm	40	cc/min
	Styrene balanced N2 200 ppm	20	cc/min
	N2 dilute flow rate	40	cc/min
	total flow rate	100	cc/min

Inlet concentration	NH3	200	ppm	peak area(avg)	190
	Styrene	40	ppm	peak area(avg)	6119
Current:	0.3	mA	SV	55.8	hr^{-1}

			Peak Area (NH3)		Concentration (NH3)		Efficiency		Peak Area (Styrene)		Concentration (Styrene)		Efficiency	
T (^0C)	V (kV)	P (W)	Cout, 0 mA (avg)	Cout	Cout, 0 mA (avg)	Cout	ψ,(-)	ψ',(-)	Cout, 0 mA (avg)	Cout	Cout, 0 mA (avg)	Cout	ψ,(-)	ψ',(-)
33	9.0	2.70	171	108	180	114	0.43	0.37	3374	783	22	5	0.87	0.77
33	9.0	2.70	171	110	180	116	0.42	0.36	3374	804	22	5	0.87	0.76
100	7.7	2.31	178	120	188	127	0.37	0.33	5187	1652	34	11	0.73	0.68
100	7.7	2.31	178	139	188	147	0.27	0.22	5187	1748	34	11	0.71	0.66
100	7.7	2.31	178	132	188	139	0.30	0.26	5187	1758	34	11	0.71	0.66
200	6.0	1.80	186	167	196	176	0.12	0.10	5824	2502	38	16	0.59	0.57
200	6.0	1.80	186	169	196	178	0.11	0.09	5824	2521	38	16	0.59	0.57
300	4.0	1.20	188	160	198	169	0.16	0.15	5670	2777	37	18	0.55	0.51
300	4.0	1.20	188	164	198	173	0.14	0.13	5670	2501	37	16	0.59	0.56

Date: 26/4/44

Subject: Removal of NH3-Styrene from N2

Gas flow rate:	NH3 balanced N2 500 ppm	40	cc/min
	Styrene balanced N2 200 ppm	40	cc/min
	N2 dilute flow rate	20	cc/min
	total flow rate	100	cc/min

Inlet concentration	NH3	200	ppm	peak area(avg)	121
	Styrene	80	ppm	peak area(avg)	10043

Current: 0.3 mA SV 55.8 hr^{-1}

			Peak Area (NH3)		Concentration (NH3)		Efficiency		Peak Area (Styrene)		Concentration (Styrene)		Efficiency	
T (^0C)	V (kV)	P (W)	Cout, 0 mA (avg)	Cout	Cout, 0 mA (avg)	Cout	ψ,(-)	ψ',(-)	Cout, 0 mA (avg)	Cout	Cout, 0 mA (avg)	Cout	ψ,(-)	ψ',(-)
33	10.0	3.00	110	-	182	50	0.75	0.73	6585	347	52	3	0.97	0.95
100	9.7	2.91	111	-	183	50	0.75	0.73	8050	404	64	3	0.96	0.95
150	8.2	2.46	117	-	193	60	0.70	0.69	8567	487	68	4	0.95	0.94
200	7.0	2.10	116	-	192	120	0.40	0.37	8910	845	71	7	0.92	0.91
300	4.9	1.47	120	91	198	150	0.25	0.24	8721	4057	69	32	0.60	0.53

Date: 25/4/44

Subject: Removal of NH3-Styrene from N2-H2O 5250 ppm

Gas flow rate: NH3 balanced N2 500 ppm 40 cc/min
Styrene balanced N2 200 ppm 20 cc/min
N2 bubbling water 10 cc/min (water bath 34^{0}C)
N2 dilute flow rate 30 cc/min
total flow rate 100 cc/min

Inlet concentration NH3 200 ppm peak area(avg) 121
Styrene 40 ppm peak area(avg) 5053
Current: 0.3 mA SV 55.8 hr^{-1}

			Peak Area (NH3)		Concentration (NH3)		Efficiency		Peak Area (Styrene)		Concentration (Styrene)		Efficiency	
T (^{0}C)	V (kV)	P (W)	Cout, 0 mA (avg)	Cout	Cout, 0 mA (avg)	Cout	ψ,(-)	ψ',(-)	Cout, 0 mA (avg)	Cout	Cout, 0 mA (avg)	Cout	ψ,(-)	ψ',(-)
33	9.8	2.94	110	-	182	100	0.50	0.45	3134	259	25	2	0.95	0.92
100	9.5	2.85	113	-	187	100	0.50	0.46	3872	219	31	2	0.96	0.94
150	8.4	2.52	110	-	182	100	0.50	0.45	4205	262	33	2	0.95	0.94
200	6.8	2.04	116	85	192	140	0.30	0.27	4507	1150	36	9	0.77	0.74
300	4.5	1.35	120	97	198	160	0.20	0.19	4229	1646	33	13	0.67	0.61

Date: 3/5/44

Subject: Removal of NH3-Styrene from N2-H2O 5250 ppm

Gas flow rate: NH3 balanced N2 500 ppm 40 cc/min

Styrene balanced N2 200 ppm 40 cc/min

N2 bubbling water 10 cc/min (water bath 34^{0}C)

N2 dilute flow rate 10 cc/min

total flow rate 100 cc/min

Inlet concentration NH3 200 ppm peak area(avg) 121

Styrene 80 ppm peak area(avg) 11106

Current: 0.3 mA SV 55.8 hr^{-1}

			Peak Area (NH3)		Concentration (NH3)		Efficiency		Peak Area (Styrene)		Concentration (Styrene)		Efficiency	
T (^{0}C)	V (kV)	P (W)	Cout, 0 mA (avg)	Cout	Cout, 0 mA (avg)	Cout	ψ,(-)	ψ',(-)	Cout, 0 mA (avg)	Cout	Cout, 0 mA (avg)	Cout	ψ,(-)	ψ',(-)
33	10.5	3.15	108	-	179	50	0.75	0.72	7460	542	54	4	0.95	0.93
100	10.0	3.00	110	-	182	50	0.75	0.73	8124	492	59	4	0.96	0.94
150	8.7	2.61	112	-	185	60	0.70	0.68	8567	525	62	4	0.95	0.94
200	7.4	2.22	115	-	190	70	0.65	0.63	8712	803	63	6	0.93	0.91
300	5.7	1.71	120	91	198	150	0.25	0.24	8551	4634	62	33	0.58	0.46

Date: 20/4/44

Subject: Removal of Styrene from N2-O2 (5%)

Gas flow rate:	Styrene balanced N2 200 ppm	20	cc/min
	O2 flow rate	5	cc/min
	N2 dilute flow rate	75	cc/min
	total flow rate	100	cc/min

Inlet concentration	40	ppm	peak area(avg)		5314
Current:	0.1	mA	SV	55.8	hr^{-1}

			Peak Area (NH3)		Concentration (NH3)		Efficiency		Peak Area (Styrene)		Concentration (Styrene)		Efficiency	
T (^{0}C)	V (kV)	P (W)	Cout, 0 mA (avg)	Cout	Cout, 0 mA (avg)	Cout	ψ,(-)	ψ',(-)	Cout, 0 mA (avg)	Cout	Cout, 0 mA (avg)	Cout	ψ,(-)	ψ',(-)
33	11.9	1.19	-	-	-	-	-	-	3665	-	28	0	1.00	1.00
100	9.2	0.92	-	-	-	-	-	-	3871	-	29	0	1.00	1.00
150	8.4	0.84	-	-	-	-	-	-	4107	-	31	0	1.00	1.00
200	7.1	0.71	-	-	-	-	-	-	4318	249	33	2	0.95	0.94
300	4.9	0.49	-	-	-	-	-	-	4215	1760	32	13	0.67	0.58

Date: 19/4/44

Subject: Removal of NH3-Styrene from N2-O2 (5%)

Gas flow rate:	NH3 balanced N2 500 ppm	20	cc/min
	Styrene balanced N2 200 ppm	20	cc/min
	O2 flow rate	5	cc/min
	N2 dilute flow rate	55	cc/min
	total flow rate	100	cc/min

Inlet concentration	NH3	100	ppm	peak area(avg)	-
	Styrene	40	ppm	peak area(avg)	5267

Current: 0.1 mA SV 55.8 hr^{-1}

			Peak Area (NH3)		Concentration (NH3)		Efficiency		Peak Area (Styrene)		Concentration (Styrene)		Efficiency	
T (^{0}C)	V (kV)	P (W)	Cout, 0 mA (avg)	Cout	Cout, 0 mA (avg)	Cout	ψ,(-)	ψ',(-)	Cout, 0 mA (avg)	Cout	Cout, 0 mA (avg)	Cout	ψ,(-)	ψ',(-)
33	11.0	1.10	-	-	85	0	1.00	1.00	3675	-	28	0	1.00	1.00
100	9.0	0.90	-	-	90	0	1.00	1.00	4123	-	31	0	1.00	1.00
150	8.2	0.82	-	-	90	10	0.90	0.89	4471	-	34	0	1.00	1.00
200	7.2	0.72	-	-	95	58	0.42	0.39	4248	377	32	3	0.93	0.91
300	4.9	0.49	-	-	95	83	0.17	0.13	3621	2031	28	15	0.61	0.44

Date:	19/4/44		
Subject:	Removal of NH_3-Styrene from N_2-O_2 (5%)		
Gas flow rate:	NH_3 balanced N_2 500 ppm	20	cc/min
	Styrene balanced N_2 200 ppm	20	cc/min
	O_2 flow rate	5	cc/min
	N_2 dilute flow rate	55	cc/min
	total flow rate	100	cc/min

Inlet concentration	NH_3	100	ppm	peak area(avg)	-
	Styrene	40	ppm	peak area(avg)	5267

Current: 0.1 mA SV 55.8 hr^{-1}

			Peak Area (NH_3)		Concentration (NH_3)		Efficiency		Peak Area (Styrene)		Concentration (Styrene)		Efficiency	
T (^{0}C)	V (kV)	P (W)	Cout, 0 mA (avg)	Cout	Cout, 0 mA (avg)	Cout	ψ,(-)	ψ',(-)	Cout, 0 mA (avg)	Cout	Cout, 0 mA (avg)	Cout	ψ,(-)	ψ',(-)
33	11.0	1.10	-	-	85	0	1.00	1.00	3675	-	28	0	1.00	1.00
100	9.0	0.90	-	-	90	0	1.00	1.00	4123	-	31	0	1.00	1.00
150	8.2	0.82	-	-	90	10	0.90	0.89	4471	-	34	0	1.00	1.00
200	7.2	0.72	-	-	95	58	0.42	0.39	4248	377	32	3	0.93	0.91
300	4.9	0.49	-	-	95	83	0.17	0.13	3621	2031	28	15	0.61	0.44

Date: 10/4/44

Subject: Removal of NH3-Styrene from N2-O2 (5%)

Gas flow rate:	NH3 balanced N2 500 ppm	40	cc/min
	Styrene balanced N2 200 ppm	20	cc/min
	O2 flow rate	5	cc/min
	N2 dilute flow rate	35	cc/min
	total flow rate	100	cc/min

Inlet concentration	NH3	200	ppm	peak area(avg)	164
	Styrene	40	ppm	peak area(avg)	5017

Current: 0.3 mA SV 55.8 hr^{-1}

			Peak Area (NH3)		Concentration (NH3)		Efficiency		Peak Area (Styrene)		Concentration (Styrene)		Efficiency	
T (^{0}C)	V (kV)	P (W)	Cout, 0 mA (avg)	Cout	Cout, 0 mA (avg)	Cout	ψ,(-)	ψ',(-)	Cout, 0 mA (avg)	Cout	Cout, 0 mA (avg)	Cout	ψ,(-)	ψ',(-)
33	11.5	1.15	127	-	155	0	1.00	1.00	3114	-	25	0	1.00	1.00
100	9.5	0.95	120	-	146	0	1.00	1.00	3388	-	27	0	1.00	1.00
150	9.2	0.92	125	-	152	0	1.00	1.00	4399	-	35	0	1.00	1.00
200	7.4	0.74	148	-	180	65	0.68	0.61	4321	-	34	0	1.00	1.00
300	5.2	0.52	154	131	188	145	0.27	0.23	3946	962	31	8	0.81	0.76

Date: 10/4/44

Subject: Removal of NH3-Styrene from N2-O2 (5%)

Gas flow rate:	NH3 balanced N2 500 ppm	40	cc/min
	Styrene balanced N2 200 ppm	20	cc/min
	O2 flow rate	5	cc/min
	N2 dilute flow rate	35	cc/min
	total flow rate	100	cc/min

Inlet concentration	NH3	200	ppm	peak area(avg)	164
	Styrene	40	ppm	peak area(avg)	5017

Current: 0.1 mA SV 55.8 hr^{-1}

			Peak Area (NH3)		Concentration (NH3)		Efficiency		Peak Area (Styrene)		Concentration (Styrene)		Efficiency	
T (^{0}C)	V (kV)	P (W)	Cout, 0 mA (avg)	Cout	Cout, 0 mA (avg)	Cout	ψ,(-)	ψ',(-)	Cout, 0 mA (avg)	Cout	Cout, 0 mA (avg)	Cout	ψ,(-)	ψ',(-)
33	11.5	1.15	127	-	155	0	1.00	1.00	3114	-	25	0	1.00	1.00
100	9.5	0.95	120	-	146	0	1.00	1.00	3388	-	27	0	1.00	1.00
150	9.2	0.92	125	-	152	10	0.95	0.93	4399	-	35	0	1.00	1.00
200	7.4	0.74	148	-	180	95	0.53	0.47	4321	286	34	2	0.99	0.93
300	5.2	0.52	154	131	188	160	0.20	0.15	3946	1722	31	14	0.66	0.56

Date: 27/3/44

Subject: Removal of NH_3-Styrene from N_2-O_2 (10%)

Gas flow rate:	NH_3 balanced N_2 500 ppm	40	cc/min
	Styrene balanced N_2 200 ppm	20	cc/min
	O_2 flow rate	10	cc/min
	N_2 dilute flow rate	30	cc/min
	total flow rate	100	cc/min

Inlet concentration	NH_3	200	ppm	peak area(avg)	162
	Styrene	40	ppm	peak area(avg)	5837

Current: 0.3 mA SV 55.8 hr^{-1}

			Peak Area (NH_3)		Concentration (NH_3)		Efficiency		Peak Area (Styrene)		Concentration (Styrene)		Efficiency	
T (^{0}C)	V (kV)	P (W)	Cout, 0 mA (avg)	Cout	Cout, 0 mA (avg)	Cout	ψ,(-)	ψ',(-)	Cout, 0 mA (avg)	Cout	Cout, 0 mA (avg)	Cout	ψ,(-)	ψ',(-)
33	13.2	3.96	157	-	193	0	1.00	1.00	4335	-	30	0	1.00	1.00
100	12.1	3.63	150	-	185	0	1.00	1.00	4674	-	32	0	1.00	1.00
100	12.1	3.63	150	-	185	0	1.00	1.00	4674	-	32	0	1.00	1.00
200	9.0	2.70	152	-	188	55	0.73	0.71	4338	-	30	0	1.00	1.00
200	9.0	2.70	152	-	188	60	0.70	0.68	4338	-	30	0	1.00	1.00
300	6.0	1.80	161	110	199	136	0.32	0.32	4817	-	33	0	1.00	1.00
300	6.0	1.80	161	113	199	140	0.30	0.30	4817	-	33	0	1.00	1.00

Date: 29/3/44

Subject: Removal of NH_3-Styrene from N_2-O_2 (20%)

Gas flow rate:	NH_3 balanced N_2 500 ppm	40	cc/min
	Styrene balanced N_2 200 ppm	20	cc/min
	O_2 flow rate	20	cc/min
	N_2 dilute flow rate	20	cc/min
	total flow rate	100	cc/min

Inlet concentration	NH_3	200	ppm	peak area(avg)	167
	Styrene	40	ppm	peak area(avg)	6127

Current: 0.1 mA SV 55.8 hr^{-1}

			Peak Area (NH_3)		Concentration (NH_3)		Efficiency		Peak Area (Styrene)		Concentration (Styrene)		Efficiency	
T (^{0}C)	V (kV)	P (W)	Cout, 0 mA (avg)	Cout	Cout, 0 mA (avg)	Cout	ψ,(-)	ψ',(-)	Cout, 0 mA (avg)	Cout	Cout, 0 mA (avg)	Cout	ψ,(-)	ψ',(-)
33	12.1	1.21	121	-	145	0	1.00	1.00	4138	-	27	0	1.00	1.00
100	10.3	1.03	145	-	174	0	1.00	1.00	4855	-	32	0	1.00	1.00
200	8.1	0.81	159	-	190	40	0.80	0.79	5117	-	33	0	1.00	1.00
300	6.0	0.60	162	-	194	110	0.45	0.43	5210	258	34	2	0.99	0.95
300	6.0	0.60	162	-	194	120	0.40	0.38	5210	251	34	2	0.99	0.95

Date: 28/3/44

Subject: Removal of NH_3-Styrene from N_2-O_2 (20%)

Gas flow rate:	NH_3 balanced N_2 500 ppm	40	cc/min
	Styrene balanced N_2 200 ppm	20	cc/min
	O_2 flow rate	20	cc/min
	N_2 dilute flow rate	20	cc/min
	total flow rate	100	cc/min

Inlet concentration	NH_3	200	ppm	peak area(avg)	130
	Styrene	40	ppm	peak area(avg)	6158

Current: 0.3 mA SV 55.8 hr^{-1}

			Peak Area (NH_3)		Concentration (NH_3)		Efficiency		Peak Area (Styrene)		Concentration (Styrene)		Efficiency	
T (^{0}C)	V (kV)	P (W)	Cout, 0 mA (avg)	Cout	Cout, 0 mA (avg)	Cout	ψ,(-)	ψ',(-)	Cout, 0 mA (avg)	Cout	Cout, 0 mA (avg)	Cout	ψ,(-)	ψ',(-)
33	13.4	4.02	105	-	161	0	1.00	1.00	3764	-	24	0	1.00	1.00
100	12.4	3.72	126	-	194	0	1.00	1.00	4785	-	31	0	1.00	1.00
200	10.2	3.06	130	-	200	0	1.00	1.00	5062	-	33	0	1.00	1.00
300	7.1	2.13	161	-	248	10	0.95	0.96	5016	-	33	0	1.00	1.00

Date: 2/5/44

Subject: Removal of NH_3-Styrene from N_2-O_2 (5%)

Gas flow rate:	NH_3 balanced N_2 500 ppm	40	cc/min
	Styrene balanced N_2 200 ppm	40	cc/min
	O_2 flow rate	5	cc/min
	N_2 dilute flow rate	15	cc/min
	total flow rate	100	cc/min

Inlet concentration	NH_3	200	ppm	peak area(avg)	137
	Styrene	80	ppm	peak area(avg)	12452

Current: 0.1 mA SV 55.8 hr^{-1}

			Peak Area (NH_3)		Concentration (NH_3)		Efficiency		Peak Area (Styrene)		Concentration (Styrene)		Efficiency	
T (^{0}C)	V (kV)	P (W)	Cout, 0 mA (avg)	Cout	Cout, 0 mA (avg)	Cout	ψ,(-)	ψ',(-)	Cout, 0 mA (avg)	Cout	Cout, 0 mA (avg)	Cout	ψ,(-)	ψ',(-)
33	11.7	1.17	101	-	147	0	1.00	1.00	7774	-	25	0	1.00	1.00
100	9.4	0.94	109	-	159	10	0.95	0.94	9582	-	31	0	1.00	1.00
150	8.3	0.83	117	-	171	50	0.75	0.71	10795	-	35	0	1.00	1.00
200	7.1	0.71	120	68	175	99	0.50	0.43	10867	945	35	3	0.92	0.91
300	4.7	0.47	131	102	191	149	0.26	0.22	10527	5844	34	19	0.53	0.44

Date:	21/4/44		
Subject:	Removal of NH_3 from N_2-O_2 (5%)		
Gas flow rate:	NH_3 balanced N_2 500 ppm	40	cc/min
	O_2 flow rate	5	cc/min
	N_2 dilute flow rate	55	cc/min
	total flow rate	100	cc/min

Inlet concentration NH3 200 ppm peak area(avg) 93

Current: 0.1 mA SV 55.8 hr^{-1}

			Peak Area (NH3)		Concentration (NH3)		Efficiency		Peak Area (Styrene)		Concentration (Styrene)		Efficiency	
T (^{0}C)	V (kV)	P (W)	Cout, 0 mA (avg)	Cout	Cout, 0 mA (avg)	Cout	ψ,(-)	ψ',(-)	Cout, 0 mA (avg)	Cout	Cout, 0 mA (avg)	Cout	ψ,(-)	ψ',(-)
33	11.4	1.14	61	-	131	0	1.00	1.00	-	-	-	-	-	-
100	9.5	0.95	68	-	146	10	0.95	0.93	-	-	-	-	-	-
150	8.7	0.87	78	-	168	80	0.60	0.52	-	-	-	-	-	-
200	6.0	0.60	87	75	187	161	0.19	0.14	-	-	-	-	-	-
300	unstable	-	-	-	-	-	-	-	-	-	-	-	-	-

Date:	9/5/44		
Subject:	Removal of NH_3-Styrene from N_2-O_2 (5%) H_2O 5250 ppm		
Gas flow rate:	NH_3 balanced N_2 500 ppm	40	cc/min
	Styrene balanced N_2 200 ppm	40	cc/min
	N_2 bubbling water	10	cc/min (water bath 34.5 ^{0}C)
	O_2 flow rate	5	cc/min
	N_2 dilute flow rate	5	cc/min
	total flow rate	100	cc/min

Inlet concentration	NH_3	200	ppm	peak area(avg)	121
	Styrene	80	ppm	peak area(avg)	10396

Current: 0.1 mA SV 55.8 hr^{-1}

			Peak Area (NH_3)		Concentration (NH_3)		Efficiency		Peak Area (Styrene)		Concentration (Styrene)		Efficiency	
T (^{0}C)	V (kV)	P (W)	Cout, 0 mA (avg)	Cout	Cout, 0 mA (avg)	Cout	ψ,(-)	ψ',(-)	Cout, 0 mA (avg)	Cout	Cout, 0 mA (avg)	Cout	ψ,(-)	ψ',(-)
33	11.6	1.16	108	-	179	0	1.00	1.00	7598	0	58	0	1.00	1.00
100	9.3	0.93	110	-	182	20	0.90	0.89	8612	0	66	0	1.00	1.00
150	8.2	0.82	112	-	185	80	0.60	0.57	9299	277	72	2	0.97	0.97
200	7.2	0.72	115	-	190	100	0.50	0.47	8997	1014	69	8	0.90	0.89
300	4.5	0.45	120	85	198	170	0.15	0.14	7330	5347	56	41	0.49	0.27

Date: 10/5/44

Subject: Removal of NH_3-Styrene from N_2-O_2 (5%) H_2O 10500 ppm

Gas flow rate:	NH_3 balanced N_2 500 ppm	40	cc/min
	Styrene balanced N_2 200 ppm	40	cc/min
	N_2 bubbling water	15	cc/min (water bath 40 ^{0}C)
	O_2 flow rate	5	cc/min
	total flow rate	100	cc/min

Inlet concentration	NH_3	200	ppm	peak area(avg)	120
	Styrene	80	ppm	peak area(avg)	12243

Current: 0.1 mA SV 55.8 hr^{-1}

			Peak Area (NH_3)		Concentration (NH_3)		Efficiency		Peak Area (Styrene)		Concentration (Styrene)		Efficiency	
T (^{0}C)	V (kV)	P (W)	Cout, 0 mA (avg)	Cout	Cout, 0 mA (avg)	Cout	ψ,(-)	ψ',(-)	Cout, 0 mA (avg)	Cout	Cout, 0 mA (avg)	Cout	ψ,(-)	ψ',(-)
33	11.8	1.18	108	-	180	0	1.00	1.00	7593	0	50	0	1.00	1.00
100	9.6	0.96	110	-	183	0	1.00	1.00	8583	0	56	0	1.00	1.00
150	8.2	0.82	112	-	187	30	0.85	0.84	8739	0	57	0	1.00	1.00
200	7.2	0.72	115	-	192	100	0.50	0.48	9533	1173	62	8	0.90	0.88
300	4.9	0.49	120	85	200	170	0.15	0.15	7997	5605	52	37	0.54	0.30

Date: 31/3/44

Subject: Removal of NH_3-Styrene from N_2-O_2 (20%) H_2O 10500 ppm

Gas flow rate:	NH_3 balanced N_2 500 ppm	40	cc/min
	Styrene balanced N_2 200 ppm	20	cc/min
	N_2 bubbling water	20	cc/min (water bath 34 ^{0}C)
	O_2 flow rate	20	cc/min
	total flow rate	100	cc/min

Inlet concentration	NH_3	200	ppm	peak area(avg)	120
	Styrene	40	ppm	peak area(avg)	5120

Current: 0.1 mA SV 55.8 hr^{-1}

			Peak Area (NH_3)		Concentration (NH_3)		Efficiency		Peak Area (Styrene)		Concentration (Styrene)		Efficiency	
T (^{0}C)	V (kV)	P (W)	Cout, 0 mA (avg)	Cout	Cout, 0 mA (avg)	Cout	ψ,(-)	ψ',(-)	Cout, 0 mA (avg)	Cout	Cout, 0 mA (avg)	Cout	ψ,(-)	ψ',(-)
33	11.6	1.16	101	-	168	0	1.00	1.00	3692	-	29	0	1.00	1.00
100	10.0	1.00	104	-	173	0	1.00	1.00	4092	-	32	0	1.00	1.00
200	8.3	0.83	106	-	177	20	0.90	0.89	4187	-	33	0	1.00	1.00
300	6.2	0.62	115	-	192	120	0.40	0.37	3624	305	28	2	0.94	0.92
300	6.2	0.62	115	-	192	120	0.40	0.37	3624	299	28	2	0.94	0.92

Date:	3/4/44			
Subject:	Removal of NH_3-Styrene from N_2-O_2 (20%) H_2O 24344 ppm			
Gas flow rate:	NH_3 balanced N_2 500 ppm	40	cc/min	
	Styrene balanced N_2 200 ppm	20	cc/min	
	N_2 bubbling water	20	cc/min	(water bath 50 ^{0}C)
	O_2 flow rate	20	cc/min	
	total flow rate	100	cc/min	

Inlet concentration	NH_3	200	ppm	peak area(avg)	190
	Styrene	40	ppm	peak area(avg)	5429
Current:	0.1	mA	SV	55.8	hr^{-1}

			Peak Area (NH_3)		Concentration (NH_3)		Efficiency		Peak Area (Styrene)		Concentration (Styrene)		Efficiency	
T (^{0}C)	V (kV)	P (W)	Cout, 0 mA (avg)	Cout	Cout, 0 mA (avg)	Cout	ψ,(-)	ψ',(-)	Cout, 0 mA (avg)	Cout	Cout, 0 mA (avg)	Cout	ψ,(-)	ψ',(-)
33	11.6	1.16	161	-	169	0	1.00	1.00	3973	-	29	0	1.00	1.00
100	10.0	1.00	172	-	181	0	1.00	1.00	4257	-	31	0	1.00	1.00
200	8.0	0.80	176	-	185	30	0.85	0.84	4627	-	34	0	1.00	1.00
300	6.0	0.60	179	-	188	120	0.40	0.36	4280	345	32	3	0.94	0.92
300	6.0	0.60	179	-	188	120	0.40	0.36	4280	309	32	2	0.94	0.93

Date: 17/4/44

Subject: Removal of NH_3-Styrene from N_2-O_2 (5%) H_2O 5250 ppm

Gas flow rate:	NH_3 balanced N_2 500 ppm	40	cc/min
	Styrene balanced N_2 200 ppm	20	cc/min
	N_2 bubbling water	10	cc/min (water bath 34 ^{0}C)
	N_2 flow rate	25	cc/min
	O_2 flow rate	5	cc/min
	total flow rate	100	cc/min

Inlet concentration	NH_3	200	ppm		peak area(avg)	163
	Styrene	40	ppm		peak area(avg)	5853
Current:	0.1	mA		SV	55.8	hr^{-1}

			Peak Area (NH_3)		Concentration (NH_3)		Efficiency		Peak Area (Styrene)		Concentration (Styrene)		Efficiency	
T (^{0}C)	V (kV)	P (W)	Cout, 0 mA (avg)	Cout	Cout, 0 mA (avg)	Cout	ψ,(-)	ψ',(-)	Cout, 0 mA (avg)	Cout	Cout, 0 mA (avg)	Cout	ψ,(-)	ψ',(-)
33	11.3	1.13	126	-	155	0	1.00	1.00	3965	-	27	0	1.00	1.00
100	9.3	0.93	136	-	167	0	1.00	1.00	4762	-	33	0	1.00	1.00
150	8.6	0.86	137	-	168	55	0.73	0.67	4931	-	34	0	1.00	1.00
200	7.4	0.74	147	-	180	100	0.50	0.45	4558	452	31	3	0.92	0.90
300	5.0	0.50	150	-	184	160	0.20	0.13	3994	2300	27	16	0.61	0.42

Date:	18/4/44		
Subject:	Removal of NH_3-Styrene from N_2-O_2 (5%) H_2O 10500 ppm		
Gas flow rate:	NH_3 balanced N_2 500 ppm	40	cc/min
	Styrene balanced N_2 200 ppm	20	cc/min
	N_2 bubbling water	20	cc/min (water bath 34 ^{0}C)
	N_2 flow rate	15	cc/min
	O_2 flow rate	5	cc/min
	total flow rate	100	cc/min

Inlet concentration	NH_3	200	ppm		peak area(avg)		162
	Styrene	40	ppm		peak area(avg)		5271
Current:	0.1	mA		SV	55.8	hr^{-1}	

			Peak Area (NH_3)		Concentration (NH_3)		Efficiency		Peak Area (Styrene)		Concentration (Styrene)		Efficiency	
T (^{0}C)	V (kV)	P (W)	Cout, 0 mA (avg)	Cout	Cout, 0 mA (avg)	Cout	ψ,(-)	ψ',(-)	Cout, 0 mA (avg)	Cout	Cout, 0 mA (avg)	Cout	ψ,(-)	ψ',(-)
33	11.1	1.11	125	-	154	0	1.00	1.00	3894	-	30	0	1.00	1.00
100	9.0	0.90	136	-	168	0	1.00	1.00	4604	-	35	0	1.00	1.00
150	8.4	0.84	137	-	169	60	0.70	0.65	4931	-	37	0	1.00	1.00
200	7.2	0.72	145	-	179	105	0.48	0.41	4569	559	35	4	0.89	0.88
300	5.1	0.51	151	-	186	165	0.18	0.11	4056	2451	31	19	0.54	0.40

APPENDIX G

SIMULTANEOUS REMOVAL OF STYRENE AND AMMONIA IN TWO SERIAL REACTORS

Date:	18/4/44		
Subject:	Removal of NH3-Styrene 200-40 ppm from N2-O2 (5%)		
Gas flow rate:	NH3 balanced N2 500 ppm	40	cc/min
	Styrene balanced N2 200 ppm	20	cc/min
	N2 flow rate	35	cc/min
	O2 flow rate	5	cc/min
	total flow rate	100	cc/min

Inlet concentration	NH3	200	ppm	peak area(avg)	-
	Styrene	40	ppm	peak area(avg)	5168

Temperature: 35 ^{0}C SV 55.8 hr^{-1}

I (mA)	V (kV)	Cout, NH3 (ppm)	Cout, Styrene (ppm)	Reaction by products
0	0	150	24	
0.01	unstable	-	-	
0.02	10.1	100	0	NI
0.03	10.5	85	0	NI
0.05	11.0	50	0	O3- 400 ppm
0.07	11.4	30	0	O3- 460 ppm
0.10	11.7	0	0	O3- 620 ppm

Date: 21/5/44

Subject: Removal of NH3-Styrene 200-40 ppm from N2-O2 (5%) by series reactors

Gas flow rate:			
	NH3 balanced N2 500 ppm	40	cc/min
	Styrene balanced N2 200 ppm	20	cc/min
	N2 flow rate	35	cc/min
	O2 flow rate	5	cc/min
	total flow rate	100	cc/min

Inlet concentration					
	NH3	200	ppm	peak area(avg)	-
	Styrene	40	ppm	peak area(avg)	6251

SV 55.8 hr^{-1}

First reactor temperature 35 ^{0}C

I (mA)	V (kV)	Cout, NH3 (ppm)	Cout, Styrene (ppm)	Reaction by products
0	0	150	28	NI
0.01	unstable	-	-	NI
0.03	9.4	80	0	NI

Fixed current of first reactor at 0.03 mA

Second reactor temperature 185 ^{0}C

I (mA)	V (kV)	Cout, NH3 (ppm)	Reaction by products
0	0	15	NI
0.01	8.1	0	NOx – 1 ppm
0.02	8.2	0	NOx – 3 ppm

Second reactor temperature 300 ^{0}C

I (mA)	V (kV)	Cout, NH3 (ppm)	Reaction by products
0	0	10	NI
0.01-0.10	unstable	-	-
0.20	5.8	0	NOx – 60 ppm
0.30	6.0	0	NOx – 80 ppm
0.40	6.3	0	NOx – 90 ppm

Date: 23/5/44

Subject: Removal of NH_3-Styrene 200-40 ppm from N_2-O_2 (5%)-H_2O 5250 ppm by series reactors

Gas flow rate:			
	NH_3 balanced N_2 500 ppm	40	cc/min
	Styrene balanced N_2 200 ppm	20	cc/min
	N_2 flow rate	10	cc/min (water bath 34 ^{0}C)
	O_2 flow rate	5	cc/min
	N_2 flow rate	25	cc/min
	total flow rate	100	cc/min

Inlet concentration					
	NH_3	200	ppm	peak area(avg)	-
	Styrene	40	ppm	peak area(avg)	6251

SV 55.8 hr^{-1}

First reactor temperature 150 ^{0}C

Fixed current of first reactor at 0.10 mA

Second reactor temperature 185 ^{0}C

I (mA)	V (kV)	Cout, NH_3 (ppm)	Reaction by products
0	0	20	O_3- 5ppm NOx- 0 ppm
0.01	8	5	O_3- 1ppm NOx- 1 ppm
0.02	8.1	0	O_3- 3ppm NOx- 1 ppm
0.03	8.1	0	O_3- 4ppm NOx- 2 ppm
0.04	8.2	0	O_3- 5ppm NOx- 2 ppm

Second reactor temperature 300 ^{0}C

I (mA)	V (kV)	Cout, NH_3 (ppm)	Reaction by products
0	0	10	O_3- 1ppm NOx- 3 ppm
0.01-0.10	unstable	-	-
0.20	5.8	0	O_3- 12ppm NOx- 30 ppm
0.30	6.0	0	O_3- 10ppm NOx- 55 ppm
0.40	6.3	0	O_3- 10ppm NOx- 100 ppm

Date: 19/5/44

Subject : Removal of O3 from first reactor

Gas flow rate :

NH3 balanced N2 500 ppm	40 cc/min
Styrene balanced N2 200 ppm	20 cc/min
O2	5 cc/min
N2	35 cc/min
total flow rate	100 cc/min

Current 0.1 mA

Inlet conc. O3 Second reactor 620 ppm

Outlet conc. O3 Second reactor 500 ppm (room temperature, no current)

Outlet from first reactor flows to second reactor

Second reactor condition

Temperature	190	C		
I (mA)	V (kV)	P (W)	Cout, O3 (ppm)	Cout, NOx (ppm)
0	0	0	30	0
0.01	8.1	0.08	33	0
0.05	8.5	0.43	34	0
0.15	9.5	1.43	20	0
0.30	10.8	3.24	6	8
0.50	11.7	5.85	13	40

Temperature	300	C		
I (mA)	V (kV)	P (W)	Cout, O3 (ppm)	Cout, NOx (ppm)
0	0	0	5	20
0.15	8.1	1.22	13	55
0.30	8.5	2.55	15	80
0.50	9.5	4.75	15	100
0.70	10.8	7.56	12	130

Date: 27/5/44

Subject : Effect of water vapor on O3 generation

Gas flow rate :

N2 flow rate	95 cc/min
O2 flow rate	5 cc/min
total flow rate	100 cc/min

Temperature 35 C

			Cout
I(mA)	V(kV)	P(W)	O3 Concentration (ppm)
0.01	7.7	0.08	80
0.03	9.5	0.29	270
0.05	10.6	0.53	360
0.10	11.4	1.14	510

Gas flow rate :

N2 flow rate	85 cc/min
O2 flow rate	5 cc/min
N2 bubbling water flow rate	10 cc/min(34 C)
total flow rate	100 cc/min

Temperature 35 C

			Cout
I(mA)	V(kV)	P(W)	O3 Concentration (ppm)
0.01	8.3	0.08	50
0.03	9.3	0.28	170
0.05	10.1	0.51	210
0.10	11.0	1.10	360

Date: 28/5/44

Subject: Substantiation of ozone effect

1)Ozone disappear in second reactor

1) Gas flow rate:	First reactor			Second reactor					
	N2 flow rate	75	cc/min	Flow rate from first reactor	80	cc/min			
	O2 flow rate	5	cc/min	add N2 flow rate	20	cc/min			
	total flow rate	80	cc/min	total flow rate	100	cc/min			
Current 0.1	mA	Voltage 11.4	kV	Current	0	mA	Voltage	0	kV
				Cin, O3	500	ppm	Cout, O3	430	ppm

2) NH3 disappear in second reactor

2) Gas flow rate:	First reactor			Second reactor					
	N2 flow rate	0	cc/min	N2 flow rate	80	cc/min			
	NH3 balanced N2	0	cc/min	NH3 balanced N2	20	cc/min			
	total flow rate	0	cc/min	total flow rate	100	cc/min			
Current 0	mA	Voltage 0	kV	Current	0	mA	Voltage	0	kV
				Cin, NH3	100	ppm	Cout, NH3	75	ppm

3)Ozone effect on NH3

3) Gas flow rate:	First reactor			Second reactor					
	N2 flow rate	75	cc/min	Flow rate from first reactor	80	cc/min			
	O2 flow rate	5	cc/min	add NH3 balanced N2	20	cc/min			
	total flow rate	80	cc/min	total flow rate	100	cc/min			
Current 0.1	mA	Voltage 11.4	kV	Current	0	mA	Voltage	0	kV
				Cin, O3	500	ppm	Cout, O3	400	ppm
				Cin, NH3	100	ppm	Cout, NH3	25	ppm

APPENDIX H
FT-IR SPECTRUM OF DEPOSIT ON THE ANODE PLATE

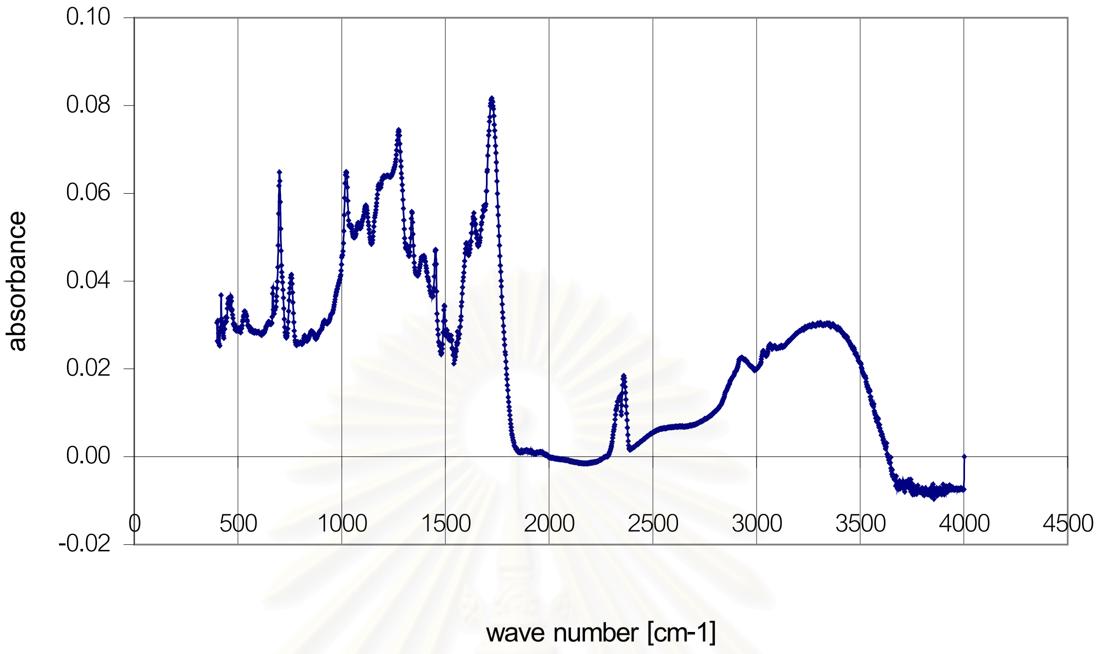

FT-IR spectrum of deposit on the anode plate from styrene removal without any pre-heating

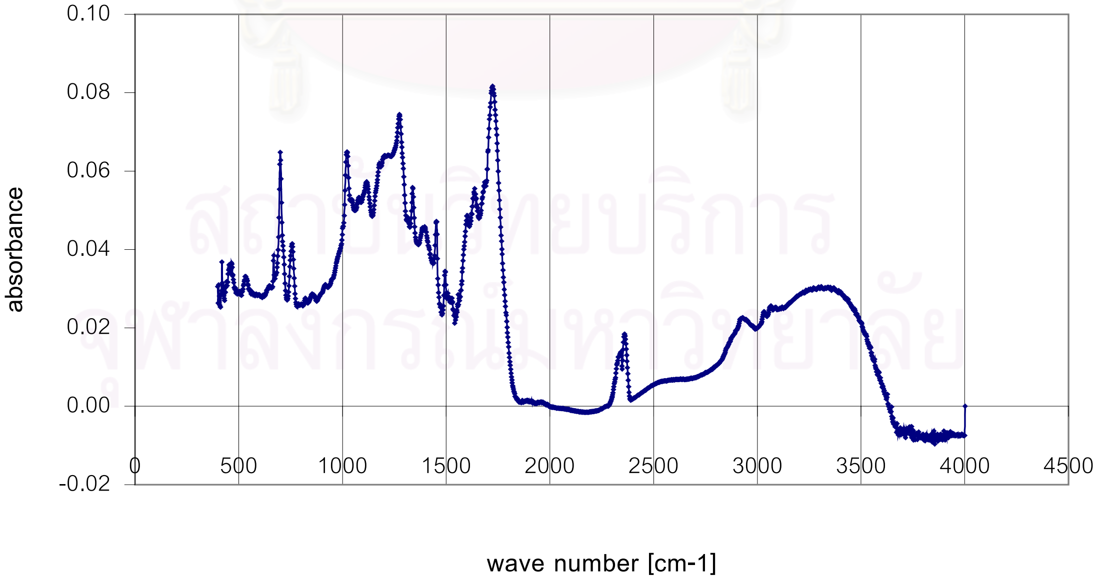

FT-IR spectrum of deposit on the anode plate from styrene removal after pre-heating to 60^0C with hot air to evaporate out water moisture.

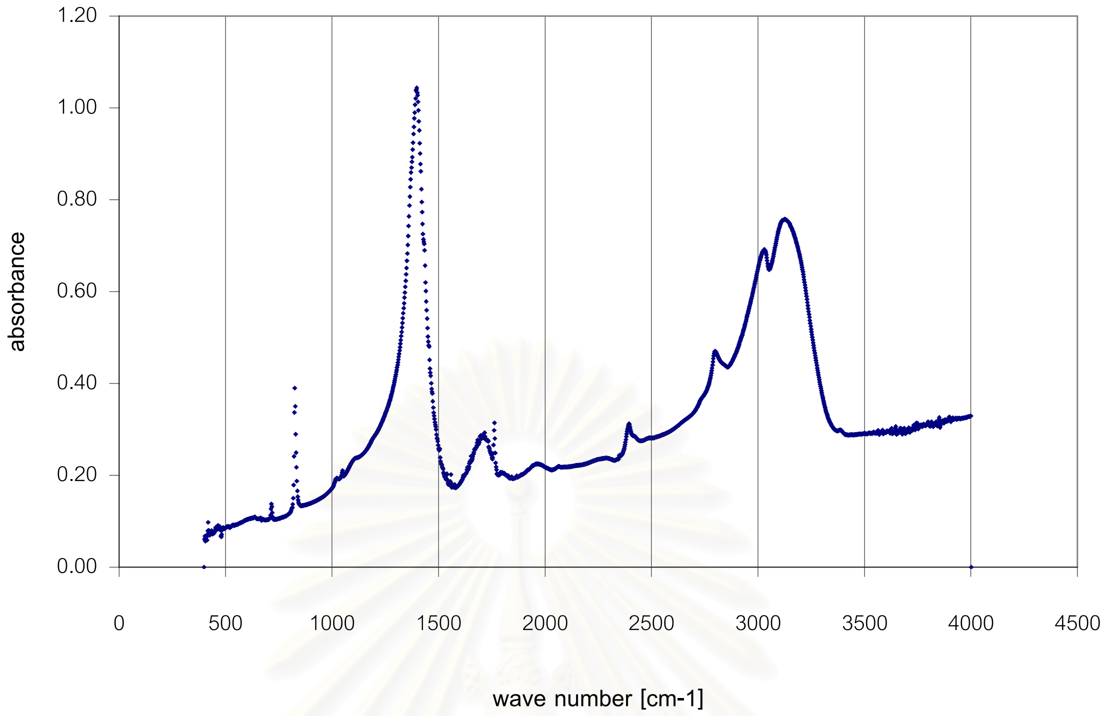

FT-IR absorbance spectrum of deposit on the anode plate from NH_3 removal from N_2-O_2

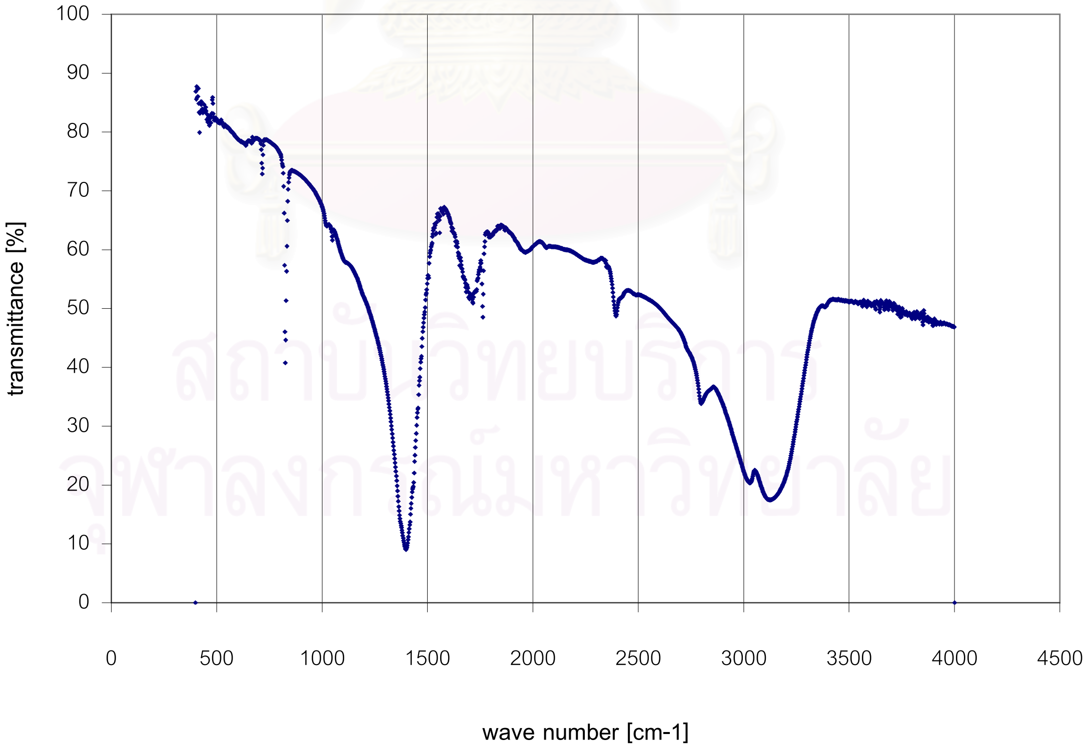

FT-IR transmittance spectrum of deposit on the anode plate from NH_3 removal from N_2-O_2

APPENDIX I

DEPOSITION-TYPE REACTOR FOR COLLECT DEPOSIT

A specially designed deposition-type reactor with a detachable plate

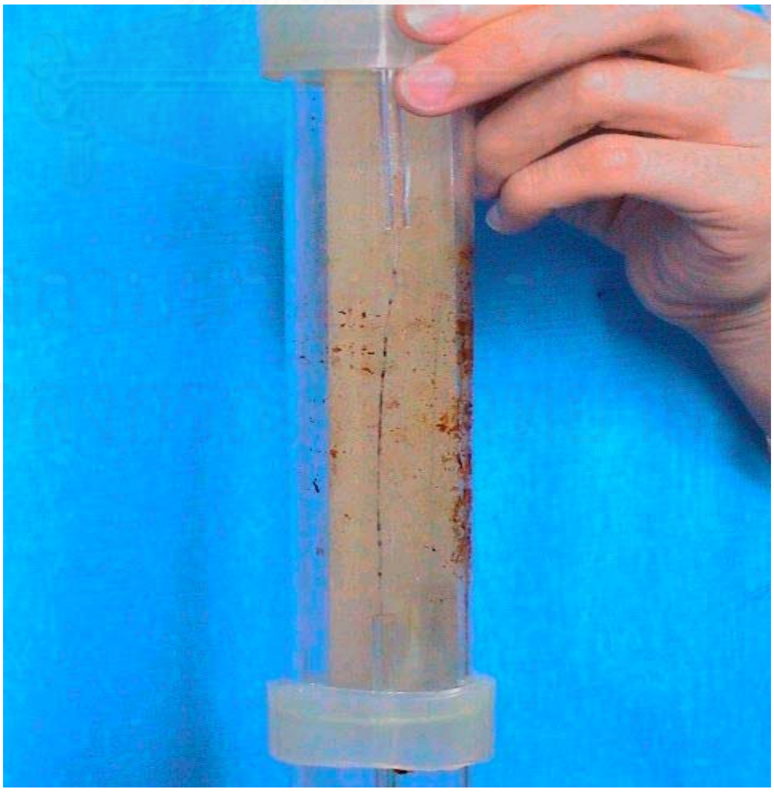

Anode plate used to collect deposit from styrene removal (1000 ppm) from N_2-O_2 at room temperature, SV 55.8 hr-1, 60 hr of deposition

APPENDIX J

PUBLICATIONS CO-AUTHORED BY S.CHAIYO

1. Tanthapanichakoon, W., Dhattavorn, N., **Chaiyo, S.**, Tamon, H. and Sano, N. “Development of Odor Control Technology for Crematory Furnace Using Corona Discharge Reaction” Journal of Multidisciplinary Research, Vol. 14(no.1), 34-41, spring 2001, published by Multidisciplinary Research Council of Japan.

2. Tanthapanichakoon, W., Charinpanitkul, T., **Chaiyo, S.**, Siriwongrangsan, V., Suthiprasit, P., Tamon, H. and Sano, N. “Removal of Styrene from Nitrogen and Air by Electron Attachment Reaction at various temperatures”, accepted for publication in Proceedings of 11th National Conference on Chemical Engineering and Applied Chemistry, November 2001.

Development of Odor Control Technology for Crematory Furnace Using Corona Discharge Reaction

Wiwut Tanthapanichakoon[*1], Nantamas Dhattavorn[*2], Sahat Chaiyo[*3]
Department of Chemical Engineering, Chulalongkorn University, Thailand
Hajime Tamon[*4]
Department of Chemical Engineering, Kyoto University, Japan
Noriaki Sano[*5]
Department of Chemical Engineering, Himeji Institute of Technology, Japan

This article investigates the feasibility of purifying the exhaust gas from cremation using corona discharge reactor with electron attachment effect. Firstly, in a survey of the common gas species emitted from the cremation, it was found that extremely low concentrations of some organic compounds can still cause malodorous smell. Next, the article summarizes the experimental results on removal of sulfur compounds, nitrogen compounds, and organic compounds, including NOx, SOx, and some other malodorous gases from nitrogen or air using corona discharge reactors. In this summary, the influence of coexisting oxygen and water vapor in the treated gas is discussed, indicating that the presence of oxygen and water vapor in the gas contributes to the increase of the removal efficiency in many cases. As for the influence of temperature on treating exhaust gas from incineration such as cremation, temperature elevation negatively affects the removal of SO_2. Furthermore, the reactor structure in terms of the shapes of cathode and anode are discussed.

Introduction

One of the national air pollution problems in Thailand is emission gas from the crematoria during cremation rites. There are nearly 23,000 temples nationwide, including approximately 300 temples with crematory furnaces in Bangkok Metropolitan Area. Various malodorous gases and particulate are emitted during cremation, causing frequent complaints from vicinal communities. Table 1 lists the commonly reported components in crematory emission. Typically crematory gases are emitted from a stack to the atmosphere without adequate treatment. A few rich temples have installed furnaces with after-burning systems but an overwhelming majority of Bangkok temples have inadequate systems, not to mention those in the country side.

Table 2 compares the generic technologies with corona discharge technology for odor control. Under suitable conditions, corona discharge is a novel efficient method that can simultaneously remove several gases. As an important character of the corona discharge, a sufficient number of low energy electrons are produced in gas stream easily. When discharged electrons collide with malodorous gas molecules, some electrons are captured by the gas molecules to form negative ions, which can be separated from the main gas stream in an electric field as solid deposit on the anode surface. First proposed for gas purification by Tamon et al.[6], this phenomenon of "electron attachment" depends on the electron energy, the

---

[*1] Dr. Wiwut Tanthapanichakoon (born in 1949)
Professor, Department of Chemical Engineering and Thai Powder Technology Center, Faculty of Engineering, Chulalongkorn University, Thailand. Ph. D. in University of Texas at Austin.

[*2] Nantamas Dhattavorn (born in 1975)
Master Student, Department of Chemical Engineering, Faculty of Engineering, Chulalongkorn University.

[*3] Sahat Chaiyo (born in 1978)
Master Student, Department of Chemical Engineering, Faculty of Engineering, Chulalongkorn University.

[*4] Dr. Hajime Tamon (born in 1952)
Professor, Department of Chemical Engineering, Kyoto University, Japan. Ph. D. in Kyoto Universitiy.

[*5] Dr. Noriaki Sano (born in 1967)
Reseach Associate, Department of Chemical Engineering, Himeji Institute of Technology, Japan. Ph. D. in Kyoto University.

Table 1. Types and concentrations of gaseous emission from a crematorium after 100-fold dilution[16,17,18]

	Components	Concentration	
Air	N_2	78	%
	O_2	20~21	%
Low Concentration	CO_2	0.01-0.02	%
	H_2O	0.22	%
	NO_x	80	ppm (max)
	SO_x	5.8	ppm (max)
	Acetic acid (CH_3COOH)	24	ppm
	Hydrocarbons	230	ppm (as propane)
Very dilute concentration (malodorous)	Acetaldehyde	0.04	ppm
	Styrene	0.01	ppm
	Hydrogen sulfide	0.01	ppm
	Methyl mercaptan	0.01	ppm
	Dimethyl sulfide	0.001	ppm
	Ammonia	0.0005	ppm
	Trimethyl amine	0.023	ppm

structure of the gas molecules and its electron affinity [13,14,15,19]. It can lead to very high selectivity in the formation of negative ions from electronegative impurities even at low concentrations. Under suitable conditions clusters of ions with gas molecules are formed, which greatly enhance the removal efficiency. In the presence of O_2, oxygen radicals and ozone are formed and contribute to decomposition and oxidation of the malodorous gas molecules.

Principle of gas purification

Figure 1 illustrates the principle of gas purification. An impurity AB is to be removed from an inert gas in a cylindrical corona discharge reactor. Its cathode is a wire tightened at the center of the reactor and the stainless steel cylinder is the anode. High DC voltage (-5~-15 kV) is applied to the cathode to induce corona discharge in the reactor. During their drift to the anode, electrons emitted by the discharge collide with some of the gas molecules and the resulting negative ions drift to and deposit on the anode. The present paper describes the joint development of the corona discharge reactor by Tamon et al., Sano et al. and Tanthapanichakoon et al. to control malodorous crematory emission.

Experimental Setup

As illustrated in Figure 2, the experimental set-up and experimental procedure have been reported elsewhere [1,6,21] and are omitted here. Infrared lamps are used to raise and control the reactor temperature up to 400°C. Since most emission gases are exhausted at relatively high temperatures, it is indispensable to investigate the effect of temperature on the removal efficiency.

Result and Discussion

In addition to the malodorous gas found in crematory

Table 2 Odor control methods

Method	Suitable condition	Advantage	Disadvantage
After-burning (thermal combustion)	- Uniform furnace temperature (800-900 °C) - Residence time about 0.5~2 sec - Steady state operation	- Simple and widely available	- Unsuitable for unsteady state operation - Require sizable furnace
Catalytic reaction (catalytic combustion)	- Known fixed gas species - Steady state operation	- Can be operated at relatively low temperature - High selectivity	- One catalyst can not simultaneously be effective for many species - Combustion is not good when the gas species change
Adsorption	- Relatively low temperature and space velocity - Steady and unsteady operation	- No problem with unsteady operation	- Regeneration is necessary - Relatively high pressure drop - Batch operation with multiple units
Gas absorption	- Low to very high temperature - Steady and unsteady operation	- Can simultaneously remove particulate and odor	- Difficult to find the appropriate liquid absorbent - Complicated operation
Corona discharge, including electron attachment	- Low space velocity - Steady and unsteady operation	- Rapidly reach the steady state - Multiple removal mechanisms	- Relatively big reactor - High voltage

emission, the authors have investigated a wide variety of gas species. Table 3 summarized the types of gas species and the effect of various factors on their observed removal efficiencies. As an example, Table 3 reveals that the inlet concentration of $(CH_3)_2S$ to the reactor was investigated in the range 4-89 ppm; the concentration of coexisting O from 0(nil) to 22 vol% and H_2O vapor from 600- 9,10 ppm. The identified reaction byproducts were SO_2 in th cases of coexisting O_2 alone and O_2 plus H_2O vapor. Th removal efficiency of $(CH_3)_2S$ decreased as its inle

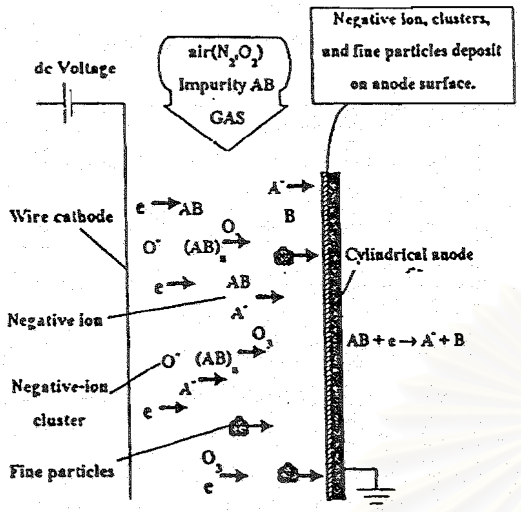

Figure 1 Principle of gas purification

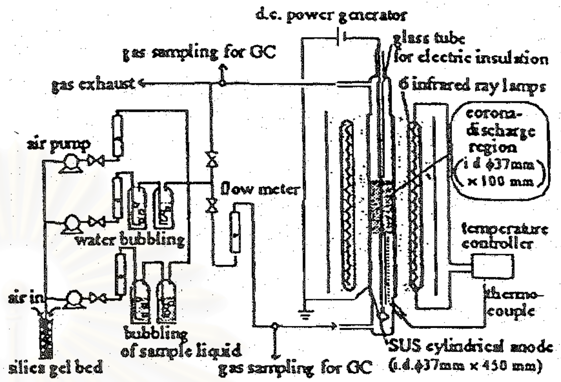

Figure 2. Experimental set-up for gas purification at high temperature

concentration increased. In contrast, when the concentration of coexisting O_2, H_2O vapor or both increased, the removal efficiency of $(CH_3)_2S$ tended to rise. Moreover, the observed maximum removal efficiency of $(CH_3)_2S$ was higher than 80% at 4 ppm (symbol A) in the case of pure N_2, coexisting O_2 or O_2 plus H_2O vapor. One can notice that the removals of most gases investigated here also show very high removal efficiency in the presence of oxygen. Obviously, the corona discharge reactor is applicable to such malodorous crematory gas species as $(CH_3)_3N$, H_2S, CH_3CHO, CH_3SH, $(CH_3)_2S$, SO_2 and so on.

Table 4 summarizes the role of coexisting O_2. A wide range of removal mechanisms can take place in the corona discharge reactor and in several of them O_2 often enhances the removal efficiency. To obtain good results the deposition on the anode surface should be stable. Table 5 lists the main characteristics of the solid deposits. These tables contribute to a better understanding of the dominant removal mechanism for each species.

Figure 3 shows an example of the effect of temperature on the removal of SO_2 at dry and humidified conditions. This figure shows that the removal efficiency of SO_2 decreases as the temperature increases and that H_2O vapor enhances the removal efficiency especially at low temperature condition.

Tanthapanichakoon et al.[19,20] have investigated the effect of reactor structure and come up with the following design guideline:

a. Whenever applicable, a thicker cathode wire should be used because it generally leads to higher removal efficiency.
b. For the same space velocity and reactor volume, a slender reactor has a higher removal efficiency than a stocky reactor.
c. Only a single cathode wire should be used in the reactor. The use of multiple cathodes has been shown to lead to a deterioration in the removal efficiency.

The authors have also investigated the simultaneous removal of a few pairs of gas species. However, they are omitted because of space limitation.

Conclusion

The corona discharge reactor has shown a good promise for the treatment of crematory emission. More development work, however, is necessary before its actual

Table 3. Effect of coexisting oxygen and water vapor in nitrogen on the reaction byproducts and removal efficiency

Sample Gas	Experimental conditions[1]				Reaction Byproduct	Removal efficiency								Ref No.
	C_{in} (Sample gas)	C_{O_2}	C_{H_2O}	SV		Change of removal efficiency when the gas below increases				Maximum efficiency [-]				
	[ppm]	[%]	[ppm]	[hr^{-1}]		C_{in} (in N_2 Only)	O_2	H_2O	O_2 + H_2O	C_{in} (in N_2 Only)	O_2	H_2O	O_2+ H_2O	
SF_6	0.176-298	NI	NI	18.9	NI	↓	NI	NI	NI	A	NI	NI	NI	2,6
H_2S	60	NI	400-1,100	37.8	None	↓	NI	↑	NI	A	NI	A (60ppm)	NI	1,2,6
SO_2	32.7-304	0-18	400-13,000	18.9-37.8	None	↓	↑	↑	↑	C (33ppm)	A	D (122ppm)	A	1,2,6, 12
CS_2	30-65	0-49	300-11,000	18.9-37.8	SO_2 . COS	↓	↑[5]	↑	↓	A (30ppm)	A	B (48ppm)	A	1,2,6
COS	29-53	0-50	650-10,000	18.9-37.8	SO_2	↓	↑[5]	↑	NI	B	A	B (53ppm)	NI	1,2,6
CH_3SH	40-69	0-20	1,000-10,000	18.9-37.8	SO_2 . H_2S^* or COS^*	↓	↑	↑	NI	B	A	B (40ppm)	NI	1,2,6
$(CH_3)_2S$	3.88-89	0-22	600-9,100	18.9-52.9	SO_2^{**} . SO_2^{***}	↓	↑	↑	↑	A (4ppm)	A	D (38ppm)	A	1,2,6
CH_3I	75-83	5.6-8.0	5,600-17,800	47.3-50.0	I_2 (in N_2)	↓	↑	↑	↑	C	A	A	A	2,3,4
I_2	40.4-62	0-7	8,500	44-77.9	NI	NI	↑	↓	NI	B[3]	A	A (at I=0)	NI	4,5
$C_2Cl_3F_3$	50-400	0-20	NI	18.9	HCl^* or HF^*	↓	↓	NI	NI	A	A	NI	NI	2,10, 11
CH_3CHO	9.9-35.6	0-20	0-183	80.9	NI	↓	↑	↑	NI	B	A	A	NI	2,7,9, 10
C_9H_9N (skatole)	2.4	0-20	10,000	43.5-189	NI	NI	↑	NI	↑	A	A	NI	A	7
C_6H_6 (benzene)	205-313	29-34	7,500	18.7-28.4	NI	NI	↑	NI	↑	D	A	NI	A	8
p-$C_6H_4Cl_2$ (p-dichloro benzene)	19-57	19-20	NI	20.6-45.5	NI	↓	↑	NI	NI	B	A	NI	NI	8
NH_3	49-143	0-20	3,288-6,418	75.6-189	NI	NI	↑	NI	↑	D	A	NI	A	9,12
$(CH_3)_3N$	58.6-69.4	0-20	NI	58.6-69.4	CH_3CHO, C_2H_5OH, $(CH_3)_2CO$ or CH_3NO_2	NI	↑	NI	NI	D	A	NI	NI	2,9, 12
NO_2	674-747	0-20	NI	75.6	NI	NI	NI	NI	NI	C	NI	NI	N	9
O_2[4]	1.1-6.3	NI	NI	315-846.3	NI	NI	NI	NI	NI	D[4]	NI	NI	NI	6

* byproduct observed with coexisting oxygen

** byproduct observed with coexisting water vapor

*** byproduct observed with both coexisting oxygen and water vapor

Unless stated otherwise, the same byproducts are observed for the same sample gas.

1) Current, I = 0.05 – 2.0 mA ; Voltage, V = 6.0 - 20.0 kV

2) Removal efficiency ; A > 80%, B 60-80%, C 40-60%, D < 40 %

3) Removed by wetted – wall reactor.

4) Removed by sweep-out-type type reactor

5) Complete removal at O_2 > 2%

NI not investigated

Table 4. Dominant removal mechanism in the presence of O_2

Removal mechanism	Influence of O_2 on removal efficiency	Deposition at anode	Example	Removal efficiency
Reaction with O_3	Increase	Stable	I_2 . CH_3I . C_9H_7N .CH_3CHO .$(CH_3)_3N$	High
Formation of ion clusters induced by O^*	Increase	Stable	SO_2 . CS_2 . COS . CH_3SH . $(CH_3)_2S$. CH_3CHO . CH_3I	High
Polycondensation by reaction with O^*	Increase	Stable	C_6H_6	High
Polycondensation by dissociative electron attachment	None	Stable	p-$C_6H_4Cl_2$	High
Dissociative electron attachment	Decrease	Stable	$C_2F_3Cl_3$	Low
Dissociative electron attachment	None	Unstable	F_2 . Cl_3	Low

*Electrons are attached to coexisting oxygen

Table 5 Deposit on anode surface in the presence of O_2

Sample gas	Feature of deposit
Sulfur compounds	Solid containing S compound
I_2	Yellow powder (I_4O_9)
CH_3I	Black particles (not identified)
$C_2F_3Cl_3$	Black particles containing F . Cl
C_6H_6 . p-$C_6H_4Cl_2$	Polycyclic aromatic compounds of high boiling point
CH_3CHO	Hard brown coating containing CH_3CHO
$(CH_3)_3N$	Carbon compounds of high boiling point

application. Since most of the previous studies were carried out at room temperature, the effect of high temperature on the removal efficiency should be investigated further. So should the simultaneous removal of several malodorous gas species commonly found in crematory emission.

Acknowledgement

W. T., N. D. and S. C. receive partial financial support from Thailand Research Fund. H. T. and N. S. visited with them under the OECF-TJTTP scheme.

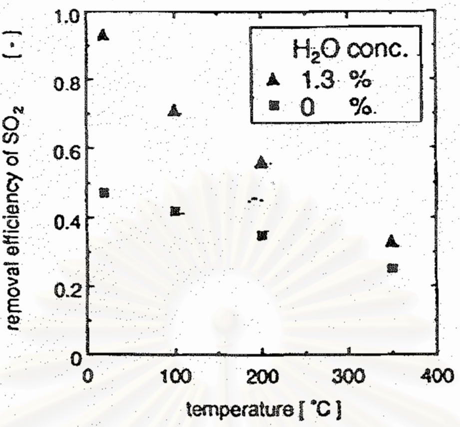

Figure 3. Removal efficiency of SO_2 from N_2-O_2 (-H_2O) mixture at various temperatures; $[SO_2]_{inlet} = 4{,}000$ ppm , $[O_2] = 20\%$

Reference

1. Tamon, H., Sano, N. and Okazaki, M. " Influence of Oxygen and Water Vapor on Removal of Sulfur Compounds by Electron Attachment," AIChE J., 1996, 42,pp.1481-1486.
2. Tanthapanichakoon, W., Larpsuriyakul, K., Khongprasarnkal, P., Charinpanitkul, T., Tamon, H., and Okazaki, M." Basic Study on the Application of Electron Attachment Reaction to the Treatment of Crematory Emission Gas, " J. National Res. Council of Thailand, 1996, vol 28,pp.282-313.
3. Sano, N., Nagamoto, T., Tamon, H., Suzuki, T. and Okazaki, M." Removal of Methyl Iodide in Gas by Corona-Discharge Reactor," J. Chem. Eng. Japan,1997,vol 30, pp.944-946 .
4. Sano, N., Nagamoto, T., Tamon, H. and Okazaki, M." Removal of Iodine and Methyl Iodide in Gas by Wetted-Wall Reactor Based on Selective Electron Attachment," J. Chem. Eng. Japan, 1996, 29, pp.59-64.
5. Sano, N., Tamon, H. and Okazaki, M." Removal of Iodine in Gas by Corona-Discharge Reactor," J. Chem. Eng. Japan, 1996, 29,pp.59-64.
6. Tamon H., Mizota, H., Sano, N., Schulze, S. and Okazaki, M." New Concept of Gas Purification by Electron Attachment," AIChE J:, 1995, 41, pp.1701-1711.
7. Sano, N., Nagamoto, T., Tamon, H., Suzuki, T. and Okazaki, M." Removal of Acetaldehyde and Skatole in Gas by Corona-Discharge," Ind. Eng. Chem. Res., 1997b, 36, pp.3783-3791.
8. Tamon, H., Imanaka, H., Sano, N., Okazaki, M. and Tanthapanichakoon, W." Removal of Aromatic Compounds in Gas by Electron Attachment," Ind. Eng. Chem. Res., 1998, 37,pp.2770-2774.
9. P. Khongphasarnkarn," Removal of Trimethylamine Acetaldehyde and Ammonia Gases using Electron Attachment Reaction," Master's thesis, Chulalongkorn University, Bangkok, Thailand (1998), ISBN 974-639-484-3.
10. Tanthapanichakoon, W., Larpsuriyakul, K., Charinpanitkul, T., Sano, N., Tamon, H. and Okazaki, M. " Effect of structure of corona-discharge reactor on removal of dilute gaseous pollutants using selective electron attachment," J. Chem. Eng. Japan, 1998,vol 31

,pp.7-13

11. Sano ,N.,Tamon ,H and Okazaki , M. "Removal of Chlorofluorocarbon ,1,1,2-Trichloro-1,2,2-Trifluoroethane , in Gas by a Corona-Discharge Reactor," Ind. Eng. Chem. Res., 1998, 37, pp. 1428-1434.
12. Tanthapanichakoon, W., Tamon, H., Khongphasamkaln, P., Sano, N., Charinpanitkul, T., and Okazaki, M. " Removal of Trimethylamine and Ammonia Using Electron Attachment Reaction," Journal of the Science Society of Thailand (Science Asia), 1999, 1, pp. 57-63.
13. Caledonia, G. E. A Survey of the Gas-Phase Negative Ion Kinetics of Inorganic Molecules. Electron Attachment Reactions. Chem. Rev., 1975, 75, 333-351.
14. Massey, S. H. Negative Ions. Cambridge Univ. Press, Cambridge, England, 1976.
15. Massey, S. H. Atomic and Molecular Collisions. Taylor & Francis, London, 1979.
16. Nishida, K. and Matsuda Y. Malodor of exhaust gas from crematory. J. Odor Control, 1981, 1-11 (in Japanese).
17. Nishida, K. Malodor at Cremation Facility (Part I). PPM, 1988, 3, 49-58 (in Japanese).
18. Nishida, K. Malodor at Cremation Facility (Part II). PPM, 1988, 4, 51-59 (in Japanese).
19. Tamon, H., Yano, H. and Okazaki, M. A New Method of Gas Mixture Separation Based on Selective Electron Attachment. Kagaku Kogaku Ronbunshu, 1989, 15, 663-668.
20. Tanthapanichakoon, W., Larpsuriyakul, K., Sano, N., Tamon, H. and Okazaki, M. Effect of reactor structure on removal of methyl iodide and chlorofluorocarbon in gas using selective electron attachment. Proc. Regional Sym. Chem. Eng. 1996, Jakarta, Indonesia, October 1996, 3.2.1-3.2.14.
21. Sano, N., Fukuoka, M., Kanki, T., Tamon, H., Tanthapanichakoon, W. and Charinpanitkul, T. Influence of Temperature on Removal of Sulfur Dioxide and Benzene from Air by Corona Discharge Reactor. Proc. of Asia Pacific Conference on Sustainable Energy and Environmental Technologies, Hong Kong, Dec. 2000, 99-103.

[2000.5.19受稿，2000.9.18採録]

Removal of Styrene from Nitrogen and Air by Electron Attachment Reaction at Various Temperatures

Wiwut Tanthapanichakoon*, Tawatchai Charinpanitkul, Sahat Chaiyo,
Vilailuck Siriwongrangsan, and Paphawan Suthiprasit

Department of Chemical Engineering, Chulalongkorn University
Payathai Road, Pathumwan, Bangkok 10400 Thailand
email: tchw[illegible]

Noriaki Sano

Department of Chemical Engineering, Himeji Institute of Technology
2167 Shosha, Himeji, Hyogo 671-2201, Japan

Hajime Tamon

Department of Chemical Engineering, Kyoto university
Yoshida-Honmachi, Sakyo-ku, Kyoto 606-8501, Japan.

Abstract

In the present research electron attachment reaction involving negative ions produced by the collision between electrons and electronegative gas molecules is investigated experimentally. First the corona-discharge characteristics of an electron attachment reactor at various elevated temperatures (30-300^{0}C) are obtained. Next the reactor is employed to remove styrene (C_8H_8) from N_2 and from the air at room temperature to 300 ^{0}C. Compared to the removal of styrene from only N_2, the removal efficiency of styrene from the air is greatly enhanced by the presence of O_2 due to the generation of ozone. As reported by Noriaki Sano et al. (1997), ozonation reaction contributes to the removal of CH_3CHO and skatole. The same ozonation phenomenon is found to enhance styrene removal efficiency. When the reaction temperature is increased, the removal efficiency is found to decrease because ozone becomes less stable at high temperatures. The effect of styrene inlet concentration is also investigated. As expected, the higher the inlet concentration, the lower the removal efficiency becomes. This is because the discharged current is kept constant, so the number ratio of discharge electrons to styrene molecules decreases as the inlet styrene concentration increases.

Introduction

Nowadays air pollution in Thailand is one of the most serious environmental problems. There are many sources of air pollutants such as heavy concentration of vehicles that release a large amount of toxic and obnoxious emissions. One unconventional source in Thailand is emission gas from the crematoria during cremation rites. There are nearly 23,000 temples nationwide, including approximately 300 temples with crematory furnaces in Bangkok Metropolitan Area. Various malodorous gases and particulate are emitted during cremation, causing frequent complaints from vicinal communities. Typically crematory gases are emitted from a stack to the atmosphere without adequate treatment. A few rich temples have installed furnaces with satisfactory after-burning systems but an overwhelming majority of the temples have inadequate systems. For this reason it is worthwhile to try to develop an alternative gas treatment method that achieves high efficiency and low energy consumption. Electron attachment is a reaction involving low energy electrons having high selectivity for electronegative gases. When an electron collides with a gas molecule, a negative ion is produced with a probability depending on the electron energy, the structure of the gas molecule, and its electron affinity (Massey, 1976; Caledonia, 1975). This reaction is called electron attachment. A novel gas purification method was proposed (Tamon et al., 1995). Since the gas impurities contain atoms of high electron affinity such as halogens, sulfur, and oxygen, they usually have high probability of electron attachment. In the proposed gas- purification principle, the gas impurities are ionized by colliding with electrons that are produced in a corona discharge between a wire cathode and a cylindrical anode. The negative ions formed by electron attachment drift to the anode. Previous studies have revealed that gases of high electron affinity, for example sulfur compounds, halogens, malodorous gases, VOCs and CFCs are selectively removed by the proposed method (Tamon et al., 1995, 1996, 1998; Sano et al..1996. 1997a, 1997b, 1998; Tanthapanichakoon 1998; Khongphasarnkaln, 1998; Dhattavorn, 2000). This research investigates the application of electron attachment reaction to the removal of styrene that is one of crematorium gaseous.

Principle of gas purification: Figure 1 illustrates the principle of gas purification by the removal of an impurity, AB, from an inert gas with a cylindrical corona-discharge reactor (Tamon et al., 1995). The corona discharge is employed here because it is an efficient method to supply a large number of low-energy electrons to the gas stream. The cathode is a stainless steel wire stretched along the axis of the reactor and the outer cylinder acts as grounded anode. High DC voltage (-5~ -15kV) is applied to the cathode to induce corona discharge in the reactor. Electrons generated at the cathode drift to the anode along the applied electric field. During their drift to the anode, a portion of them collides with the gas molecules. Negative ions, A^-, are thus selectively produced by electron attachment and they likewise drift to the anode as the electrons do.

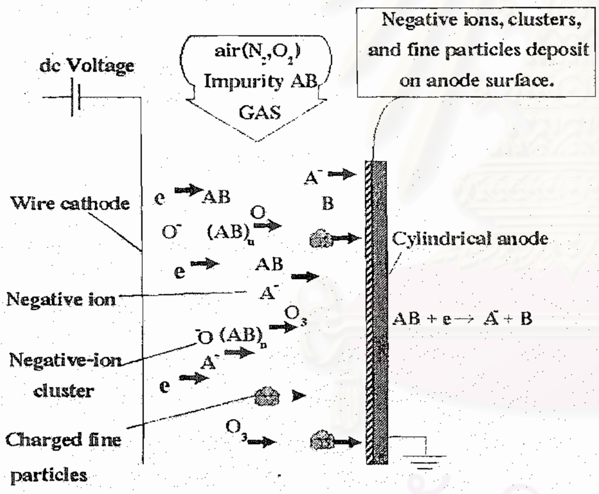

Figure 1. Principle of gas purification

Experimental Setup

Figure 2 shows a schematic diagram of the experimental setup that consists of a deposition-type corona-discharge reactor, a test gas mixing system, a high-voltage DC generator and a temperature controller. The deposition-type reactor consists of a SUS pipe, 3.7 cm. inner diameter and 80 cm. length, as the anode. The cathode is a 0.5-mm stainless-steel wire suspended from a silicone plug at the top of the reactor and straightened along the axis of the anode by a small weight. A high-voltage DC generator (Matsusada, HAR-30N5) whose maximum allowable voltage is 50 kV is utilized to supply a steady stream of energetic electrons to the corona-discharge reactor.

A slim pyrex glass tube is used to cover either end of the cathode in order to limit the corona discharge zone in the middle section of the reactor to 10 cm and to achieve a uniform axial temperature distribution within the zone. A type-K thermocouple is inserted into the reactor to measure the gas temperature in the corona discharge zone. To control the reactor temperature, 6-infrared heating lamps (200V. 700W each) are installed lengthwise around the outside perimeter of the reactor. The temperature control unit consists of a temperature controller (FENWAL. AR-24L) and a thyrister power regulator (Shimaden. PAC15C003081-NO).

The desired concentrations of styrene and coexisting oxygen are adjusted by mixing standard gases with nitrogen. The inlet concentration of styrene (C_{in}) is varied from 40-500 ppm. Inlet and outlet concentrations of styrene are analyzed using a gas chromatograph (Shimadzu Corp., GC 9A) equipped with a flame ionization detector (FID). The packed material in the GC column used for detecting the concentration of styrene is PEG-20M Uniport B (GL Science Inc.) with 60/80 mesh size and usable at maximum temperature of 230°C.

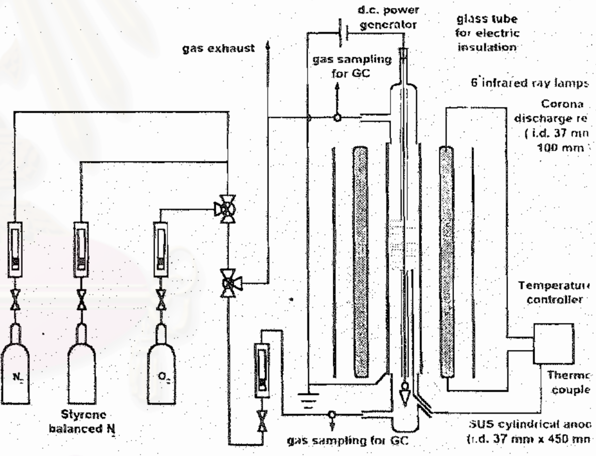

Figure 2 Experimental apparatus

Results and Discussion

Effect of reactor temperature and concentration on removal of styrene from N_2

Generally the removal efficiency is defined as Eq.1

$$\psi = \frac{(C_{in} - C_{out,anym.l})}{C_{in}} \quad [-] \qquad (1)$$

Here, ψ is the removal efficiency, C_{out} (ppm) and C_{in} (ppm) are the outlet and inlet concentrations of styrene. ψ includes the effect of adsorption inside the reactor in the absence of corona discharge. The removal efficiency ψ' in Eq.2 excludes any adsorption effect inside the reactor in the absence of corona discharge and thus represents the pure corona discharge effect.

$$\psi' = \frac{(C_{out,0mA} - C_{out,any\,mA})}{C_{out,0mA}} \quad [-] \quad (2)$$

The removal efficiency per unit residence time, ψ'', in Eq.3 is defined to take into account the actual shorter residence time of the hot gas in the reactor even though the inlet gas flow rate (mole basis) remains constant.

$$\psi'' = \frac{\psi' \times residence\ time\ at\ 25\ {}^0C}{residence\ time\ at\ T\ {}^0C} \quad (3)$$

At steady state, the equation of continuity requires that $\rho_1\langle \upsilon_1\rangle A_1 = \rho_2\langle \upsilon_2\rangle A_2$. Since $A_1 = A_2$ and ρ is a function of the gas temperature, the gas velocity at an elevated temperature T_2 will be faster than its velocity at room temperature T_1. Thus the mean residence time $\theta_2 = \frac{V}{\langle \upsilon_2\rangle}$ of this gas at T_2 is shorter than $\theta_1 = \frac{V}{\langle \upsilon_1\rangle}$ at room temperature. Here V is the effective volume of the corona discharge reactor.

Figure 3 shows the observed styrene removal efficiency ψ' versus gas temperature. We see that as the temperature increases, the value of ψ' decreases monotonically starting from room temperature to 300°C. As pointed out above, the mean residence time of the gas mixture inside the reactor decreases as the reactor temperature rises. This phenomenon is attributable to the fact that the gas mixture flows upward more quickly as its volume expands. Above 200 ^{0}C, the rate of detachment of adsorbed styrene molecules on the reactor wall is sufficiently enhanced by the lowered adsorption equilibrium to overcome the effect of electrostatic attraction, thus significantly reducing the net rate of styrene deposition on the wall when the styrene inlet concentration is below 100 ppm..

Figure 4 shows the removal efficiency per residence time ψ'' versus temperature. This figure reveals that when the negative effect of reduced residence time is taken in account, the value of ψ'' actually increases with the temperature up to 200^{0}C when the styrene inlet concentration is below 100 ppm and up to 300^{0}C when the concentration is 500 ppm. As explained above, the rate of detachment of styrene from the anode surface becomes significant at high temperatures. At sufficiently high concentration (500ppm), this detachment rate is slowed down by the remaining high concentration of styrene in the gas phase.

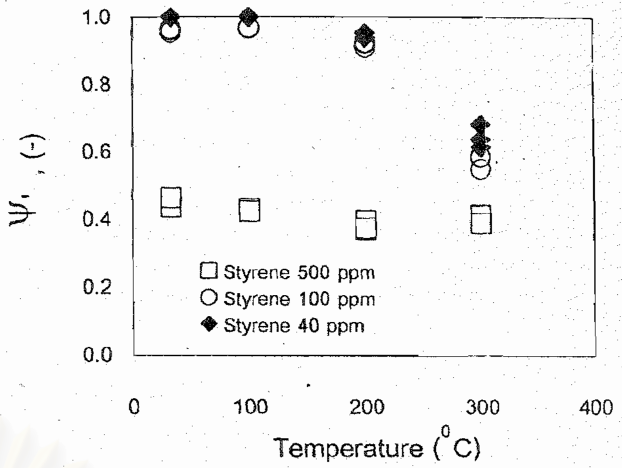

Figure 3 Effect of temperature on the removal efficiency of styrene from N_2
I = 0.5 mA , SV = 55.8 hr^{-1} at room temperature

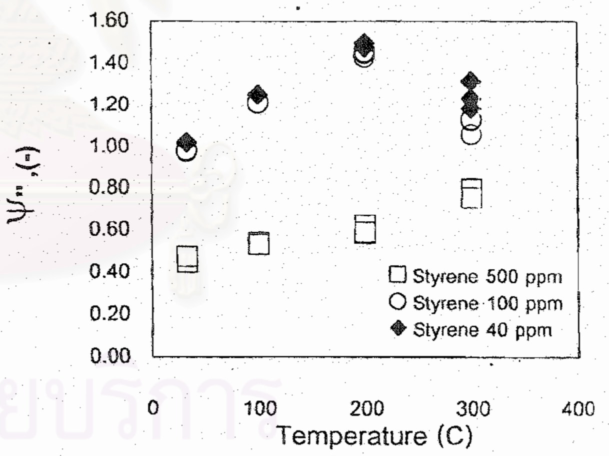

Figure 4 Effect of temperature on the removal efficiency per unit residence time of styrene from N_2
I = 0.5 mA, SV = 55.8 hr^{-1} at room temperature

Tamon et al.(1995) have found that the removal efficiency via electron attachment tends to decrease when the gas inlet concentration increases. As expected, the present experimental results on the effect of inlet styrene concentration also exhibit the same tendency. The lower the inlet concentration of styrene, the higher the removal efficiency becomes. To explain the phenomenon, we consider the number ratio of discharge electrons to the incoming styrene molecules. At a higher styrene inlet concentration, there are many more styrene molecules than at a lower inlet concentration of styrene. However, the number of discharge electrons remains more or less constant at the same discharge current. Therefore, the probability of electron attachment onto a styrene molecule becomes lower. This is the reason that the lower the inlet concentration of styrene, the higher the removal efficiency becomes regardless of the gas temperature of interest.

Removal of styrene from air

In most applications of gas purification, other kinds of gas components often coexist. Therefore it is necessary to study the influence of common coexisting gases on the removal efficiency. **Figure 5** compares the removal efficiency ψ' of styrene from N_2 and air when the styrene inlet concentration is 500 ppm. It is obvious that the presence of O_2 in N_2 greatly enhances the styrene removal efficiency despite the fact that the discharge current has been reduced tenfold to 0.05 mA compared to the case of pure N_2. This can be attributed to the fact that O_3 is produced from O_2 by the corona discharge reaction. At relatively low temperatures, O_3 is quite stable and it enhances the removal of styrene via the formation of ionic ozone-styrene clusters. It can be concluded that ozonation reaction is an important mechanism to enhance the removal efficiency, though its effect decreases when the temperature increases.

Conclusion

The removal of styrene from nitrogen and air by electron attachment was investigated. As expected, the lower the inlet concentration of styrene, the higher the removal efficiency becomes. The removal efficiency of styrene from air is much higher than from pure nitrogen because of the ozonation effect.

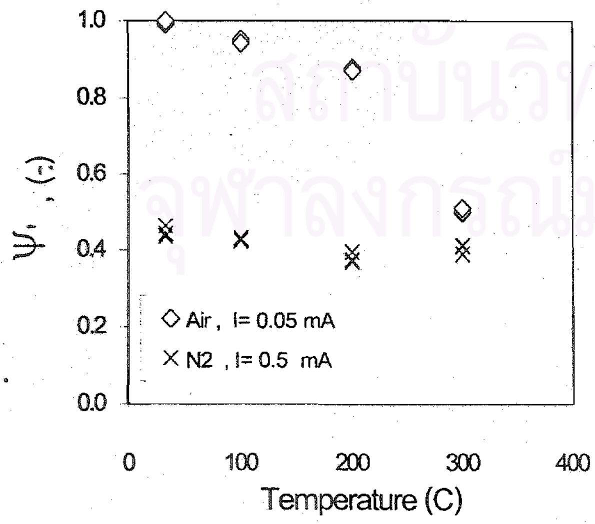

Figure 5 Effect of oxygen coexisting gas on the removal of styrene from N_2
C_{in} = 500 ppm. SV=55.8 hr^{-1} at room temperature

Acknowledgement

W.T., T.C. and S.C. receive research grant and financial support from Thailand Research Fund (High-Temperature Removal of Low-Concentration Multi-Component Air Pollutant Gases Using Electron Attachment Reaction Project and Senior Research Scholar Program). H.T. and N.S. receive support from TJTTP-JBIC Project of Chulalongkorn University to carry out research collaboration at C.U.

Notation

C = concentration, ppm
ψ = removal efficiency, (-)
ψ' = removal efficiency excluding adsorption effect, (-)
ψ'' = removal efficiency per unit residence time,(-)
SV = space velocity, hr^{-1}
θ = mean residence time, (min)
V = effective volume of the corona discharge reactor, (ml)
A = cross sectional area, (cm^2)
$\langle \upsilon \rangle$ = superficial velocity, (m/s)

Subscript

in = inlet of reactor
out,0mA = outlet of reactor at zero discharge current
out, anymA= outlet of reactor at non-zero current

Literature Cited

Caledonia, G. E. "A survey of the gas-phase negative ion kinetics of inorganic molecules - Electron Attachment Reactions," *Chem. Rev.* **75**, 333-351 (1975).

Dhattavorn, N. "Effect of temperature on removal of toluene vapor using the electron attachment reaction," Master's degree thesis., Chulalongkorn University (2000).

Khongphasarnkaln, P., "Removal of Trimethylamine Acetaldehyde and Ammonia using electron attachment reaction,". Master's degree thesis. Chulalongkorn University (1998).

Massay, S. H. *Negative Ions*. Cambridge Univ. Press, Cambridge, England (1976).

Sano, N., Nagamoto, T., Tamon, H., and Okazaki, M. "Removal Iodine and Methyl Iodide in Gas by Wetted-Wall Reactor based on Selective Electron Attachment," *J. Chem. Eng. Japan.*, **29**, 59-64 (1996)

Sano, N. "Development of Gas Purification Technology by Selective Electron Attachment," Ph.D. Diss., Kyoto Univ., Japan (1997a).

Sano, N., Nagamoto, T., Tamon, H., Suzuki, T., and Okazaki, M. "Removal of Acetaldehyde and Skatole in Gas by Corona-Discharge" *Ind. Eng. Chem. Res.*, **36**, 3783-3791 (1997b).

Sano, N., Tamon, H., and Okazaki, M. "Removal of the Chlorofluorocarbon 1,1,2-Trichloro-1,2,2-trifluoroethane in Gas by a Corona-Discharge Reactor" *Ind. Eng. Chem. Res.*, **37**, 1428(1998).

Tamon, H., et al. "New concept of gas purification by electron attachment," *AIChE J.*, **41**, 1701-1711 (1995).

Tamon, H., et al. "Influence of Oxygen and Water Vapor on Removal of Sulfur Compounds by Selective Electron Attachment," *AICHE J.*, **42**, 1481-1486(1996).

Tamon, H., et al. "Removal of Aromatic Compounds in Gas by Electron Attachment." *Ind. Eng. Chem. Res.*, **37**, 2770-2774(1998).

Tanthapanichakoon, W., Larpsuriyakul, K., Charinpanitkul, T., Sano, N., Tamon, H., and Okazaki, M. "Effect of structure of corona-discharge reactor on removal of dilute gaseous pollutants using selective electron attachment," *J. Chem. Eng. Japan.*, **31**, 7-13 (1998).

VITA

Mr. Sahat Chaiyo was born in Chiangmai, Thailand, on May 4,1978, the second son of Boonlert and Dara Chaiyo. After completing his high-school study at Montford College in Chiangmai, in March, 1995. He entered Chulalongkorn University, Bangkok, in June, 1995, he gained admission to the Graduate School of Chulalongkorn University in June 1999. He received financial support from Thailand Research Fund, which covered research materials and monthly expenses. In October 2001, he was awarded the degree of Master of Engineering in Chemical Engineering.